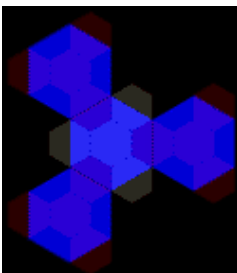**Spatial Synthesis: Volume I, Centrality and Hierarchy. Book 1.**

Sandra Lach Arlinghaus and William C. Arlinghaus
University of Michigan and Lawrence Technological University
[Institute of Mathematical Geography](), Ann Arbor, 2005
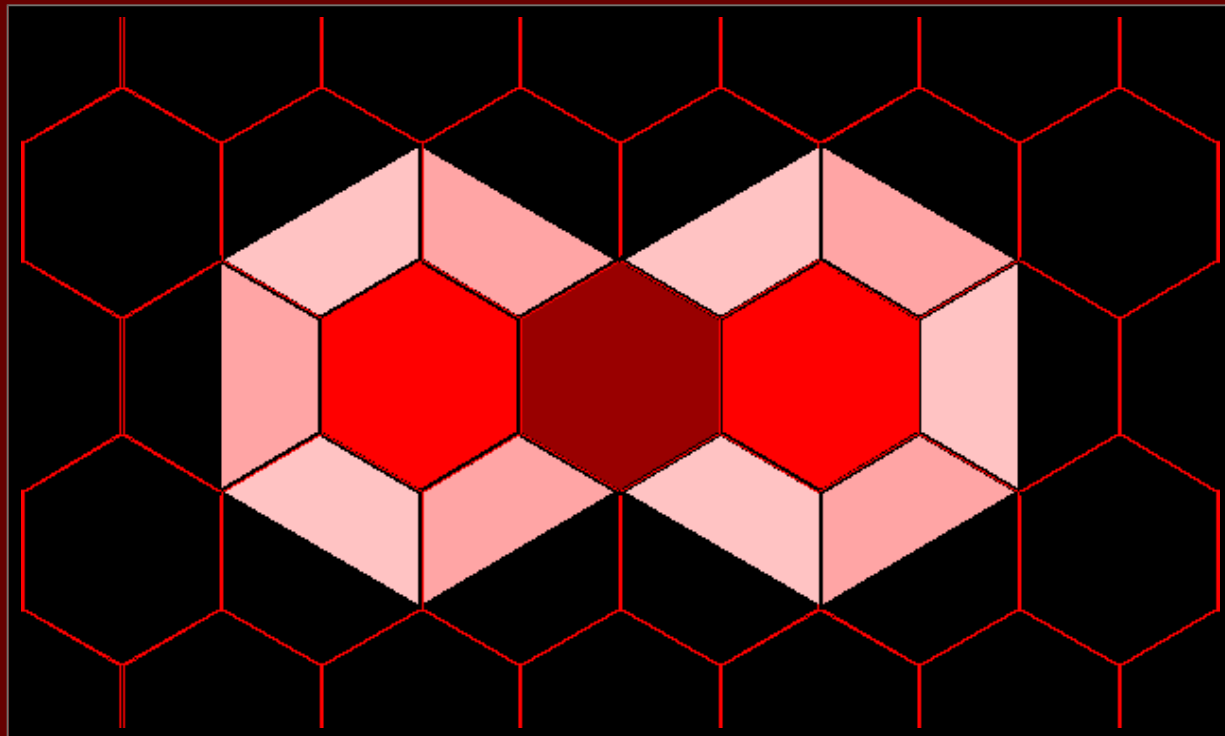
Spatial Synthesis: An eBook Series

[Sandra Lach Arlinghaus]() and [William Charles Arlinghaus]()

Volume I: Centrality and Hierarchy
Book 1: Regular Lattices, Geometry, and Number Theory.

powered by [FreeFind]()

[About the Authors]()
[Acknowledgments]()
[Dedication]()

[Download Cosmo Player (free) Browser Plug-in for interactive virtual reality]().
[Link]() showing more detail on how to use Cosmo Player.

Possible Future Volumes
Proposed topics for future volumes of Spatial Synthesis, as invited in
Solstice: An Electronic Journal of Geography and Mathematics,
Volume XIII, Number 2, Winter 2002
(http://www.InstituteOfMathematicalGeography.org).
Volume I; Centrality and Hierarchy (Books 2, 3,…)
Volume II: Distance and Geodesic
Volume III: Adjacency and Connection
Volume IV: Minimax, Absolute/relative, and Density
Volume V: Scale, Orientation, and Dimension
Volume VI: Partition, Separation, and Diffusion
Volume VII: Transformation and Symmetry

Institute of Mathematical Geography. Copyright, 2005, held by authors.

Spatial Synthesis: Centrality and Hierarchy, Volume I, Book 1.

Sandra Lach Arlinghaus and William Charles Arlinghaus

Institute of Mathematical Geography. Copyright, 2005, held by authors.

Spatial Synthesis: Centrality and Hierarchy, Volume I, Book 1.

Sandra Lach Arlinghaus and William Charles Arlinghaus

Introduction

The brain is wider than the sky,
For put them side by side;
The one the other will include,
With ease, and You beside.

Emily Dickinson

Synthesis begins with a global view and dissects that view to consider individual components, as they contribute to that whole: the whole is often more than the sum of the individual parts considered. In contrast, analysis often begins with a sequence of local views and assembles a global view from these, as a sum of parts: the assembled view may or may not fit "reality." These two different approaches to scholarship yield different results and employ different tools.   In this work, we take a synthetic approach to looking at real world issues that have mathematics as a critical, but often unseen, component. This approach permits one, also, to learn the associated mathematics as it naturally unfolds in real world settings, often in a relatively "painless" manner. The reader learns mathematics required to consider the broad problem at hand, rather than learning mathematics according to the determination of a (perhaps) artificial curriculum. The underlying philosophy is different, as is the format. The eBook is required, however, given the interactive and animated features that enliven the book and motivate the reader to explore diverse realms in the worlds of geography and mathematics and in their interface.

Figure 0.1 offers an abstract view of the idea of "spatial synthesis." Each large hexagon represents a single scholarly discipline: mathematics on the left and geography on the right (as an example). A single field (geometry, for example) is identified (deep red trapezoid) from one the broad discipline of mathematics, and is aligned with a counterpart (deep red trapezoid) field (cartography) from the other broad discipline of geography. Despite the alignment of appropriate entities, a gap remains. In institutional settings reliant on predetermined disciplinary boundaries, interdisciplinary research often founders in this gap for lack of support of various kinds. What is required, therefore, is to seal the gap and to unify aligned, related structure (represented as a single deep red hexagon formed from two trapezoids in Figure 0.1).
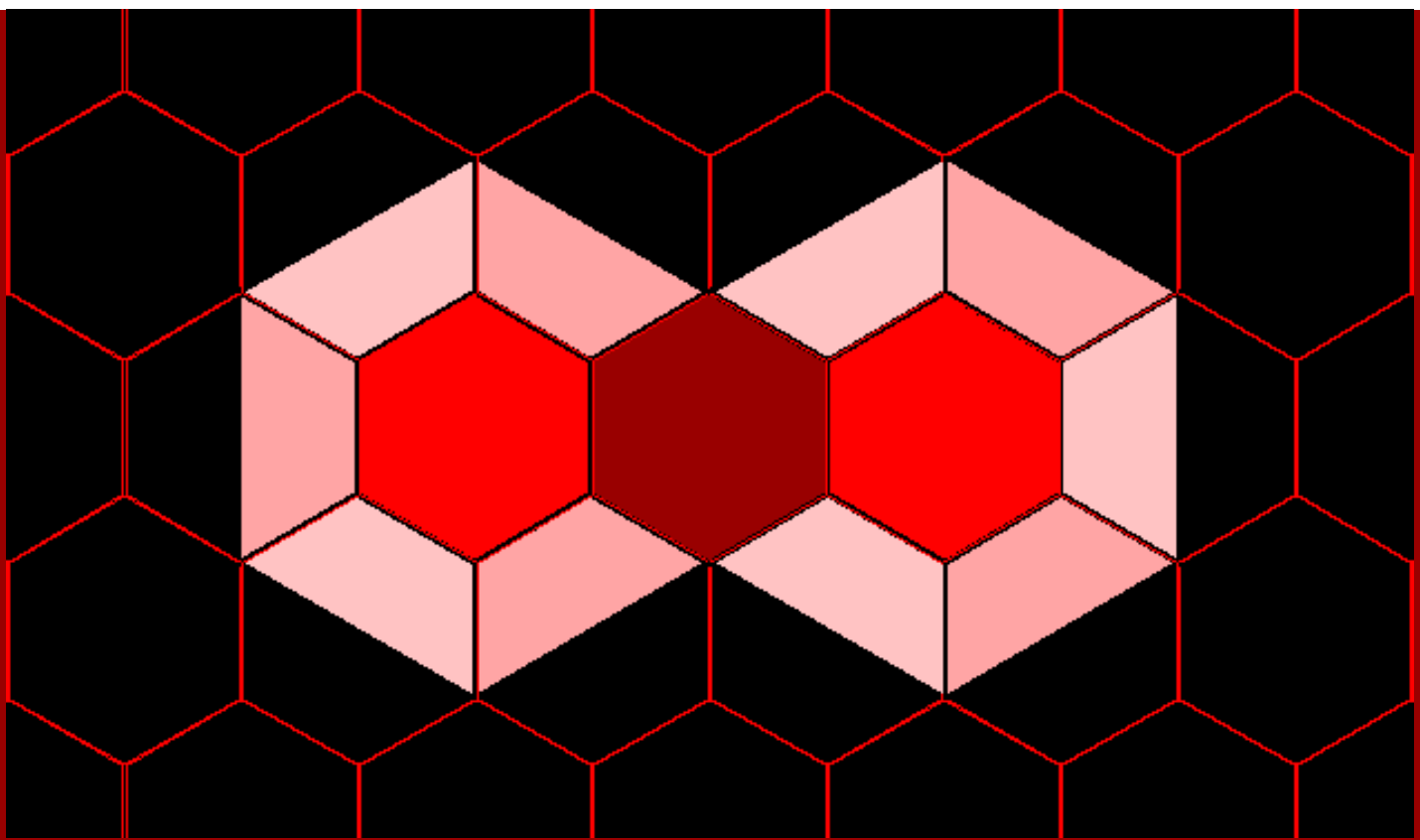
Figure 0.1. Spatial synthesis: abstract representation.

One well known classical approach to this style of scholarship appears in the work of Eratosthenes of Alexandria (c. 276-194 B.C.). Eratosthenes made critical discoveries in both mathematics and geography that might seem unrelated. His prime number sieve (see Chapter 3 of this work for more detail) permitted the complete characterization of all whole numbers and offered, therefore, an understanding of the whole number system. The idea of understanding a whole, that one could never see, also applies to his measurement of the circumference of the Earth. In his role as Librarian of the great library of Alexandria, he had access to works of his many outstanding predecessors. He worked with spherical geometry, latitude and longitude, earth-sun relations, and a variety of geometric and trigonometric ideas. Eratosthenes sealed the gap between number theory and the real world with the idea of using abstract tools to understand more than what one could see, be that an infinity of whole numbers or an Earth larger than a hometown; his brain was wider than his sky.

The astonishing scholarship of Eratosthenes serves as a model, in a variety of ways, for this effort. The body of the text draws from disciplines in pure mathematics and aligns them with real world material. The underlying mathematics is critical to the effort. Beyond the synthesis of apparently disparate disciplines, however, is the model of Eratosthenes the librarian. In our present world, each of us is an amateur librarian in the great virtual library of the Internet. Direct access to materials from all over the world is available on our desktops. Thus, where possible, we assemble a subset of this library in this electronic book. The eBook, itself, serves therefore not only as an interactive forum employing state-of-the-art techniques for communicating scientific information, but also as a library on the topic it covers. Thus, we dedicate this effort to the spirit of Eratosthenes of Alexandria: may his research strategy endure for many more millennia!

Spatial Synthesis: Centrality and Hierarchy, Volume I, Book 1.

Sandra Lach Arlinghaus and William Charles Arlinghaus

Chapter 1
Classical Central Place Hierarchies: A Real World View

eHighlights of this Chapter
Animated central place hierarchies: global view and sequence of local views
Java Applet representations of hierarchies
Virtual reality representation of sample point hierarchies (requires Cosmo Player or Cortona)
The evidence of historical maps cast in the current technological setting

___

Circular regions surrounding lattice points

A scatter of points, spread evenly across the plane, may take on a variety of configurations. If one wishes to consider circular buffers around each point, then these buffers may overlap or be widely spaced. The space between buffers, in the background behind them, is interstitial space separating buffers. A natural issue to consider is to minimize interstitial space and provide some sort of maximal coverage of the plane by the buffers: to provide a "close packing" of the plane by circles.

Two close packings of the plane with circles of identical radius are shown in Figure 1.1: one with circles centered on a square lattice and the other with circles centered on a triangular lattice.
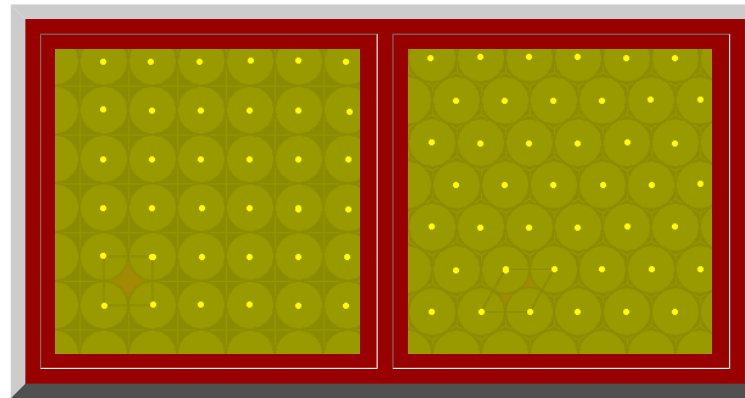

Figure 1.1 left, right. Animation shows square and triangular lattices in the plane and associated close packings with circles of identical radius. (Source of base image, no longer present at the cited url:http://www. psc.edu/~burkardt/src/graph_paper/graph_paper.html graph paper showing grid, triangular and hexagonal regions, John Burkardt, Pittsburgh Supercomputing Center, Carnegie Mellon University, University of Pittsburgh.).

It is a straightforward matter to calculate the interstitial space between circles associated with a square of side x in the square lattice and a corresponding parallelogram of side x in the triangular lattice. The radius of the circles in each figure is therefore x/2 and the area of the circles pi*x^2/4. Figure 1.2 shows a calculation of interstitial space: there is less interstitial area, between circles, within the parallelogram than there is within the square. Extrapolating this idea across the plane, one imagines naturally that the close packing of circles on the triangular lattice is denser than is the close packing of circles on the square lattice.

Side of length x, both square and parallelogram. Radius of any circle is x/2.

Area of any circle is pi*x^2/4

Red Area = area of square with four one-quarter circular sectors subtracted out = area of square with one full circular area subtracted out.
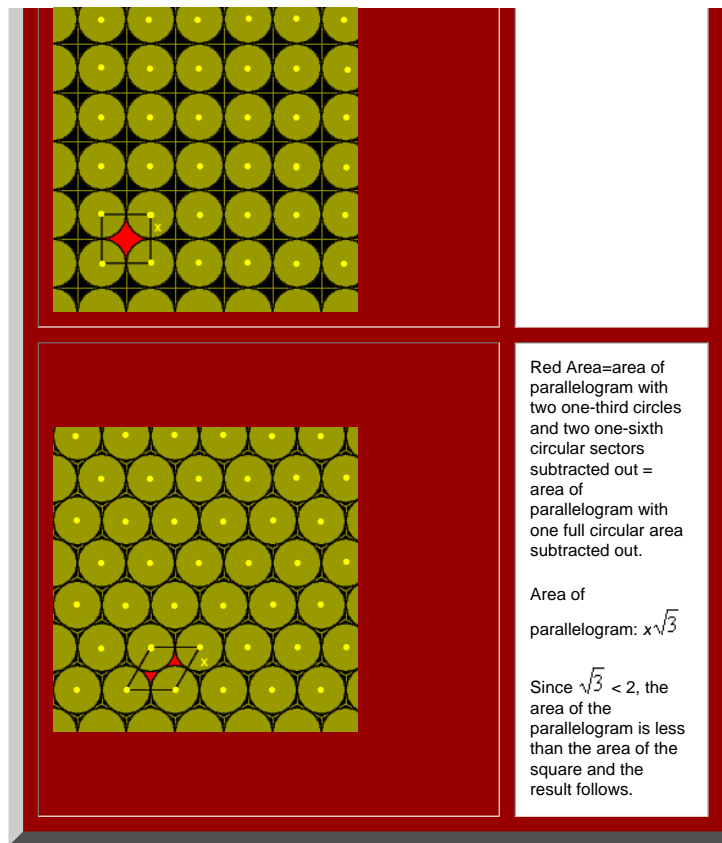
Area of square: x^2

Red Area=area of parallelogram with two one-third circles and two one-sixth circular sectors subtracted out = area of parallelogram with one full circular area subtracted out.

Area of parallelogram: $x\sqrt{3}$

Since $\sqrt{3} < 2$, the area of the parallelogram is less than the area of the square and the result follows.

Figure 1.2. There is less interstitial area between circles within the parallelogram than there is between circles within the square. (Source of base image, no longer present at the cited url:http://www.psc.edu/~burkardt/src/graph_paper/graph_paper.html graph paper showing grid, triangular and hexagonal regions, John Burkardt, Pittsburgh Supercomputing Center, Carnegie Mellon University, University of Pittsburgh.).

This chain of reasoning indicates that the close packing of the plane by circles of identical radius is denser for a triangular lattice than it is for a square lattice. Gauss (1831) proved that, in fact, the densest lattice packing of the plane is the one based on the triangular lattice. In 1940, Fejes-Toth proved that that same packing is not only the densest lattice packing of the plane but is also the densest of all possible plane packings.

If one thinks, then, of the circles as if they were bubble-foam, the circles centered on a square grid pattern expand and collide to form a grid of squares (suggested in the top figure in Figure 1.2). The circles centered on a triangular grid pattern expand and collide to form a mesh of regular hexagons (suggested in the bottom figure in Figure 1.2). Because the close packing of circles centered on points spaced in a triangular grid is the densest possible close packing of the plane, the space-filling pattern of hexagonal cells associated with that packing also possesses unique character. If one were to enter a square or triangular grid into Geographic Information System software, and ask the software to calculate Thiessen polygons the grid of square cells would emerge from the square lattice and the grid of hexagonal cells would emerge from the triangular lattice. Thus, these cells can arise in a number of technical ways.

The theoretical issues surrounding tiling in the plane are complex; even deeper are those issues involving packings in three dimensional space. We confine our interest in that matter to simply illustrating Gauss's methods and stating Fejes-Toth's extension of it. The reader interested in probing this topic further is referred to the references. Interpretation of the simple triangular grid has range sufficient to fill this volume and more.

Basic assumptions

One classical interpretation of what dots on a lattice might represent is found in the geometry of "central place theory." Readers interested in the development of this theory, over time and with regard to a clear understanding of who did what and when it was done, are referred to the references. We simply present some of the ideas in order to focus on the geometry. Geometric central place models take the complex human process of urbanization and look at it in an abstract theoretical form in order to uncover principles which might endure despite changes over time, situation, cultural tradition, and all the various

human elements that are truly the hallmarks of urbanization. Simplicity helps to reveal form: models are not representations of reality. They do, however, offer a way to look at some structural elements of complexity. Thus, consider dots on a triangular lattice as populated places (often, villages). Circles, expanding into hexagons, are areas that are tributary to the populated places. In the traditional formulation (described after Kolars and Nystuen) one considers four basic postulates (no one of which is "real" but each of which is simple):

- The backdrop of land supports uniform population density
- There is a maximum distance that residents can easily penetrate into the tributary area (often called "maximum range").
- There is slow, steady population growth
- Village residents who move, as a result of growth (or for other reasons), attempt to remain in close contact with their previous location (to maintain social or other networks).

Suppose, in a triangular lattice of villages, that one village adds to its retailing activities. After some time, growth occurs elsewhere. How might other villages compete to serve tributary areas: how will the larger, new villages share the tributary area? The answers lead to a surprising number of possible scenarios. Figure 1.3 shows the first in an infinite number of possibilities. Animated locations, for competing larger villages, are shown in Figure 1.3. The smallest villages are represented as small red dots; next nearest neighbors competing for intervening red dots are represented in blue; and, next nearest neighbors competing for intervening blue dots are represented in green. Of course, one is usually only willing to travel so far to go to a place only slightly larger, so the fact that the animated pattern could be extended to an infinite number of levels, beyond green, may not mirror the second postulate. Over time, however, one might suppose further growth and an entire hierarchy of populated places.
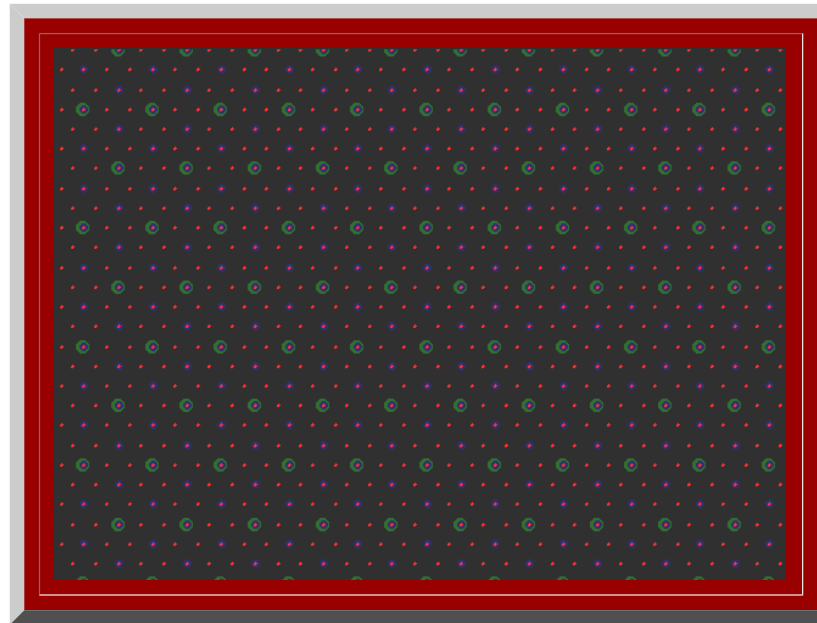

Figure 1.3. A triangular lattice of dots with animated locations for competing locations entering and vanishing from the picture.

Such a view of growth leads to another set of assumptions (after Christaller).

- The underlying market is spread evenly across an abstract geographic plane
- The underlying, discrete population is evenly spread
- There is a set of central place activities which reflects willingness to travel.

Within these added constraints, there are some embedded assumptions, as well. In particular, central place activities are viewed as themselves occupying no space: an important point in terms of retaining simplicity of form in order to look at structure. The problems of industrial location or of site plans for commercial activity are complex and important issues in themselves; however, they serve to obfuscate what is under consideration here. Hence, these complex activities are assumed to occupy mere points. Further, there is embedded the idea of a natural hierarchy of central place activities: that one might be willing to travel to get to a strip mall 5 miles away for routine shopping but for greater activities and service would be willing to travel

30 miles to a regional mall that offers all the goods and services of the smaller mall plus additional ones. These ideas are further elaborated in the following four points.

- The population of each location is a function of the number of goods and services it offers.
- The central place system is a closed system
- Each central place offers all goods and services offered by lower order places plus added ones: the number of central places in the system is therefore, in some sense, optimal
- Communication within the central place system is perfect.

With these postulates and added constraints in mind, we examine the geometric configurations that are classically identified as central place hierarchies. These are Walter Christaller's view in looking for pattern from the broad to the particular; in interpreting these ideas, however, we present the characterization of August Lösch, in working from the small to the large, as a synthesis of conceptual material.

Marketing principle: *K*=3

Consider a central place point, *A*, in a triangular lattice (Figure 1.4). Unit hexagons (fundamental cells) surround each of the points in the lattice and represent the small tributary area of each village (red hexagons in Figure 1.5a). Growth at *A* has distinguished it from other villages in the system. It will now serve a tributary area larger than will the unit hexagon. There are six villages directly adjacent to *A*. The unit hexagons represent a partition of area based on even sharing of area between *A* and these six villages. When *A* expands its central place activities, others may also desire to do so as well. Figure 1.4 shows the locations for the next nearest competitors, such as A' in blue, to enter the system. Given that they, too, will share area evenly, a set of larger hexagons emerges (blue hexagons in Figure 1.5a). The competitors that enter are spaced at a

distance, in terms of lattice points spaced one unit apart, of $\sqrt{3}$ units (Figure 1.4). The position of the competitors that enter the system in this scenario are as close as possible to *A*; expansion of goods and services at any of the six closest neighbors would constitute no change in basic pattern. One might imagine, therefore, that emphasis on distance minimization optimizes marketing capability--distance to market is at a minimum. Figure 1.5a shows the unit hexagons and the larger hexagons based on expansion of goods and services. To get a view of a large scatter of dots, arranged according to this idea, consider the linked virtual reality model. Use the Viewpoints to see an overview and a closeup; drive through it on your own.
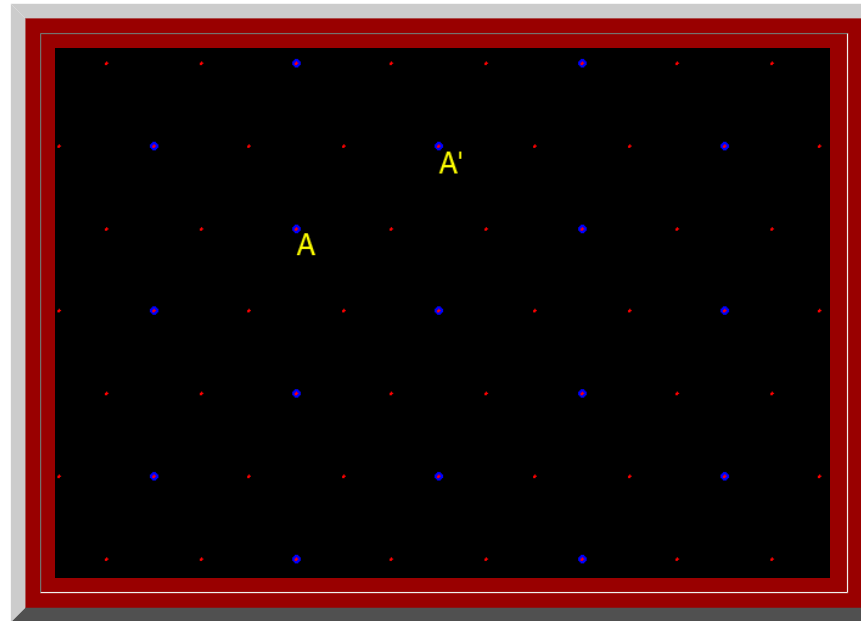

Figure 1.4. *K*=3: Marketing. Distance measurement between adjacent competing new centers, *A* and *A'*: in

this case, competing centers, blue dots, are spaced $\sqrt{3}$ units apart, assuming a distance of one unit between adjacent red dots.

Thus, when competitors are chosen in this manner, the pattern of one layer of hexagons, in relation to another, has become known as a hierarchy arranged according to a "marketing principle" (Figure 1.5a). Notationally, it is captured by the square of the distance between competing centers: as a "*K*=3" hierarchy (Figure 1.4). Each large hexagon contains the equivalent of three smaller hexagons. One large hexagon = 1 small hexagon

+ six copies of 1/3 of a small hexagon = 3 small hexagons (Figure 1.5b, c, and d). Thus, the value K=3 is not only related to distance between competing centers but also to size of tributary areas generated by competition: as a constant of the hierarchy.
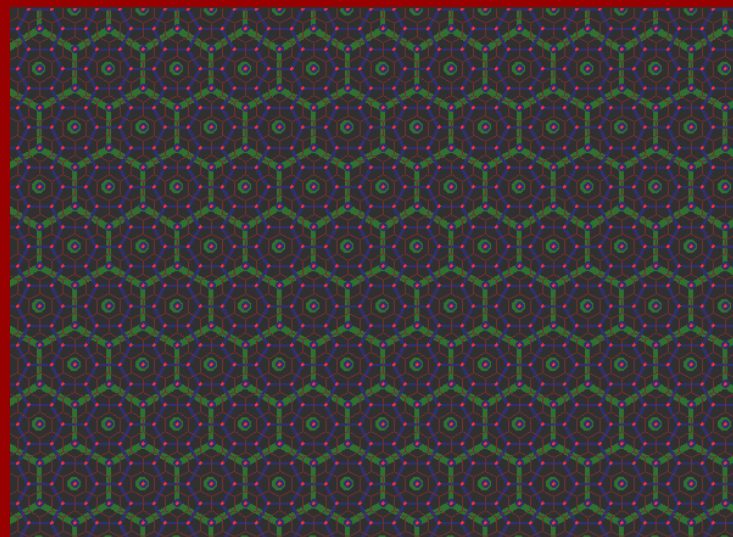

Figure 1.5a. K=3 hierarchy showing three layers of a nested hierarchy of hexagons of various sizes oriented with respect to one another according to the distance principle illustrated in Figure 1.4.
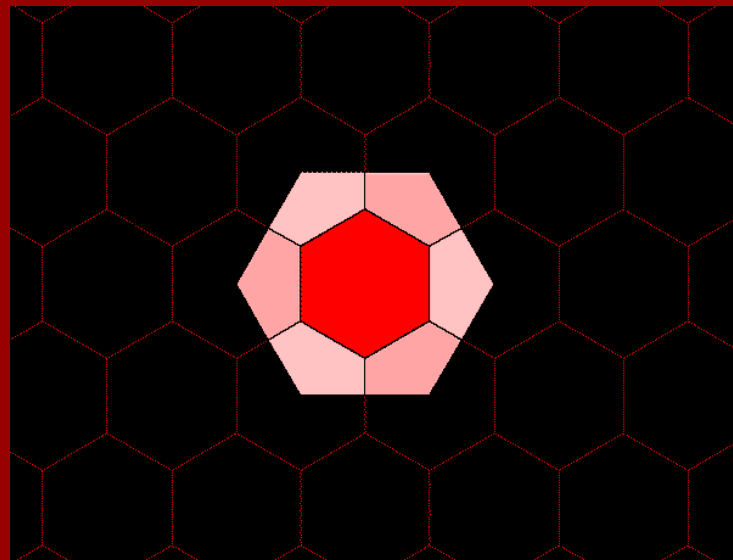

Figure 1.5b. Each blue hexagon contains the equivalent of three red hexagons: one entire red hexagon surrounded by six copies of 1/3 of a red hexagon.
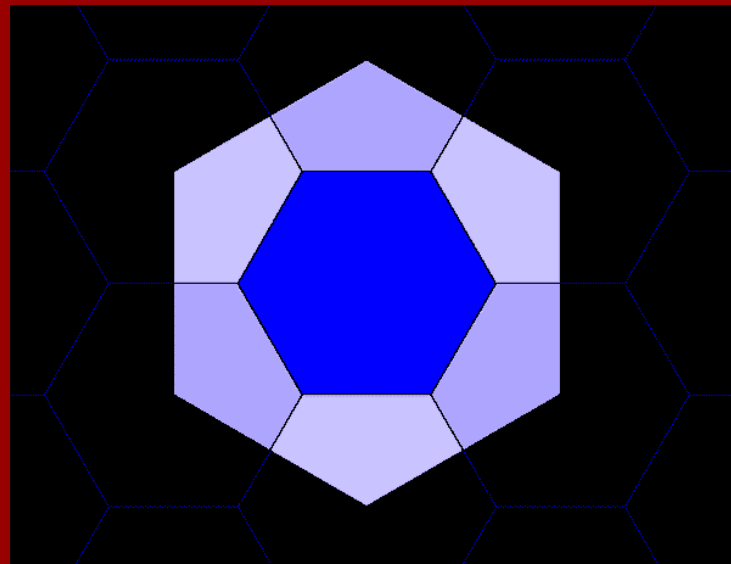
Figure 1.5c. Each green hexagon contains the equivalent of three blue hexagons: one entire blue hexagon surrounded by six copies of 1/3 of a blue hexagon.
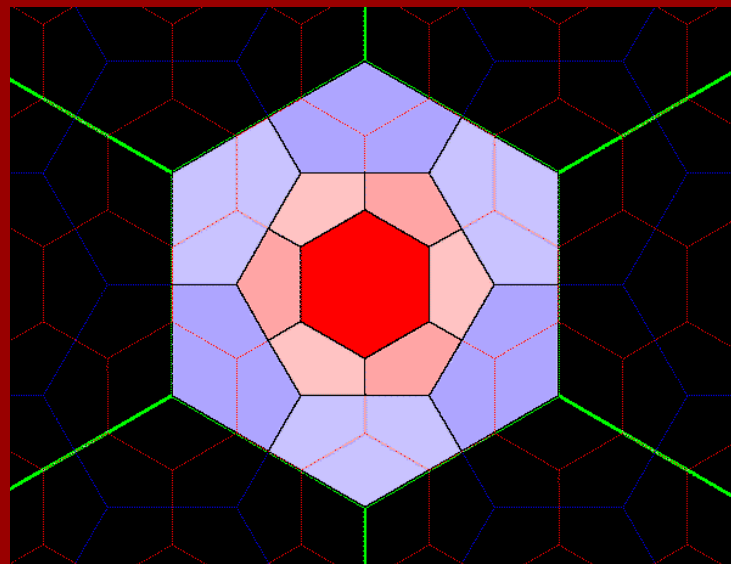

Figure 1.5d. The green hexagons contain the equivalent of 3^1 blue hexagons and 3^2 red hexagons.

Figure 1.5.
Back to Chapter 2 *K*=3 reference.

Transportation principle: *K*=4

Figure 1.6 shows the locations for the next nearest competitors, next beyond those from *K*=3, to enter the system. Given that they, too, will share area evenly, a set of even larger hexagons emerges. Figure 1.7a shows the unit hexagons and the larger hexagons based on expansion of goods and services. The competitors that enter are spaced at a distance, in terms of lattice points spaced one unit apart, of 2 units

(Figure 1.6). The position of the competitors that enter the system in this scenario lie along radials that fan outward from *A* and pass along existing boundaries to tributary areas. One might imagine, therefore, that emphasis on market penetration, or transportation, is the focus here. To get a view of a large scatter of dots, arranged according to this idea, consider the linked virtual reality model. Use the Viewpoints to see an overview and a closeup; drive through it on your own.
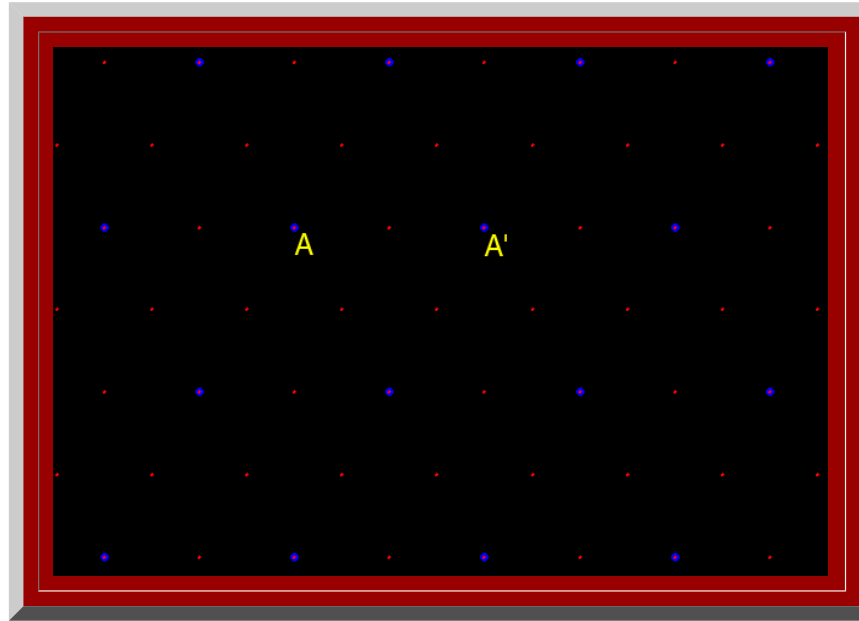

Figure 1.6. *K*=4: Marketing. Distance measurement between adjacent competing new centers, *A* and *A'* is 2 units, in this case (assuming a distance of 1 unit between adjacent red dots).

Thus, when competitors are chosen in this manner, the pattern of one layer of hexagons, in relation to another, has become known as a hierarchy arranged according to a "transportation principle" (Figure 1.7a). Notationally, it is captured by the square of the distance between competing centers: as a "*K*=4" hierarchy (Figure 1.6). Each large hexagon contains the equivalent of four smaller hexagons. One large hexagon = 1 small hexagon + six copies of 1/2 of a small hexagon = 4 small hexagons (Figure 1.7b, c, d). Thus, the value *K*=4 is not only related to distance between competing centers but also to size of tributary areas generated by competition--as a constant of the hierarchy.
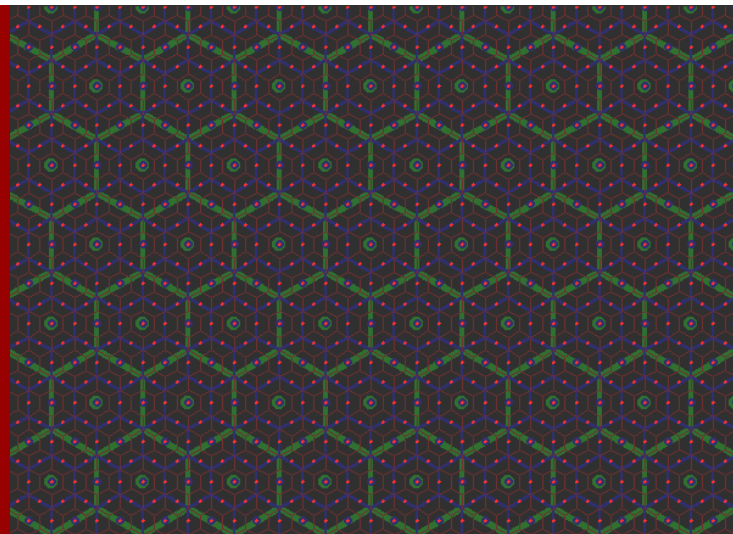
Figure 1.7a. *K*= 4 hierarchy showing three layers of a nested hierarchy of hexagons of various sizes oriented with respect to one another according to the distance principle illustrated in Figure 1.6.
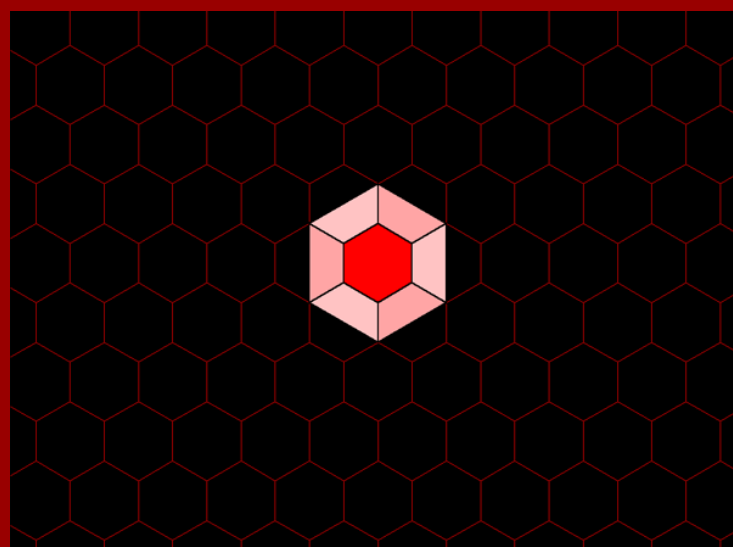

Figure 1.7b. Each blue hexagon contains the equivalent of four red hexagons: one entire red hexagon surrounded by six copies of 1/2 of a red hexagon.
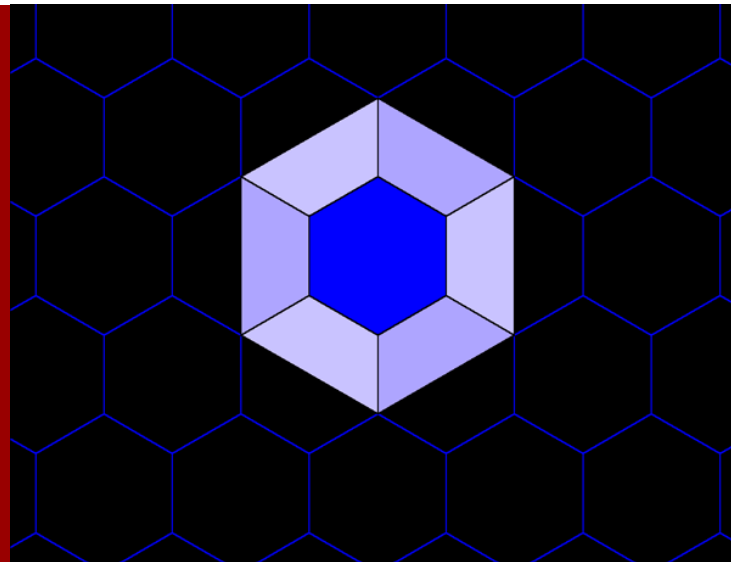
Figure 1.7c. Each green hexagon contains the equivalent of four blue hexagons: one entire blue hexagon surrounded by six copies of 1/2 of a blue hexagon.
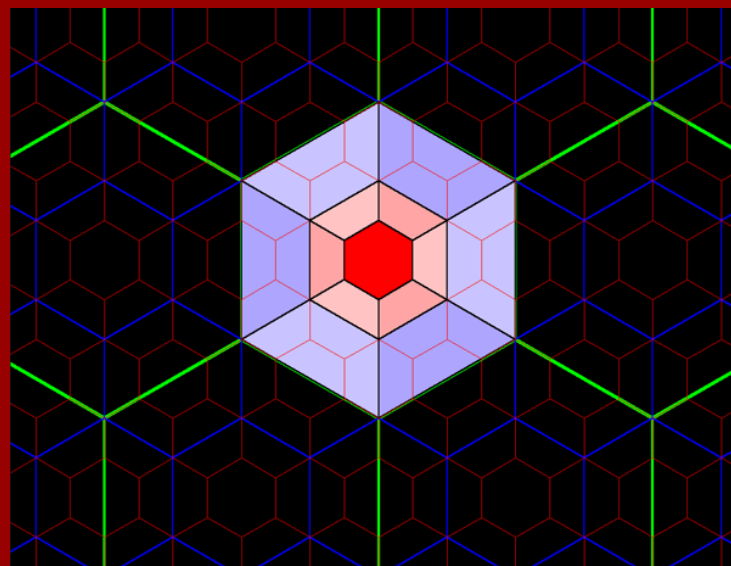

Figure 1.7d. The green hexagons contain the equivalent of 4^1 blue hexagons and 4^2 red hexagons.

Figure 1.7.

Administrative principle: *K*=7
Figure 1.8 shows the locations for the next nearest competitors, next beyond those from *K*=4, to enter the system. Given that they, too, will share area evenly, a set of even larger hexagons emerges. Figure 1.9a shows the unit hexagons and the larger hexagons based on expansion of goods and services. The

competitors that enter are spaced at a distance, in terms of lattice points spaced one unit apart, of $\sqrt{7}$ units (Figure 1.8). The position of the competitors that enter the system in this scenario create larger hexagons

whose boundaries pass through very few other populated places: hence, top-down control, or rule from the center is emphasized. One might imagine, therefore, an emphasis on administrative control here. To get a view of a large scatter of dots, arranged according to this idea, consider the linked virtual reality model. Use the Viewpoints to see an overview and a closeup; drive through it on your own.

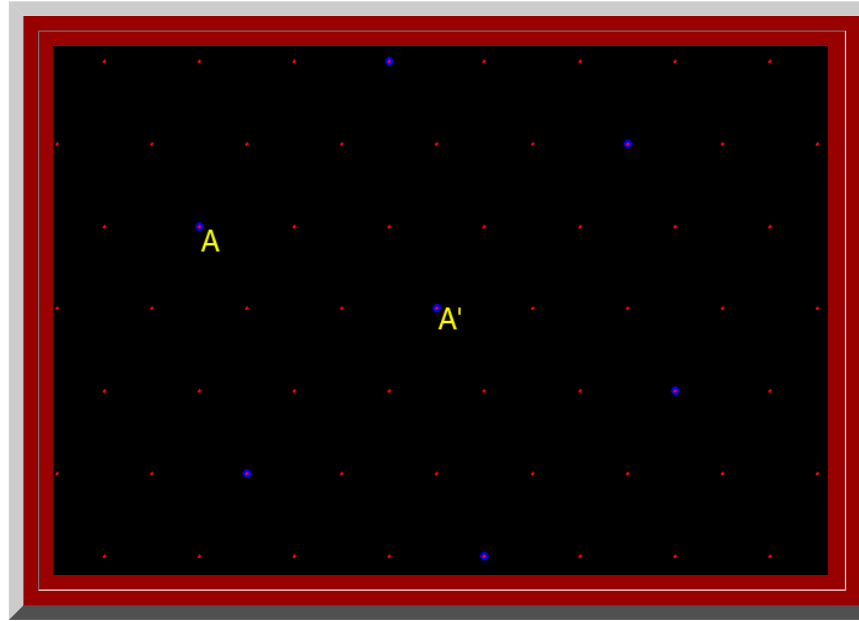**Figure 1.8.** *K*=7: Marketing. Distance measurement between adjacent competing new centers, *A* and *A'* is $\sqrt{7}$ (assuming a distance of 1 unit between adjacent red dots).

Thus, when competitors are chosen in this manner, the pattern of one layer of hexagons, in relation to another, has become known as a hierarchy arranged according to an "administration principle" (Figure 1.9a). Notationally, it is captured by the square of the distance between competing centers: as a "*K*=7" hierarchy (Figure 1.8). Each large hexagon contains the equivalent of seven smaller hexagons. One large hexagon = 1 small hexagon + six copies of a small hexagon (underfit and overfit regions balance) = 7 small hexagons (Figure 1.9b, c, d). Thus, the value *K*=7 is not only related to distance between competing centers but also to size of tributary areas generated by competition--as a constant of the hierarchy.
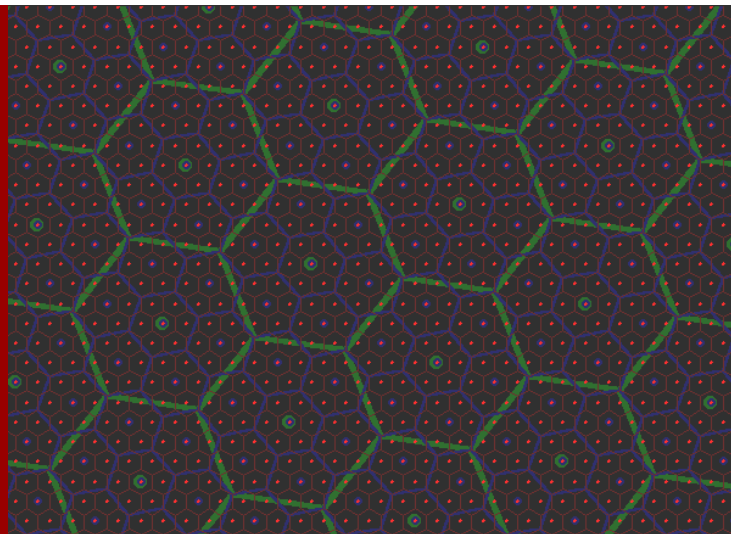
Figure 1.9a. *K*= 7 hierarchy showing three layers of a nested hierarchy of hexagons of various sizes oriented with respect to one another according to the distance principle illustrated in Figure 1.8.
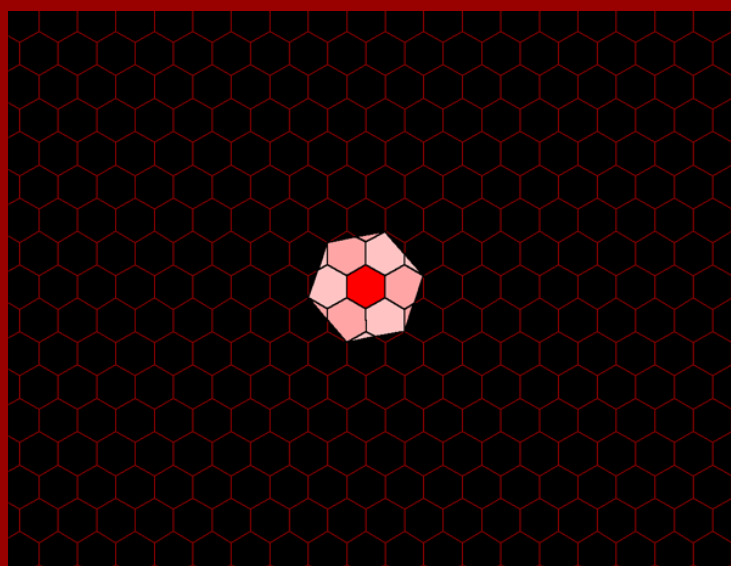
Figure 1.9b. Each blue hexagon contains the equivalent of seven red hexagons: one entire red hexagon surrounded by six copies equivalent to a single red hexagon. Each of the perimeter red hexagons is composed of 11/12 of a single red hexagonal cell plus 1/12 of an adjacent red cell: in an underfit/overfit pattern.
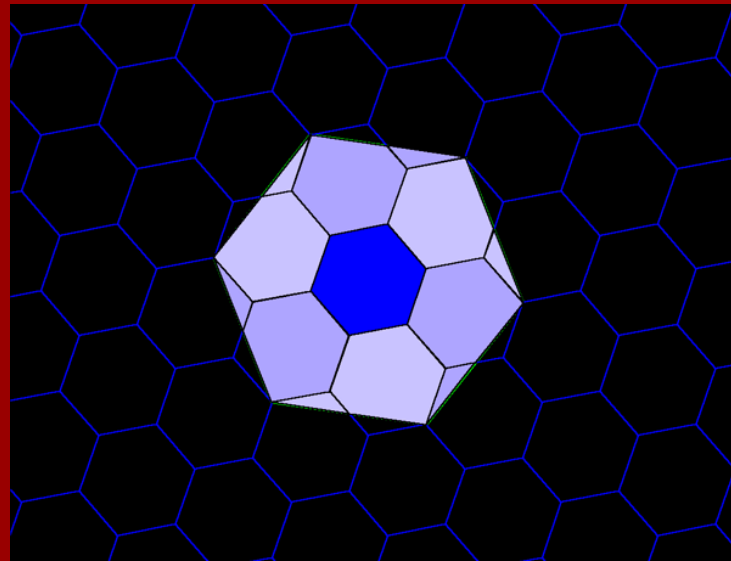
Figure 1.9c. Each green hexagon contains the equivalent of seven blue hexagons: one entire blue hexagon surrounded by six copies equivalent to a single blue hexagon. Each of the perimeter blue hexagons is composed of 11/12 of a single blue hexagonal cell plus 1/12 of an adjacent blue cell: in an underfit/overfit pattern.
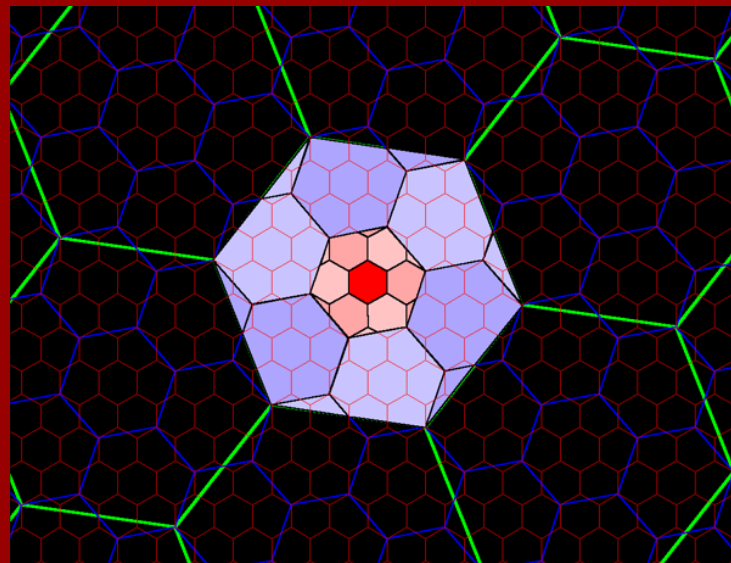

Figure 1.9d. The green hexagons contain the equivalent of 7^1 blue hexagons and 7^2 red hexagons.

Figure 1.9.

A tiled view of each hierarchy: mechanics of construction
The process of creating larger hexagons, as larger tributary areas representing expanded central place activities, can be carried out indefinitely. The set of figures above (1.5, 1.7, and 1.9) shows the general patterns that emerge and underscores, particularly, the importance of the constant of the hierarchy.

Large hexagons in one layer contain the equivalent of K^1 hexagons of the next smallest size within them; they contain the equivalent of K^2 hexagons from the level two layers down in the hierarchy, and so forth. The K value is an invariant of each geometric hierarchy that uniquely characterizes it. The mathematical search for invariants as bench marks against which to view abstract structure is equivalent to the geographical search for bench marks in the field (physical or human) against which to view mapped, spatial structure.

Virtual reality central place skylines

The initial conditions from the real world may suggest building a hierarchy from small hamlets to large cities, in the style of Christaller, or they may suggest the reverse, in the style of Lösch (or any of an infinite number of possibilities in between--we confine ourselves to the extremes). Independent of such choice, however, the resulting geometry is identical: a pattern of hexagons of various sizes, dependent on spacing between competing centers at a given hierarchical level, is the result. To see the different initial patterns of dots, and to move them around on the screen, it is useful to capture the dot patterns above as virtual reality scenes. Animation of successive virtual reality scenes, as a sequence of screen captures of the scene from various vantage points, offers the reader a chance to examine closely the three different styles of initial dot scatter used to create the geometries of hexagons associated with $K=3$, $K=4$, and $K=7$.

   The linked figures, Figures 1.L1 (derived from Figure 1.5), 1.L2 (derived from Figure 1.7), and 1.L3 (derived from Figure 1.9), offer a view of central place $K=3$, $K=4$, and $K=7$ landscapes as central place skylines in virtual reality. Links to each of these were given above, as they developed. Here, we simply accumulate the set in one set of links near each other for ease in making comparisons. Load CosmoPlayer and click on the links to drive through these landscapes and experience them as if the higher order central places represent taller urban structures, such as cell towers or other dominant skyline features. Figure 1.10 shows each of these virtual reality models, from the vantage point of "entry," as animated screen capture so that one might readily compare the three hierarchies. Figures 1.11 and 1.12 show similar animations, for purposes of comparison of pattern among $K=3$, $K=4$, and $K=7$, from the vantage point of "Overview" and "Close Up" respectively. Movies of these animations permit the reader to control the animation frame rate: Movie of 1.10, movie of 1.11, and movie of 1.12. (If the horizontal scroll bar does not show at the bottom of the linked image, expand your browser to show the full screen: in Microsoft Internet Explorer, for example, hit the F11 key.) In the next chapter, we use virtual reality to take a closer look at the geometry of these hierarchies; thus, it is worth the effort now to load the plug-in and to practice virtual navigation in a simple landscape.
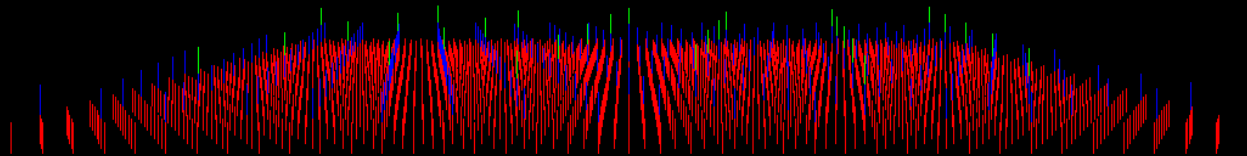
Entry View, K=7

Figure 1.10. *K*=3, *K*=4, and *K*=7 hierarchies animated as viewed from the "entry" viewpoint of associated virtual reality models.

Overview, K=7

Current Viewpoint
[Page Up] Return to this viewpoint.
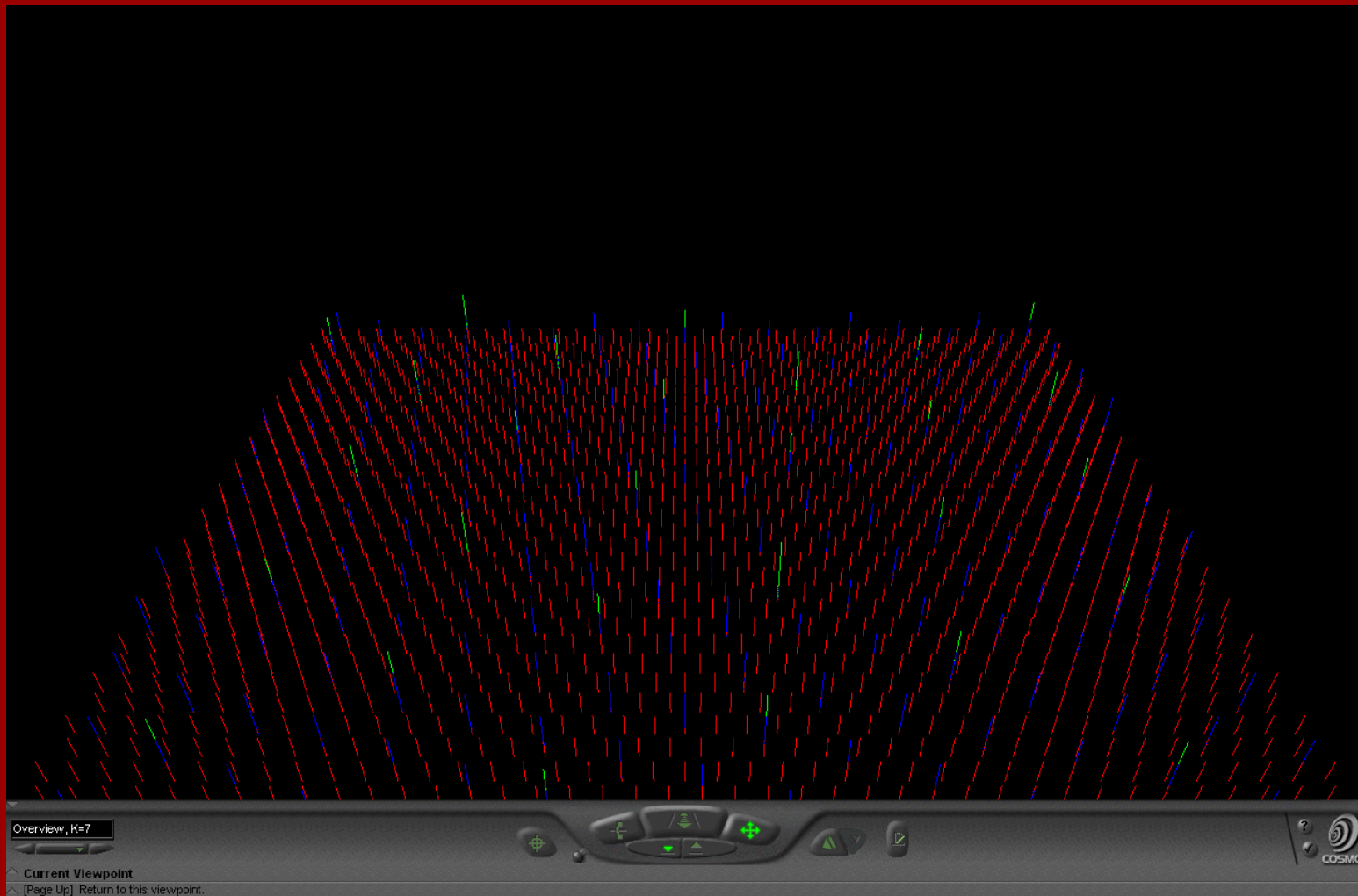
Figure 1.11. *K*=3, *K*=4, and *K*=7 hierarchies animated as viewed from the "overview" viewpoint of associated virtual reality models.
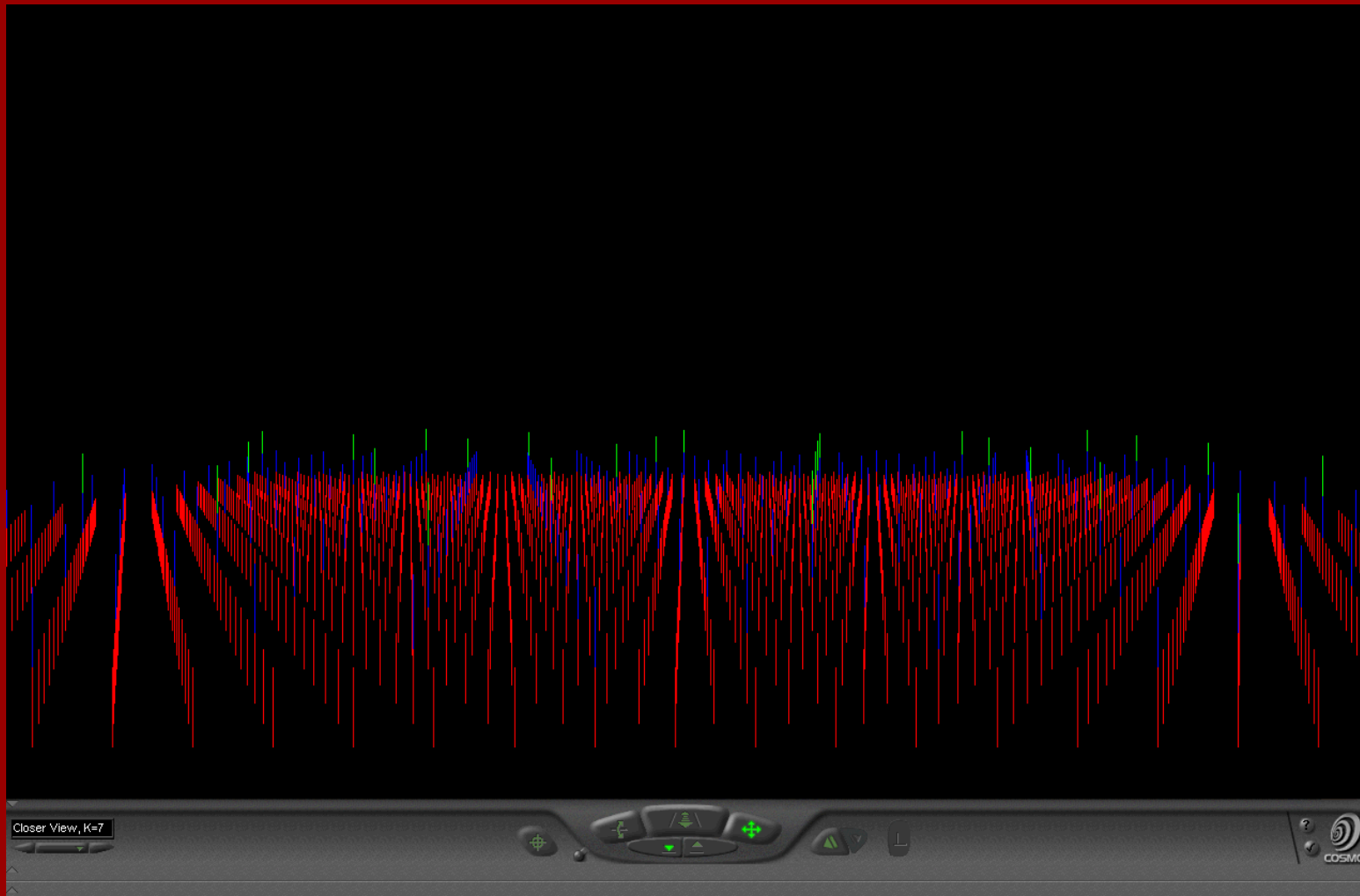
Figure 1.12. *K*=3, *K*=4, and *K*=7 hierarchies animated as viewed from the "close up" viewpoint of associated virtual reality models.

Mapplets

Another method, that is available only in current technology, for looking simultaneously at connection patterns between multiple layers of central place networks involves capturing them as Java (TM) Applets: as "Mapplets." This process also suggests some sort of stability of the geometric structure: the mapplet reflects stability in structural form. Shake the mapplet; it settles down to the expected hierarchy. Pull the mapplet; still it settles down to the underlying hierarchical form. One might speculate about real-world forces that pull on mathematical form: the form endures.
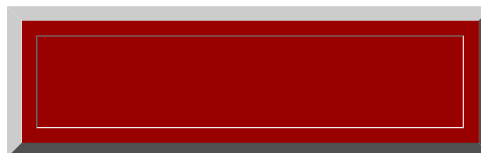
Figure 1.13. *K*=3 Mapplet
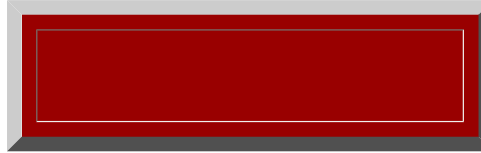
Figure 1.14.*K*=4 Mapplet
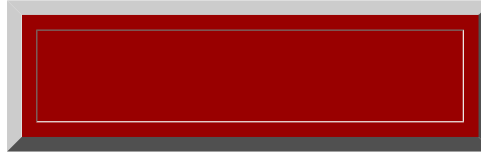
Figure 1.15. *K*=7 Mapplet

Mapplets focus on connection patterns between successive hierarchical layers and, when *K* values are loaded as distances between hierarchies, they also suggest some elusive form of structural stability of geometric form. Animated maps of the central place geometry of the plane, coupled with mapplets showing animated hierarchical pattern alone, suggest another sort of three dimensional view of central place geometry.

Central place hierarchies as Thiessen polygons

One difficulty with considering central place landscapes rests in their visualization. Slight errors in placement of points get magnified in overlay alignments. To create a meshed hierarchy in which overlays are aligned is a drafting task of substantial proportions, when done by hand. Geographic Information System software, however, offers an easy and accurate method of constructing central place landscapes at almost any level of complexity (up to the limits of hardware and software capability). Figures 1.4-1.9 were created using ArcView GIS (v. 3.2, ESRI). The method for creating GIS-generated central place landscapes employed the following steps:

- obtain as a base map a triangular lattice shape file; such a file may be created in ArcView using EdTools extension to precisely translate a point.
- ensure that each record in the underlying database has a unique code entered in "number" format (using the "add record number" feature of Animal Movement extension, if need be).
- if desired, create in a separate layer, a bounded region to serve as limits within which to calculate the landscape-- a rectangle, for example. One way to create such a region is to calculate the minimum convex polygon (convex hull) of the distribution of red dots using Home Range extension.
- load Spatial Analyst extension (ESRI) to ArcView and calculate Thiessen polygons using the Analysis| Assign Proximity command; choose the rectangle layer as the region within which to calculate the Thiessen polygons. Alternately, employ the same strategy using Home Range extension and calculate Dirichlet regions.
- The result will appear as a set of small hexagons surrounding the dots, as in the red layers in Figures 1.4-1.9.
- Repeat the procedure on other triangular lattices, with broader spacing of lattice points as in the blue and green points above, derived from the base lattice. The result will produce landscapes such as those in Figures 1.4-1.9 depending on how the broader spacing pattern is selected.

This strategy is simple to execute and straightforward to discover. Its importance, however, lies in its ease of use and its accuracy. Large environments can be created almost as easily as small ones and historical central place studies can be captured electronically. Indeed, central place studies done by hand can be checked and planning documents from the past can be recast as central place geometries.

Christaller and settlements in Central Europe

The map in Figure 1.16 shows Walter Christaller's sense of regional settlement planning in Eastern Europe. Harris and Berry, note in "Walter Christaller: An Appreciation," that central place theory served as the basis for settlement planning in Eastern Europe:

> "...Christaller's involvement in the tumultuous social movements that affected Germany profoundly influenced his life. Like many young Germans, he became aligned with left-wing causes during the 1920s, and later his work was used as the basis of Nazi settlement planning in Eastern Europe. As a result this gentle and kindly man was shunned politically by both East and West after World War II, even as he was being accorded belated recognition for his pioneering contributions to theoretical geography."

The first author contacted Harris directly, in writing and on the telephone, to find out more about the source of that statement. The linked letter shows one part of his fascinating answer. He also offers citations to appropriate documents to read. The map in Figure 1.16 is based directly on material from one of these sources.

In it, larger cities are spaced farther apart than are smaller ones. Towns and villages fill interstitial space. Surely

it must have taken Christaller much time and effort to construct this map. We have scanned it from a map in the 1941 reference and pieced together the scanned images. The scanning strategy was a multistep process because the map was quite large. First, 8.5 by 14 inch photocopies were made of the map in the book. It took 8 of those to capture the map, with overlap. Then, each piece was scanned at 600dpi on a flatbed scanner. The goal was to reassemble the scanned pieces on a canvas in Adobe Photoshop. File size of the 8 pieces prohibited such strategy and caused file oversize errors. Thus, each piece was reduced in size from 6900 pixels wide to 2000 pixels wide (preserving the aspect ratio). Then, each of these smaller images (smaller in physical size but not in resolution) was saved as a transparent .gif. The images with transparent backgrounds were then brought into Adobe Photoshop and assembled as a set of layers; use of transparency was important because it was only then that we could see how to fit the pieces together. To see an even larger version of this map (on which place names can be read easily), click here; the attached file is over 5 MB in size: scroll both horizontally and vertically to see the linked map.

DIE ZENTRALEN ORTE
IN DEN OSTGEBIETEN UND
IHRE KULTUR- UND MARKTBEREICHE

- • HAUPTDORF 600 EINW.
- ○ GEHOBENES HAUPTDORF 1 200 EINW.
- ● AMTSSTADTCHEN 3000 EINW.
- ◉ GEHOBENE AMTSSTADT (HEUTIGE KREISSTADT) 9000 EINW.
- ◎ KREISSTADT 30 000 EINW.
- ◉ GEHOBENE KREISSTADT 100 000 EINW.
- ◉ GAUHAUPTSTADT 450 000 EINW.

- ········· GRUPPENDORFGRENZE GEBIET : 2 500 EINW.
- ——— AMTSBEZIRKGRENZE GEBIET : 22 500 EINW.
- ——— KREISGRENZE GEBIET : 210 000 EINW.
- ▬▬▬ GAUGRENZE GEBIET : 2 700 000 EINW.

- · NEUGRÜNDUNG
- · ENTWICKELN AUF TYPISCHE GRÖSSE
- ^ ABWERTEN AUF TYPISCHE GRÖSSE

Walter Christaller

Figure 1.16. Walter Christaller's view of central places in Eastern Germany, 1941. Click on the map above to see a larger image.
(Source: Struktur und Gestaltung der Zentralen Orte des Deutschen Ostens, Gemeinschaftswerk im Auftrage der Reichsarbeitsgemeinschaft fur Raumforschung, Teil 1, Dr. Walter Christaller, Die Zentralen Orte in den Ostgebieten und ihre Kultur- und Marktbereiche, K. F. Koehler Verlag, Leipzig, 1941).

Digitize the original map.

One question that arises is, does the map drawn by Christaller, showing a plan for settlement in Eastern Europe, actually conform to a central place theory pattern as might be generated today? Preston (1992) notes that Christaller used an administrative hierarchy, as well as a mixed hierarchy, in creating plans for the east, mixing marketing, transportation, and administration/separation principles. A map of the sort above is complex. Current technology permits creation of geometric consideration of historical evidence.   It is a straightforward manner to digitize the dots set down by Christaller in different layers in a GIS according to assigned hierarchical level. Use of Thiessen polygons to create pattern is also simple to execute. Thus, when the image of Figure 1.16 was brought into Geographic Information System software, we separated the layers of dots as Christaller had suggested in the legend. The sizes of the colored dots in Figure 1.17 show an animated view of the seven levels of urban areas entering the system: from largest to smallest.
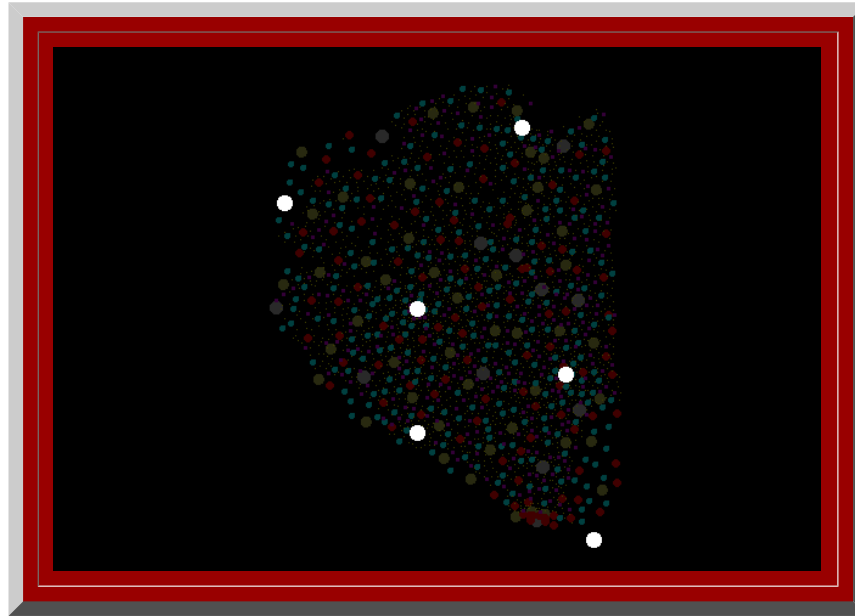
Figure 1.17. The central places of Figure 1.16 entered into a Geographic Information System.

Both the legend of Figure 1.16 and the animated map of Figure 1.17 suggest that all layers in this hierarchy are similar in nature. A closer look, however, at Figure 1.16 might see the first five layers as those with central place activities and see layers six and seven (the most rural) as working together to form a single, final layer that fills in between central places. No sixth or seventh layer places have links to subordinate places. Figure 1.18 shows those two most rural layers represented as a single layer as a scatter of yellow dots. These yellow dots are then analyzed using Thiessen polygons to create a cellular mesh that appears quite local in nature.
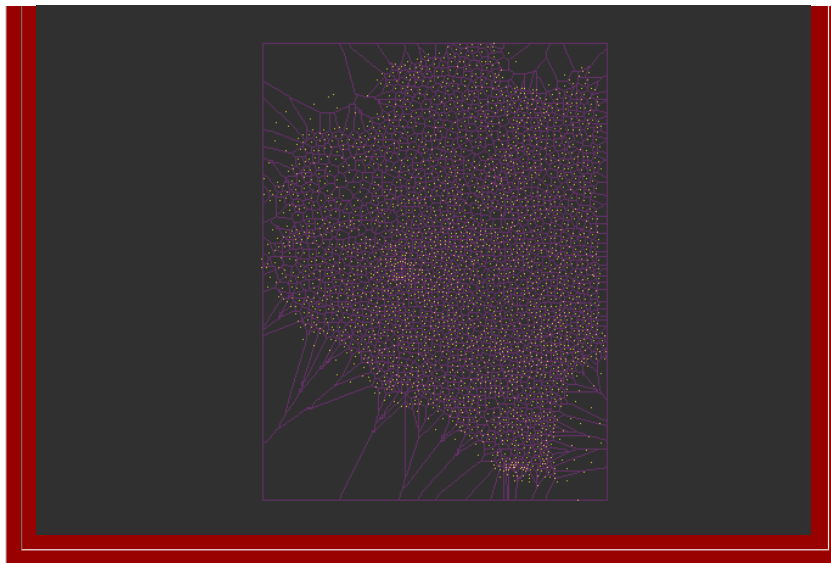
Figure 1.18. Thiessen polygons form a cellular mesh based on the two most rural layers of the hierarchy from map 1.16.

Figure 1.19 shows a sample overlay of the local cellular mesh on the original Christaller map.
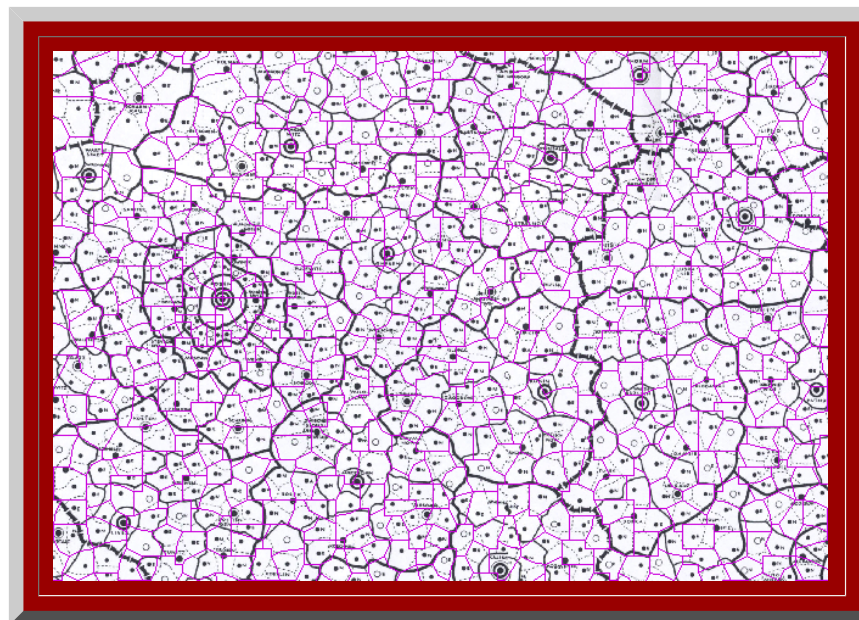
Figure 1.19. Overlay showing cellular mesh superimposed on Christaller map. Posen is the large city located near the middle/left.

Next, we constructed, using the GIS, Thiessen central place networks for each of the first five layers of the hierarchy identified by Christaller. Figure 1.20 shows these animated layers embedded in the convex hull of the map in Figure 1.16.
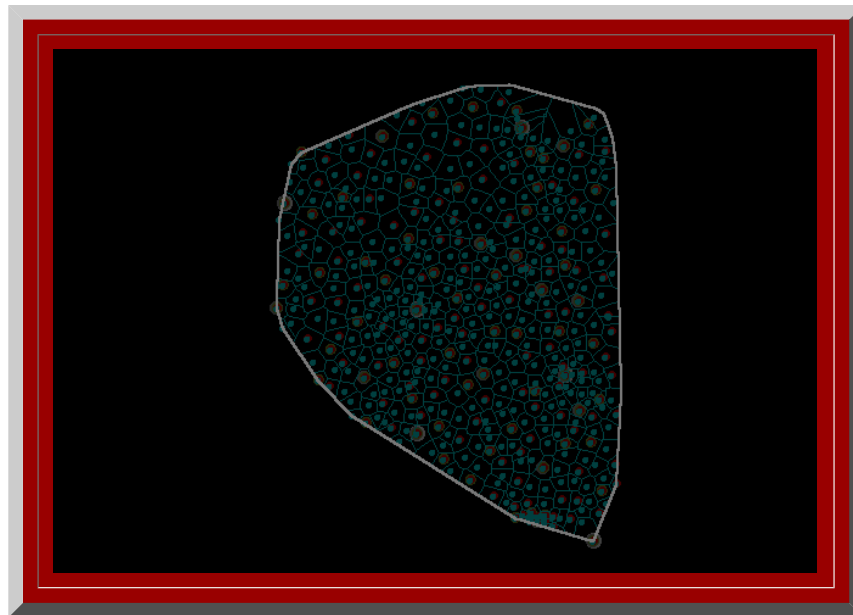
Figure 1.20. Thiessen-generated mesh for each of the five layers of largest urban places in the legend of the Christaller map.

Figure 1.21 shows a closeup comparing each of these layers to the actual map. Note the underfit/overfit pattern at the most global level (as with fractal generators for K=7).
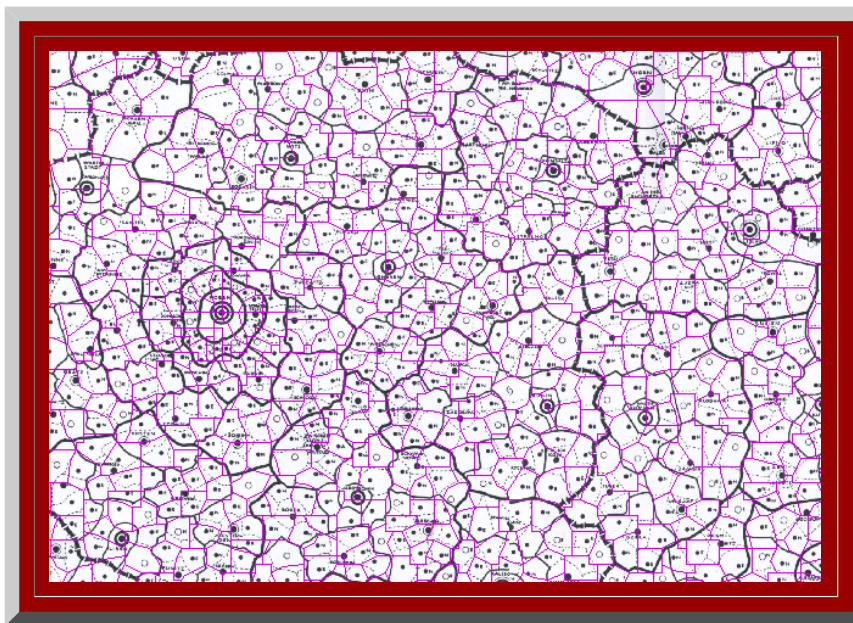
Figure 1.21. Each of the layers of Figure 1.20 overlain on the Christaller map. Posen is located left/central.
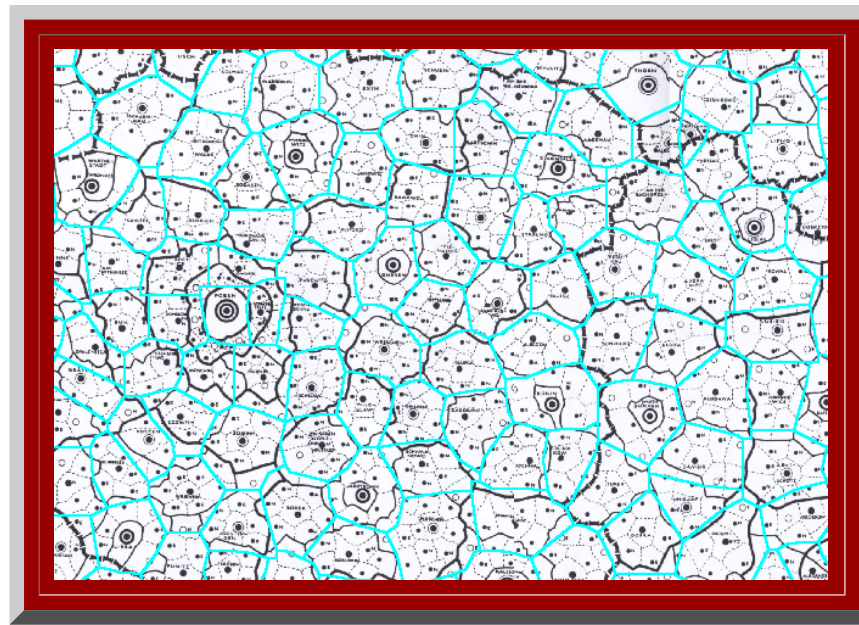
Figure 1.22. Isolated frame from the animation in Figure 1.21, showing the correspondence between the cyan Thiessen-generated polygons and the underlying Christaller map.

When the place names are linked, via the hierarchy shown in Christaller's map, as a Mapplet (Figure 1.23), the hierarchical pattern becomes clear in yet another visual manner.

Figure 1.23.

Clearly one can recreate maps from the past using techniques of the present. The strategy of aligning existing work with new technique will be carried forward into the next chapter. Establishing such alignment is interesting; projecting theorems and concepts on which it is based, into future research, is the real reason for making such alignments: to see that new procedures provide adequate results on known cases so that they serve as a procedural benchmark to extend into new theoretical and practical realms.

Chapter 2
Fractal Generation of the Classical Hexagonal Hierarchies

Concepts from fractal geometry embrace the entire geometry of classical central place theory. One type of fractal iteration sequence alone, a self-similarity transformation, produces all possible central place nets. This alignment presents more than mere technique for a verification of a geometry of central places (although it does do that, too); the geometry of the central place model is well-known and has been clearly, and comprehensively, discussed in Michael Dacey's 1965 article (Dacey 1965). The conceptual material here reveals an exact procedure for the merging of two separate theories: one from pure mathematics and one from economics and geography. In so doing, it suggests, in general, the power of one to enrich the other through the lodging of one discipline in the house of the other, and in particular, a theory in its own right derived from associating mathematically-specialized central place concepts with mathematically-broader fractal concepts.

In this chapter, we show in detail the alignment of fractal geometry with classical central place theory. In subsequent work, we illustrate how this geometry extends into far-flung realms to solve existing unsolved problems of classical central place theory and probe directions for further theoretical discovery and empirical application. The alignment of the existing classical material with fractal geometry is of interest in its own right; far more important, however, is the benchmark that this alignment creates--classical central place geometry serves as a field check for the fractal maps prior to the use of these maps as guides in the realm of theoretical geography.

"Fractals Take a Central Place"

In the material below, we illustrate, using a hexagon as an initiator, different selections of generators applied to the initial hexagon, to produce the different hexagonal hierarchies of classical central place theory (based on original concept and work of S. Arlinghaus (1985); see link). In the previous chapter we formed central place landscapes by moving from small hexagons to large ones; here, we reverse the process and dissect, using the self-similarity transformation, a large hexagon to create the smaller ones. In both processes, the results correspond exactly. The art is in generator selection, and it is simply that art that is presented in this chapter. Later work will delve into the mathematical foundations of that art.

The K=3 Hierarchy

When an hexagonal initiator is chosen and a two-sided generator, with included angle of 120 degrees, is used to make successive replacement of the sides of the hexagon (as in the animated Figure 2.1a), the outline of the next layer of the K=3 central place hierarchy is generated (the black lines in Figure 2.1a suggest interior connections). The replacement sequence applies the generator in an alternating pattern to the outside and then to the inside of the initiator. When the original generator is scaled down, with shape preserved, and applied in the outside/inside sequence to the newly formed blue polygon, the next lower level central place K=3 hierarchy is formed (as in the animated Figure 2.1b). The second, blue polygon contains three scaled-down hexagons, self-similar to the first hexagon (Figure 2.1a); the red polygon in the animation sequence contains three shapes self-similar to the blue polygon (Figure 2.1b), and 27 (or 3 cubed) hexagons self-similar to the original hexagon (Figure 2.1b). The invariant of 3, in the K=3 hierarchy, is replicated in this particular fractal iteration sequence.
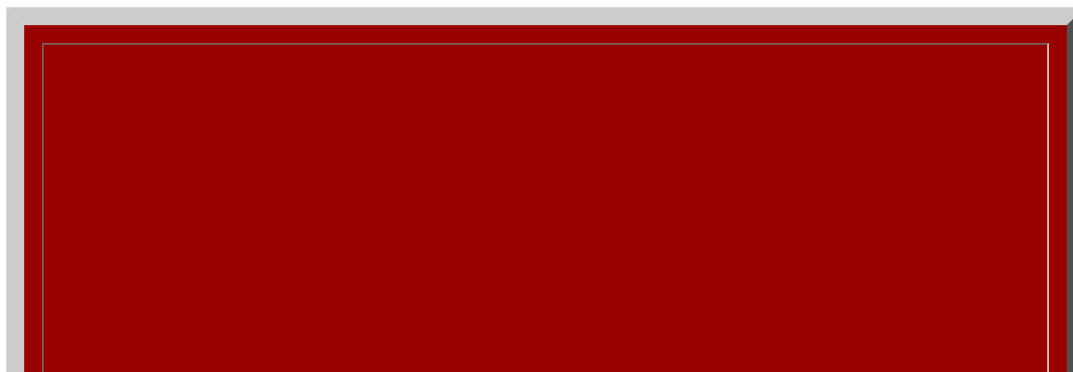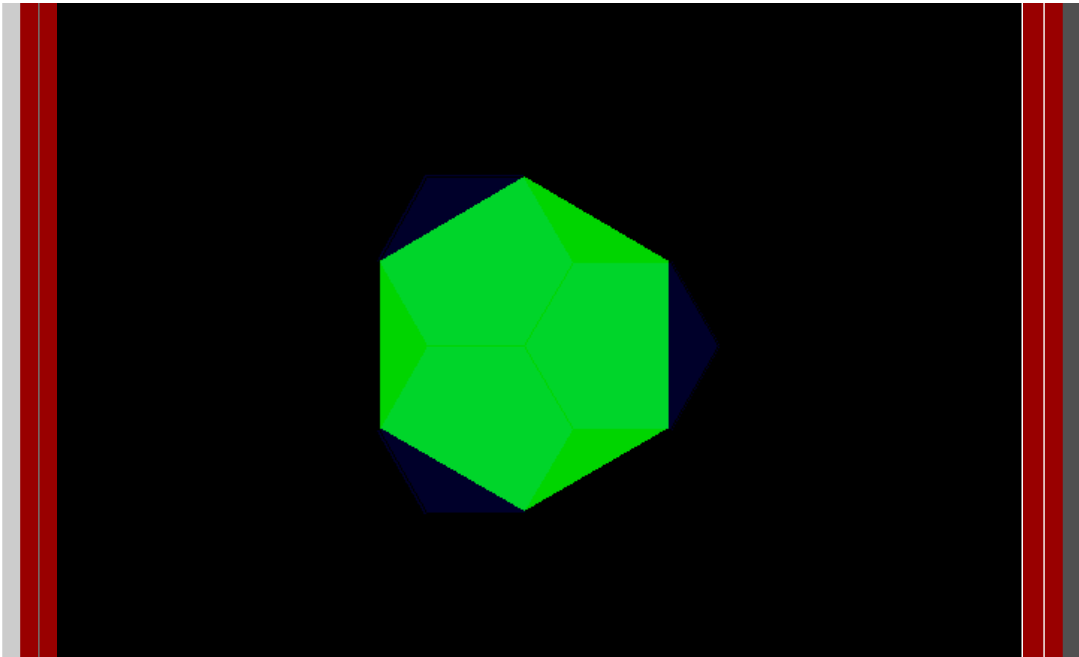
Figure 2.1a. Animated *K*=3 fractal iteration sequence: first transformation using a two-sided fractal generator applied successively to sides of the hexagonal initiator.
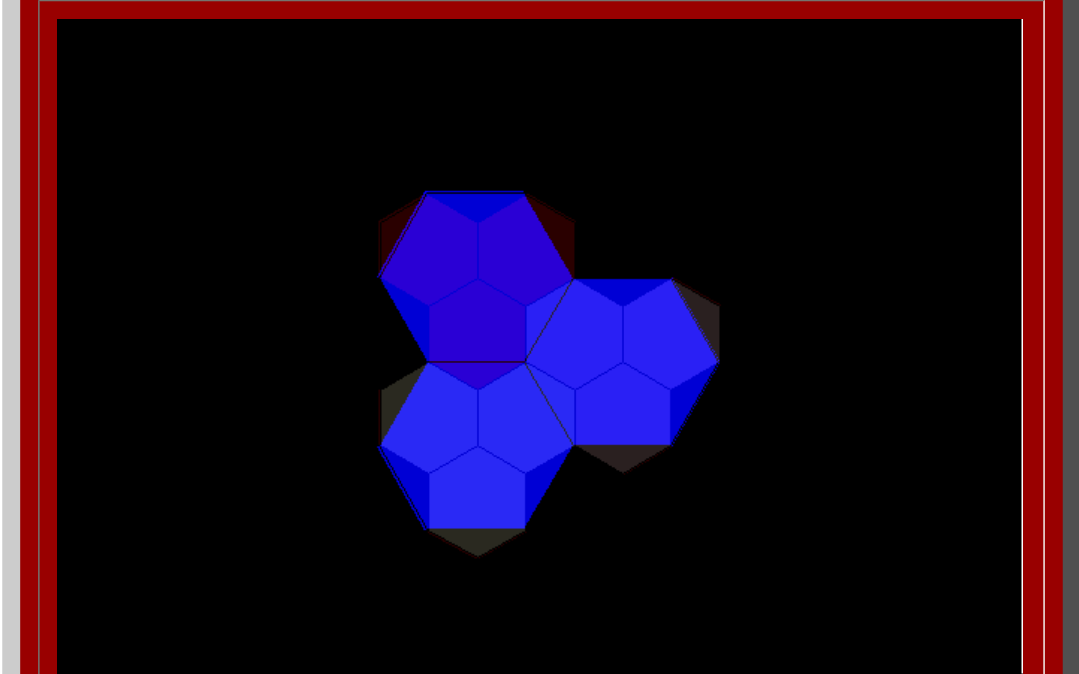
Figure 2.1b. Animated *K*=3 fractal iteration sequence: second transformation using a scaled-down two-sided fractal generator applied successively to sides of the blue polygon generated in Figure 2.1a.

It remains to determine if the polygons generated in Figure 2.1 will in fact fit together to form the broad central place landscape of arbitrary size suggested in Figure 1.5. To that end, we stack the layers generated above using the fractal iteration sequence to form a tile of layers centered on the single polygonal initiator (Figure 2.2). Click here to see a virtual solid model of the tile with which the reader can interact. Click here to see a virtual translucent model of the tile with which the reader can interact. Consider the screen captures below from those virtual reality models.
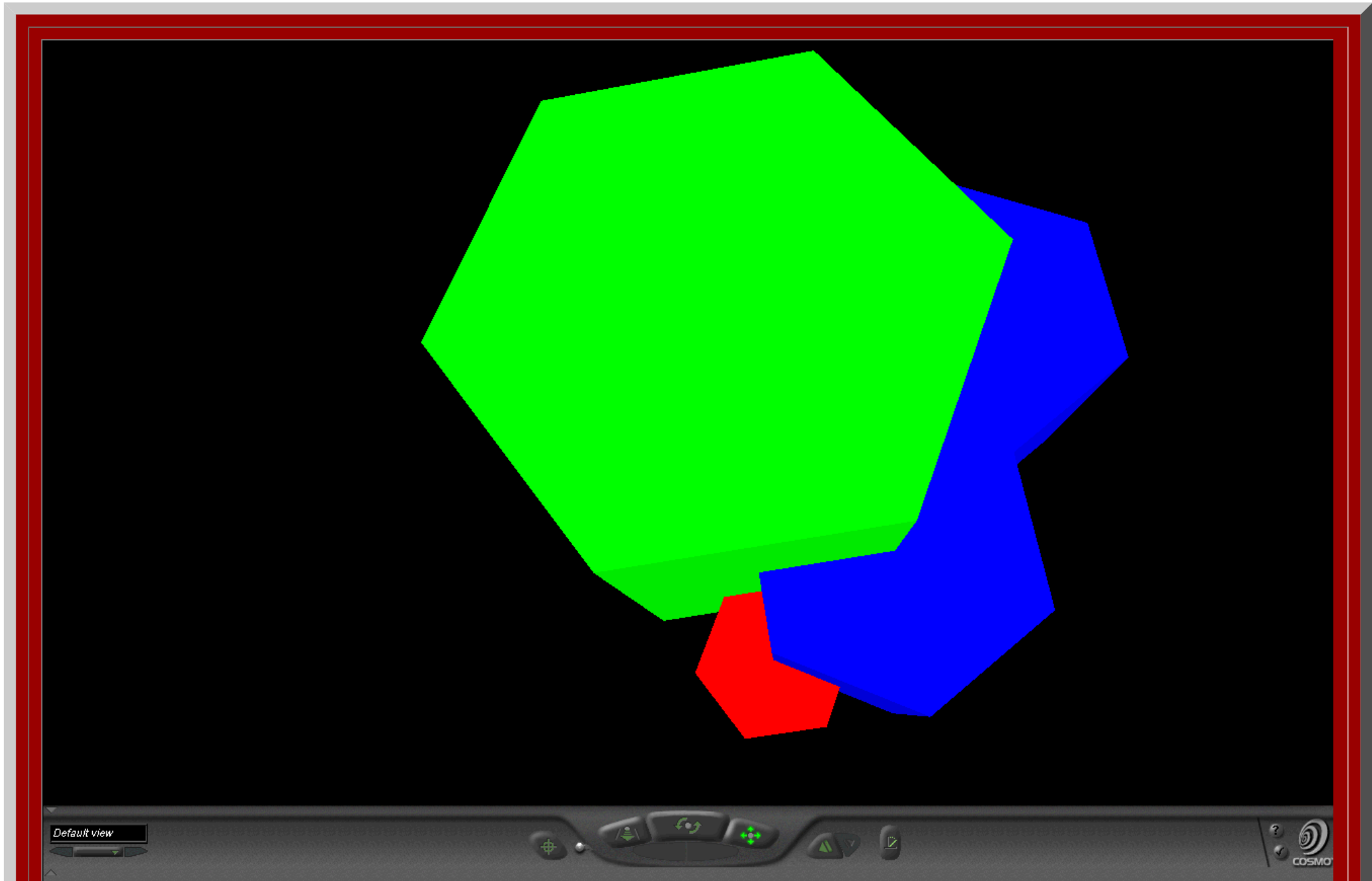
A screen shot from the virtual world linked to this image. Click on the image to enter that world!
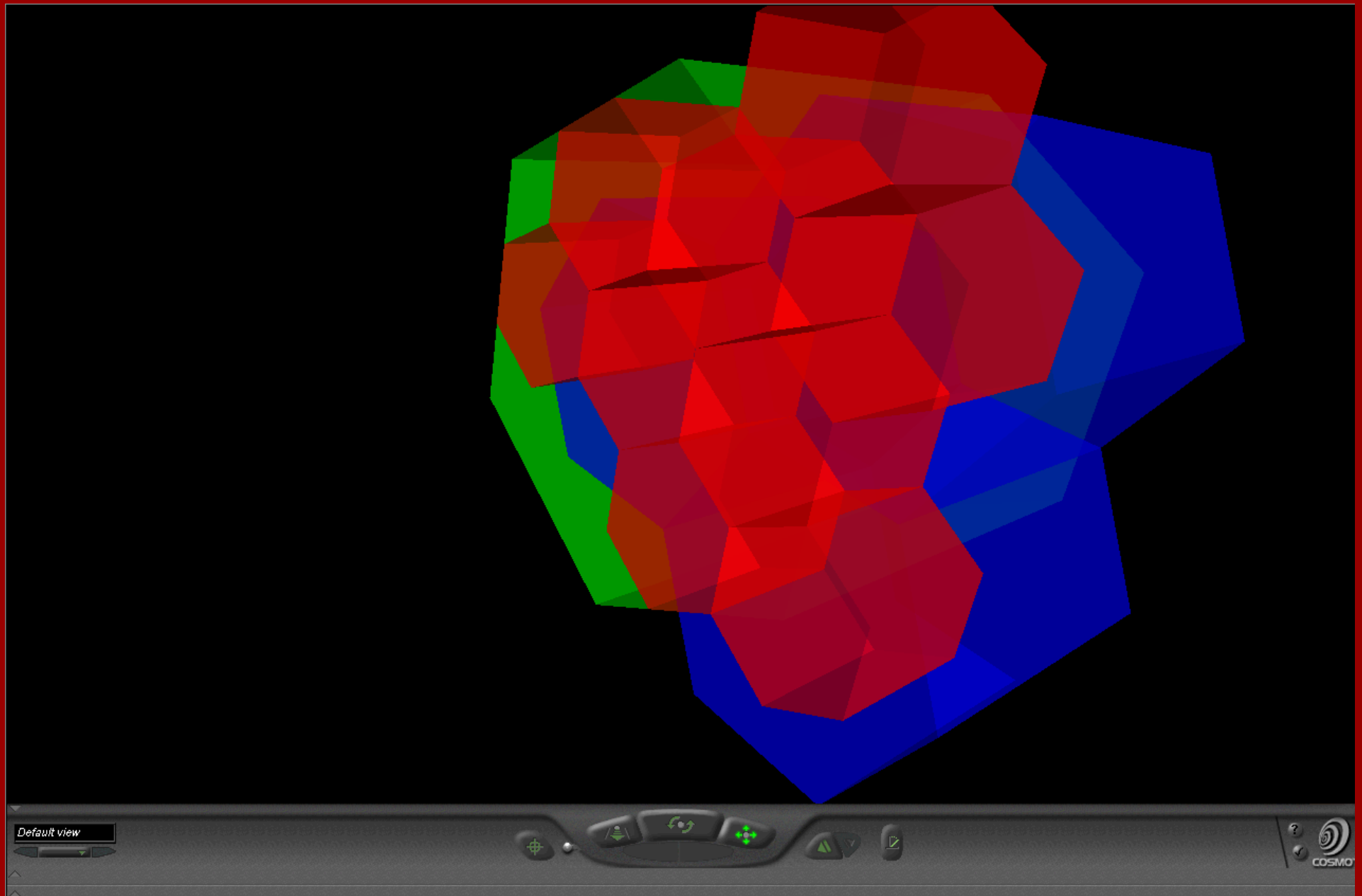
A screen shot from the virtual world linked to this image. Click on the image to enter that world! Translucent
solids permit one to see relationships among layers of the hexagonal hierarchy while travelling through the solids.
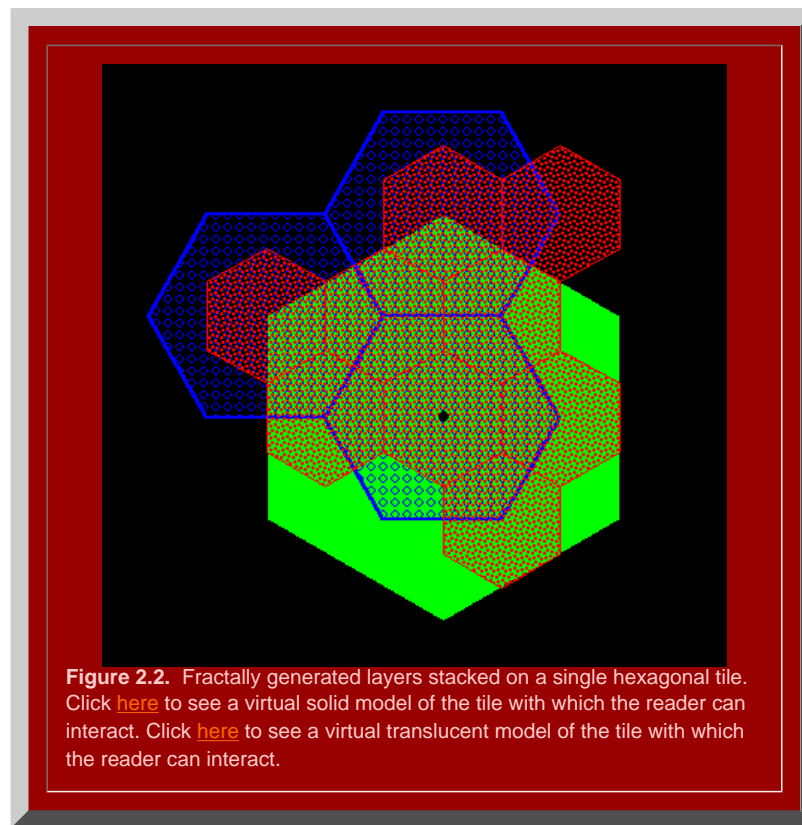
Figure 2.2. Fractally generated layers stacked on a single hexagonal tile. Click here to see a virtual solid model of the tile with which the reader can interact. Click here to see a virtual translucent model of the tile with which the reader can interact.

   Finally, we tile the plane using the hexagonal initiators, from Figure 2.2 with the attached stack of smaller hexagons, to discover if the superimposed structure also fits together perfectly (Figure 2.3). Hexagonal tiles are used to cover the plane without gaps, as is the case with the sample of green hexagons in Figure 2.3a. The hexagons mesh perfectly to cover the plane (Theorem of Gauss). In Figure 2.3b, the green outline of the hexagons remains. Each of the solid green hexagons has had the fractal generator above applied and the consequent superimposed blue tiles come into view sequentially in this animation. Again, the fit is exact, as we had hoped it might be. Finally, in Figure 2.3c, the blue outline only is retained from Figure 2.3b (along with the green outline from Figure 2.3a). The final fractally generated layer derived from the blue polygons of Figure 2.3b comes into view in shades of red (or yellow/gold for contrast). The final layer of hexagonal base of unit hexagons appears last. The fit is perfect: each green hexagon contains the equivalent of four blue hexagons and each blue hexagon contains the equivalent of four red hexagons. The fractal generation procedure created exactly the classical central place landscape of Figure 1.5 (return here using the Back button on your browser).   As the animation proceeds in Figure 2.3, further layers of the fractally generated hierarchy, attached to the tile in Figure 2.2, come into view illustrating an exact meshing of tiles at all levels to form a K=3 hierarchy.
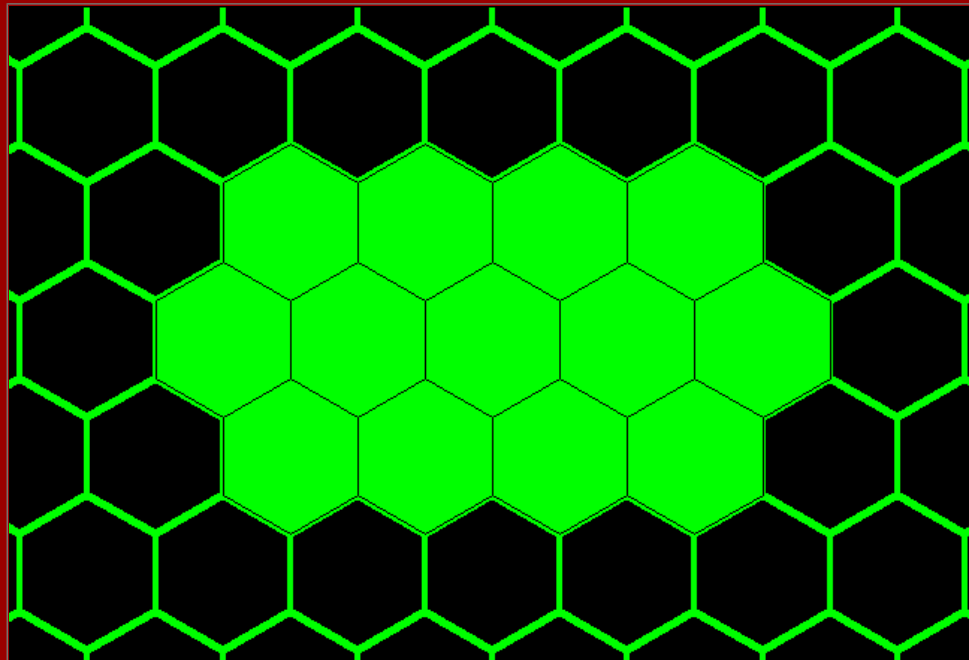
Figure 2.3a. Green layer on tile from Figure 2.2 fits exactly to tile the plane (Theorem of Gauss).
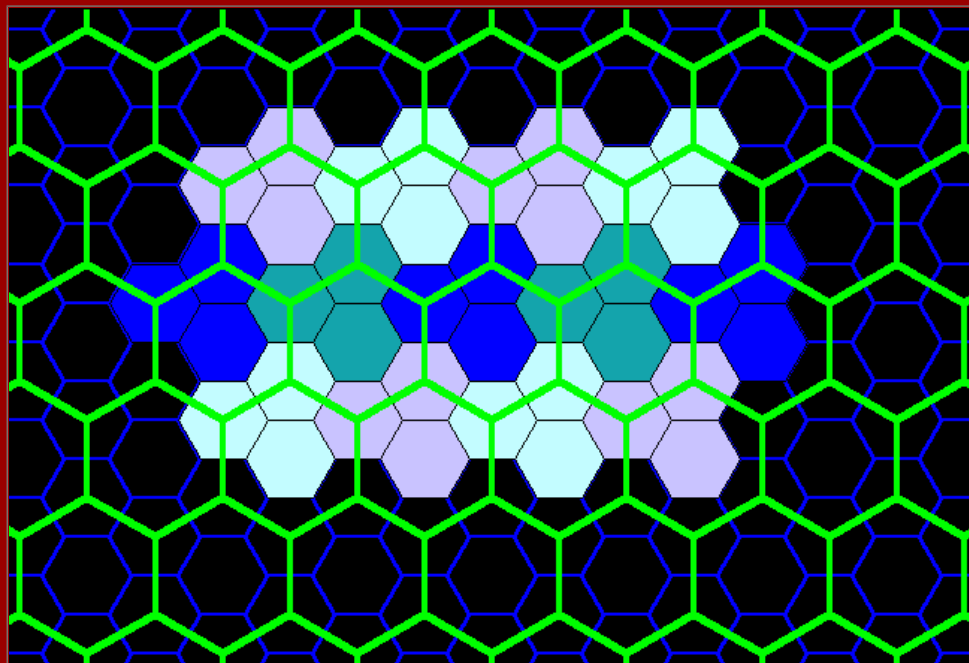
Figure 2.3b. Blue layer on tile from Figure 2.2 fits exactly to form classical *K*=3 landscape.

Figure 2.3c. Red layer on tile from Figure 2.2 fits exactly to form classical *K*=3 landscape.
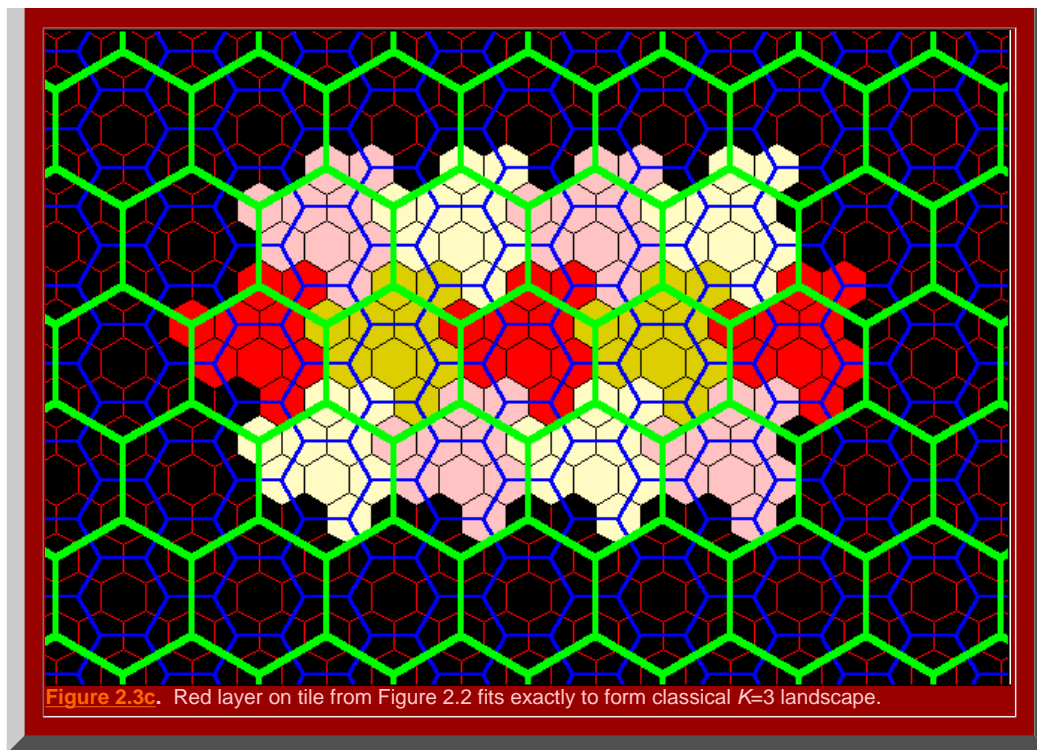
The K=4 Hierarchy

When an hexagonal initiator is chosen and a three-sided generator, with included angles of 120 degrees and shaped in the form of an isosceles trapezoid, is used to make successive replacement of the sides of the hexagon (as in the animated Figure 2.4a), the outline of the next layer of the *K*=4 central place hierarchy is generated (the black lines in Figure 2.4a suggest interior connections). The replacement sequence applies the generator in an alternating pattern to the outside and then to the inside of the initiator. When the original generator is scaled down, with shape preserved, and applied in the outside/inside sequence to the newly formed blue polygon, the next lower level central place *K*=4 hierarchy is formed (as in the animated Figure 2.4b). The second, blue polygon contains four scaled-down hexagons, self-similar to the first hexagon (Figure 2.4a); the red polygon in the animation sequence contains four shapes self-similar to the blue polygon (Figure 2.4b), and 64 (or 4 cubed) hexagons self-similar to the original hexagon (Figure 2.4b). The invariant of 4, in the *K*=4 hierarchy, is replicated in this particular fractal iteration sequence.
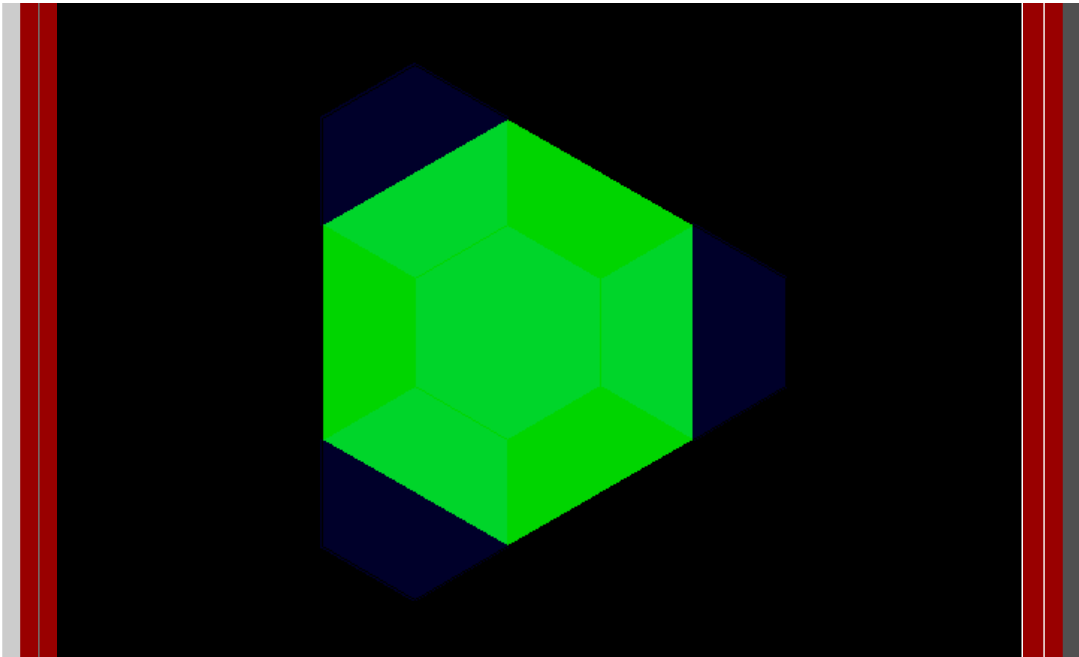
Figure 2.4a. Animated *K*=4 fractal iteration sequence: first transformation using a three-sided fractal generator applied successively to sides of the hexagonal initiator.
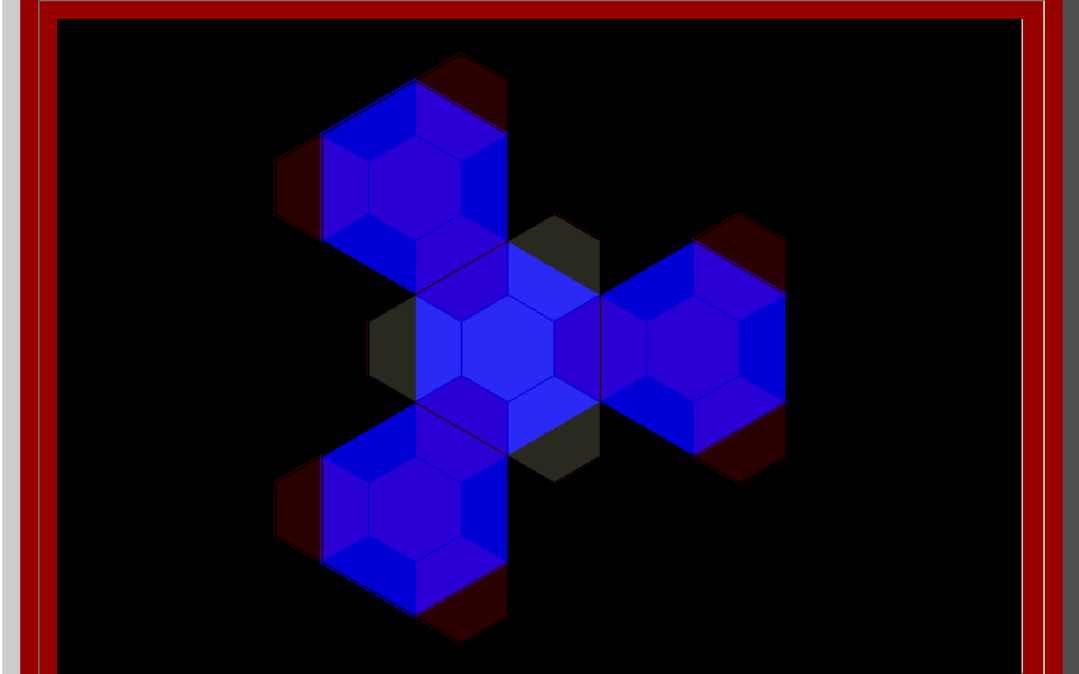
Figure 2.4b. Animated *K*=4 fractal iteration sequence: second transformation using a scaled-down three-sided fractal generator applied successively to sides of the blue polygon generated in Figure 2.4a.

It remains to determine if the polygons generated in Figure 2.4 will in fact fit together to form the broad central place landscape of arbitrary size suggested in Figure 1.7. To that end, we stack the layers generated above using the fractal iteration sequence to form a tile of layers centered on the single polygonal initiator (Figure 2.5). Click here to see a virtual solid model of the tile with which the reader can interact. Click here to see a virtual translucent model of the tile with which the reader can interact. Consider the screen captures below from those virtual reality models.

A screen shot from the virtual world linked to this image. Click on the image to enter that world!

A screen shot from the virtual world linked to this image. Click on the image to enter that world! Translucent
solids permit one to see relationships among layers of the hexagonal hierarchy while travelling through the solids.

Figure 2.5. Fractally generated layers stacked on a single hexagonal tile. Click here to see a virtual solid model of the tile with which the reader can interact. Click here to see a virtual translucent model of the tile with which the reader can interact.
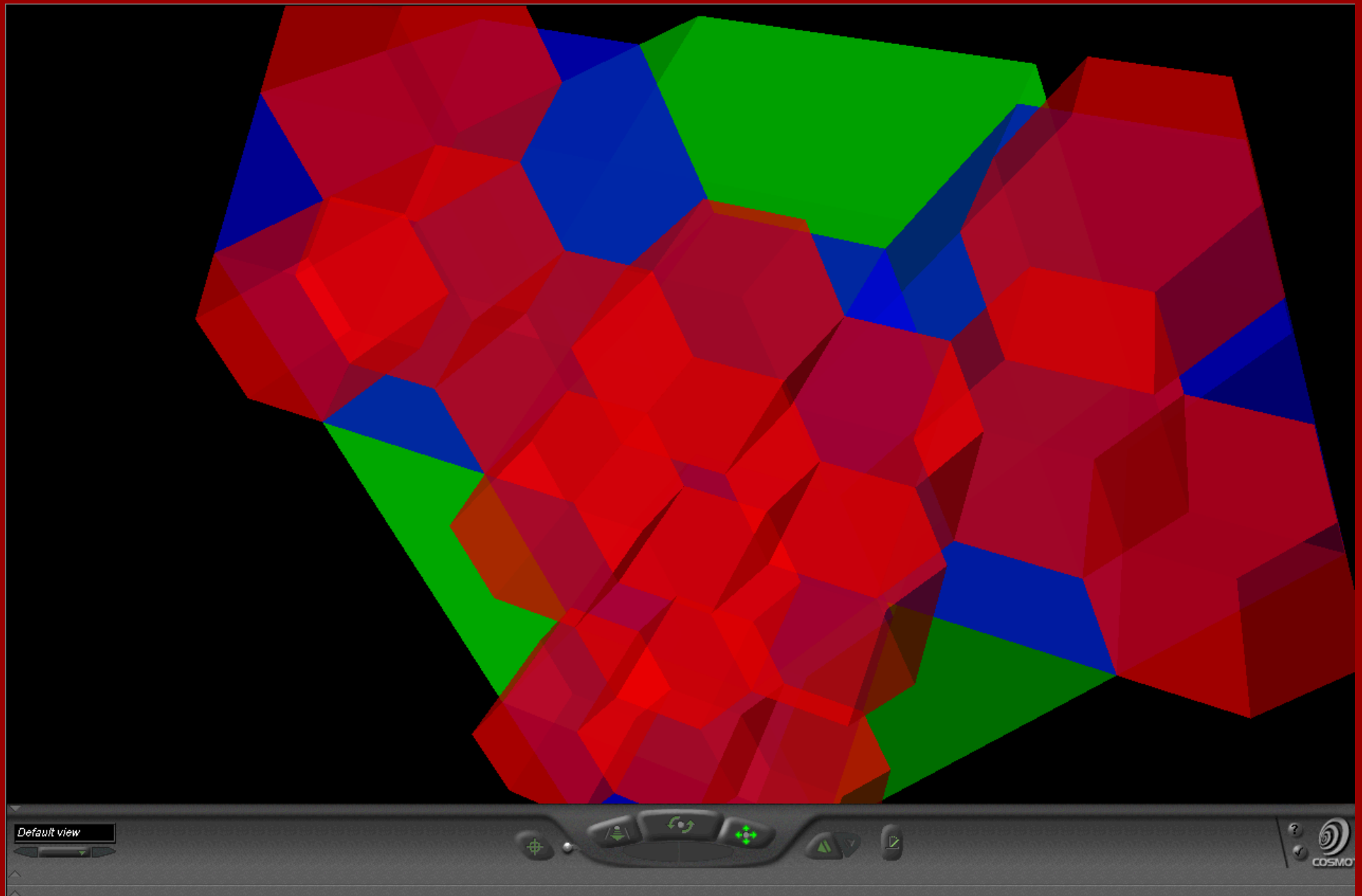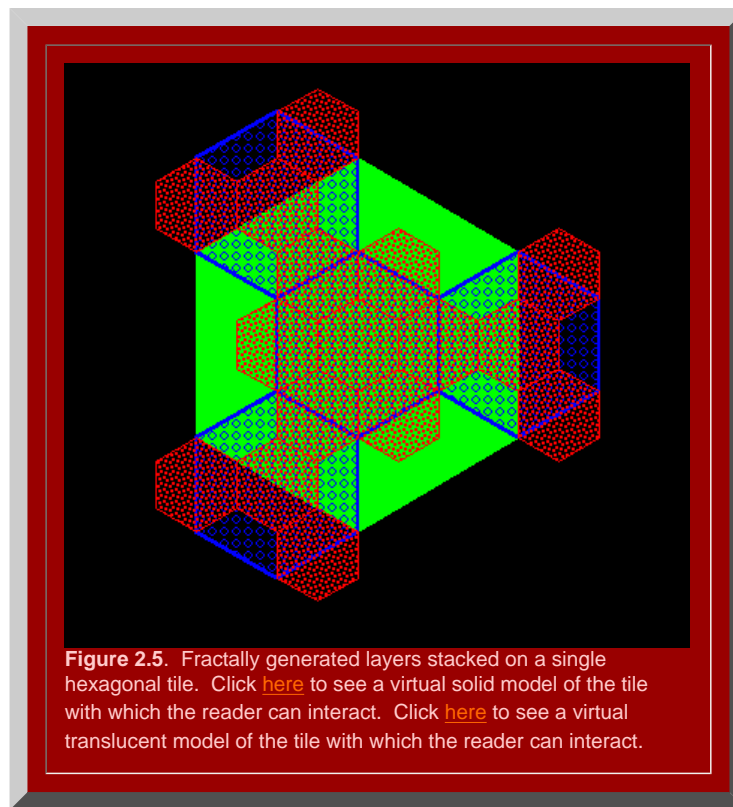
   Finally, we tile the plane using the hexagonal initiators, from Figure 2.5 with the attached stack of smaller hexagons, to discover if the superimposed structure also fits together perfectly (Figure 2.6). Hexagonal tiles are used to cover the plane without gaps, as is the case with the sample of green hexagons in Figure 2.6a. The hexagons mesh perfectly to cover the plane (Theorem of Gauss). In Figure 2.6b, the green outline of the hexagons remains. Each of the solid green hexagons has had the fractal generator above applied and the consequent superimposed blue tiles come into view sequentially in this animation. Again, the fit is exact, as we had hoped it might be. Finally, in Figure 2.6c, the blue outline only is retained from Figure 2.6b (along with the green outline from Figure 2.6a). The final fractally generated layer derived from the blue polygons of Figure 2.6b comes into view in shades of red (or yellow/gold for contrast). The final layer of hexagonal base of unit hexagons appears last. The fit is perfect: each green hexagon contains the equivalent of four blue hexagons and each blue hexagon contains the equivalent of four red hexagons. The fractal generation procedure created exactly the classical central place landscape of Figure 1.7 (return here using the Back button on your browser). As the animation proceeds in Figure 2.6, further layers of the fractally generated hierarchy, attached to the tile in Figure 2.5, come into view illustrating an exact meshing of tiles at all levels to form a K=4 hierarchy.

**Figure 2.6a.** Green layer on tile from Figure 2.5 fits exactly to tile the plane (Theorem of Gauss).

Figure 2.6b. Blue layer on tile from Figure 2.5 fits exactly to form classical K=4 landscape.

Figure 2.6c. Red layer on tile from Figure 2.5 fits exactly to form classical *K*=4 landscape.
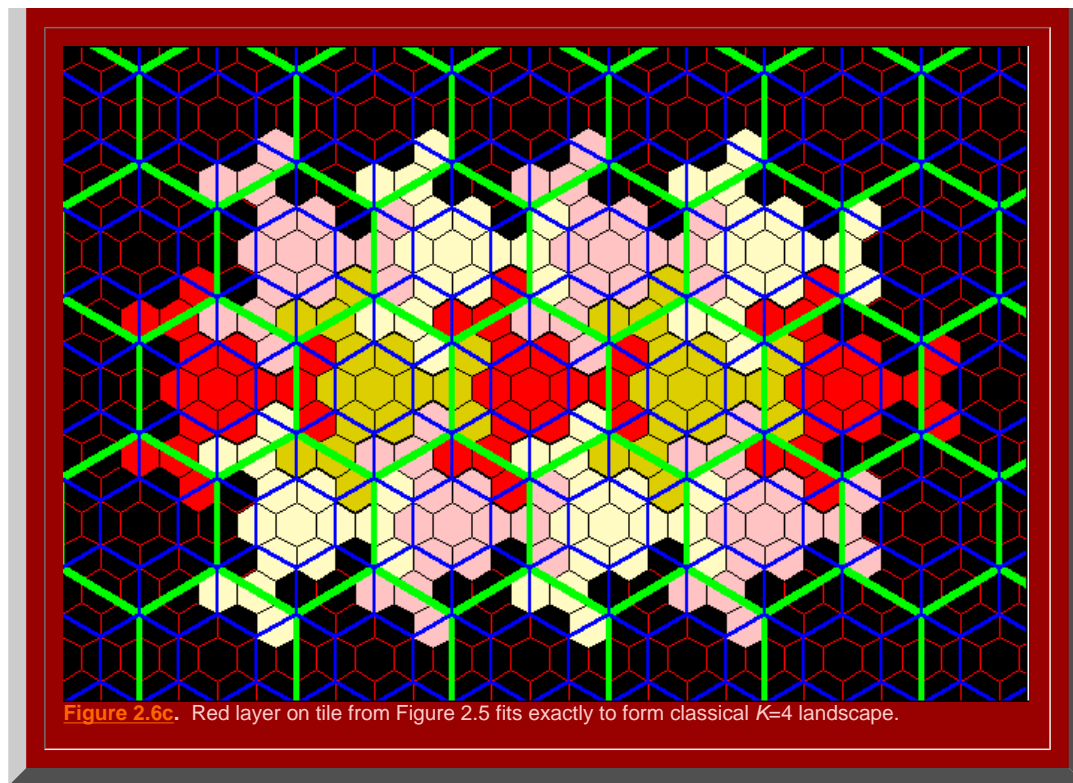
The K=7 Hierarchy

When an hexagonal initiator is chosen and a three-sided generator, with included angles of 120 degrees and shaped in a zig-zag form, is used to make successive replacement of the sides of the hexagon (as in the animated Figure 2.7a), the outline of the next layer of the *K*=7 central place hierarchy is generated (the black lines in Figure 2.7a suggest interior connections). The replacement sequence applies the generator in an alternating pattern to the outside and then to the inside of the initiator. When the original generator is scaled down, with shape preserved, and applied in the outside/inside sequence to the newly formed blue polygon, the next lower level central place *K*=7 hierarchy is formed (as in the animated Figure 2.7b). The second, blue polygon contains seven scaled-down hexagons, self-similar to the first hexagon (Figure 2.7a); the red polygon in the animation sequence contains seven shapes self-similar to the blue polygon (Figure 2.7b), and 343 (or 7 cubed) hexagons self-similar to the original hexagon (Figure 2.7b). The invariant of 7, in the *K*=7 hierarchy, is replicated in this particular fractal iteration sequence.

.
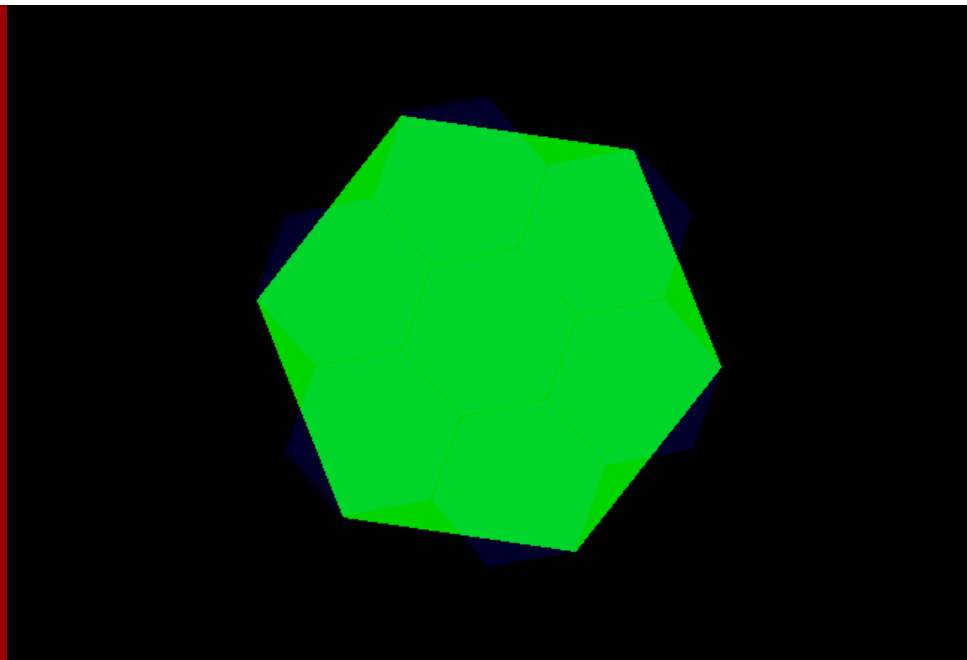
Figure 2.7a. Animated *K*=7 fractal iteration sequence: first transformation using a three-sided fractal generator applied successively to sides of the hexagonal initiator.
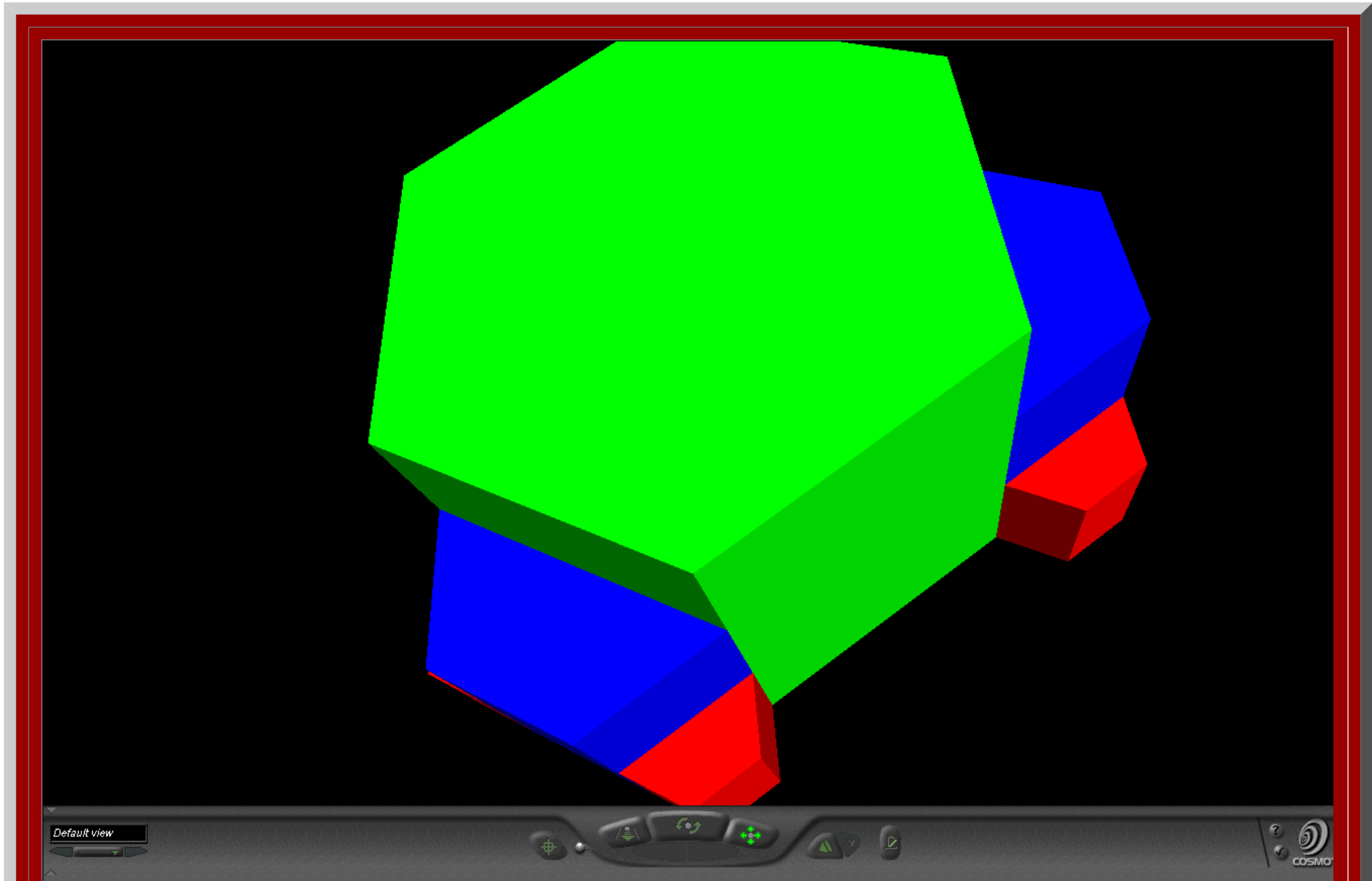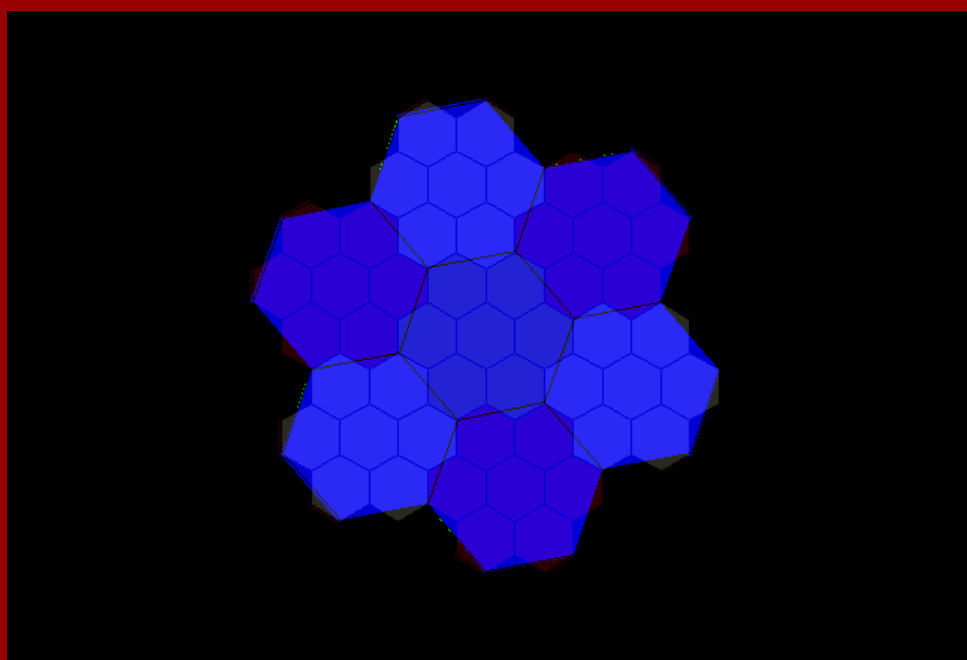

Figure 2.7b. Animated *K*=7 fractal iteration sequence: second transformation using a scaled-down three-sided fractal generator applied successively to sides of the blue polygon generated in Figure 2.7a.

It remains to determine if the polygons generated in Figure 2.7 will in fact fit together to form the broad central place landscape of arbitrary size suggested in Figure 1.9. To that end, we stack the layers generated above using the fractal iteration sequence to form a tile of layers centered on the single polygonal initiator (Figure 2.8). Click here to see a virtual solid model of the tile with which the reader can interact. Click here to see a virtual translucent model of the tile with which the reader can interact. Consider the screen captures below from those virtual reality models.

A screen shot from the virtual world linked to this image. Click on the image to enter that world!

Default view
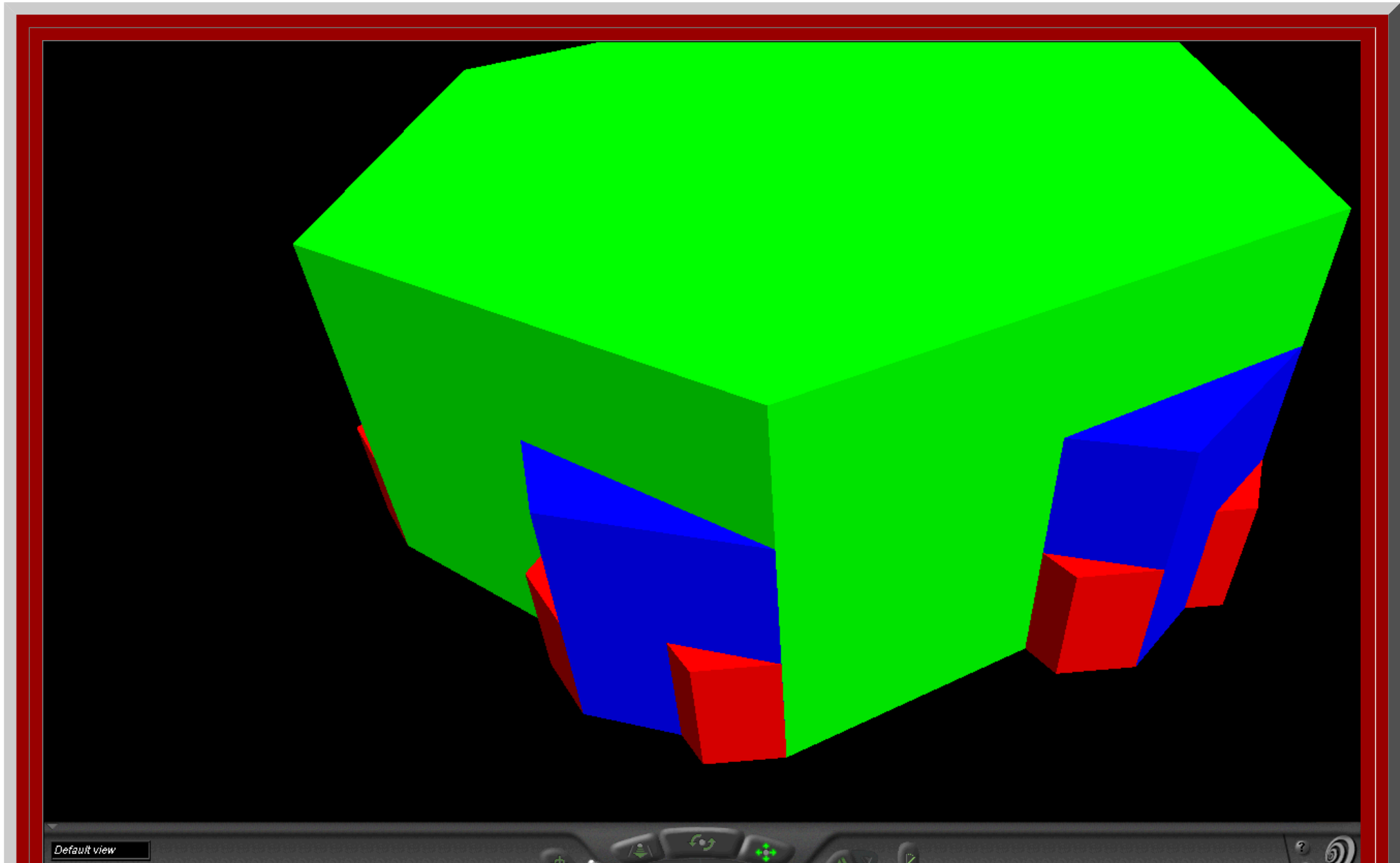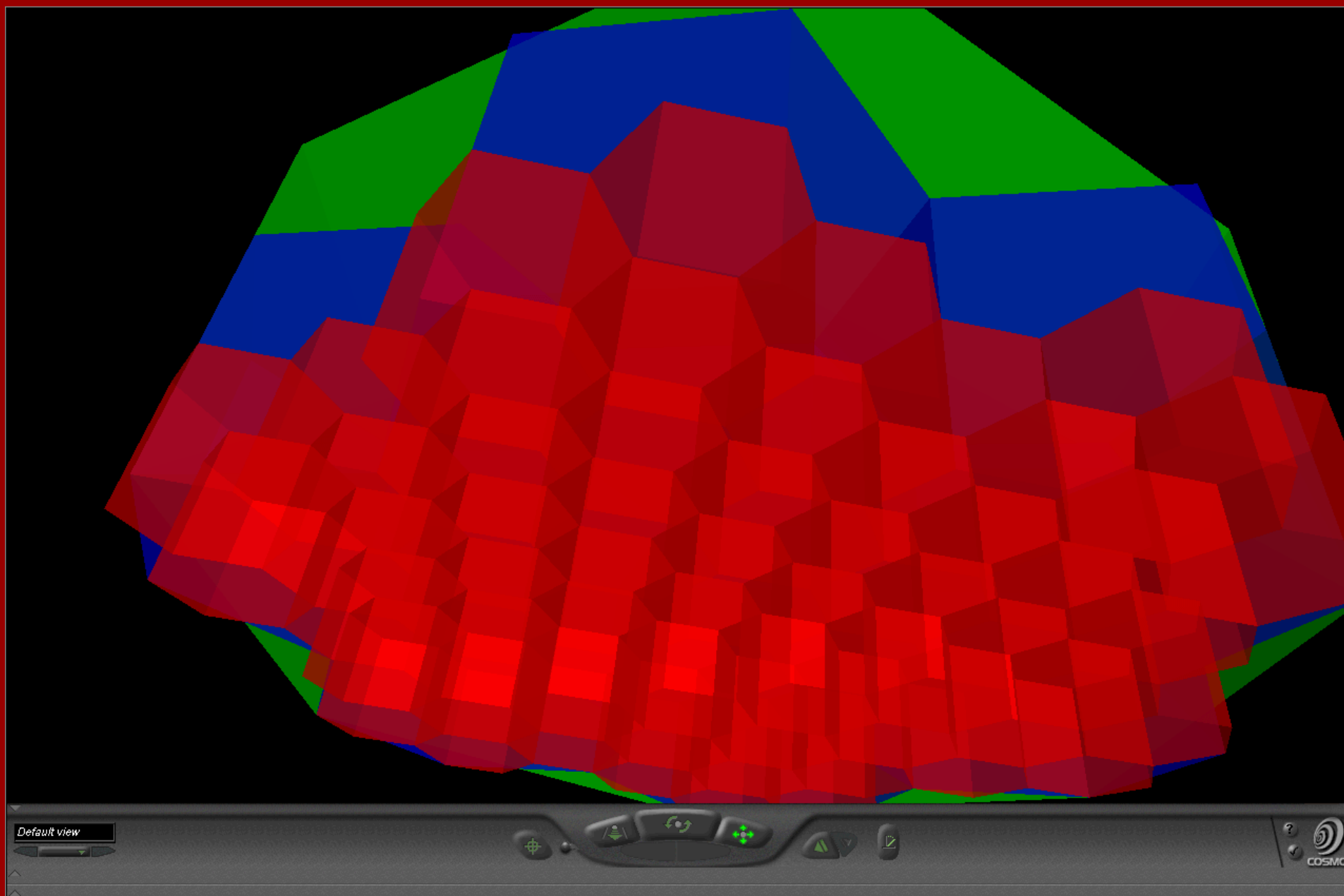
A screen shot from the virtual world linked to this image. Translucent solids permit one to see relationships among layers of the hexagonal hierarchy while travelling through the solids. Click on the image to enter that world: blast off in this virtual hexagonal space ship!

Figure 2.8. Fractally generated layers stacked on a single hexagonal tile. Click here to see a virtual solid model of the tile with which the reader can interact. Click here to see a virtual translucent model of the tile with which the reader can interact.
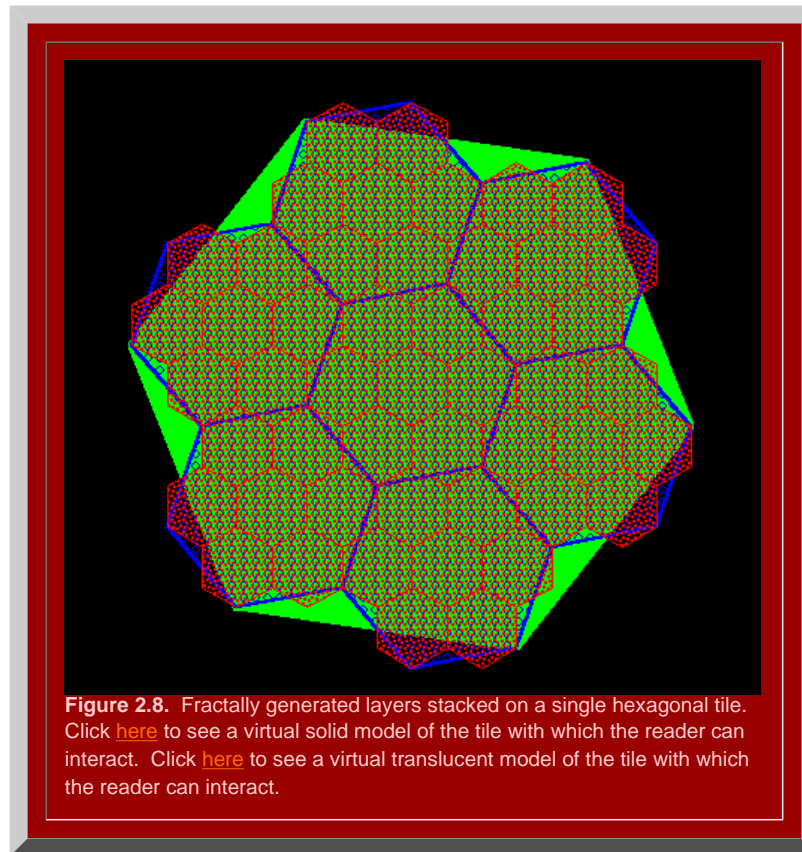
Finally, we tile the plane using the hexagonal initiators, from Figure 2.8 with the attached stack of smaller hexagons, to discover if the superimposed structure also fits together perfectly (Figure 2.9). Hexagonal tiles are used to cover the plane without gaps, as is the case with the sample of green hexagons in Figure 2.9a. The hexagons mesh perfectly to cover the plane (Theorem of Gauss). In Figure 2.9b, the green outline of the hexagons remains. Each of the solid green hexagons has had the fractal generator above applied and the consequent superimposed blue tiles come into view sequentially in this animation. Again, the fit is exact, as we had hoped it might be. Finally, in Figure 2.9c, the blue outline only is retained from Figure 2.9b (along with the green outline from Figure 2.9a). The final fractally generated layer derived from the blue polygons of Figure 2.9b comes into view in shades of red (or yellow/gold for contrast). The final layer of hexagonal base of unit hexagons appears last. The fit is perfect: each green hexagon contains the equivalent of four blue hexagons and each blue hexagon contains the equivalent of four red hexagons. The fractal generation procedure created exactly the classical central place landscape of Figure 1.9 (return here using the Back button on your browser). As the animation proceeds in Figure 2.9, further layers of the fractally generated hierarchy, attached to the tile in Figure 2.8, come into view illustrating an exact meshing of tiles at all levels to form a K=3 hierarchy.
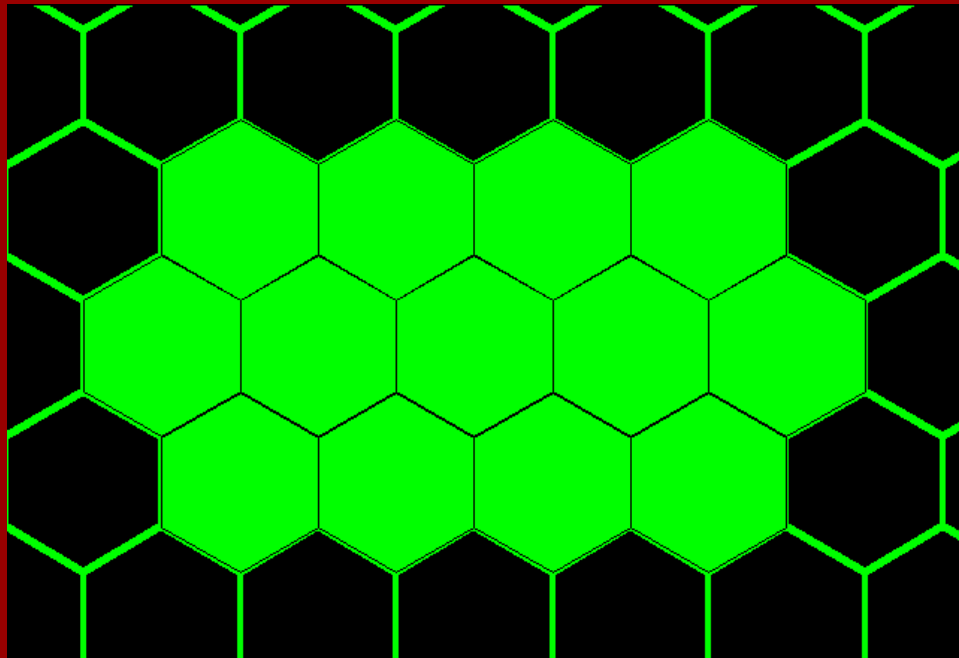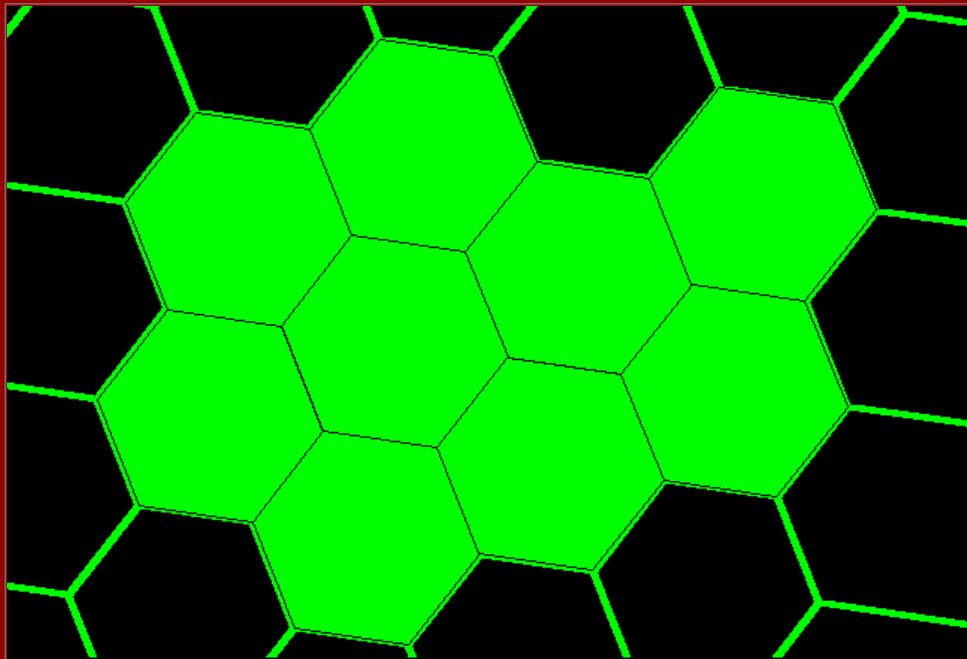
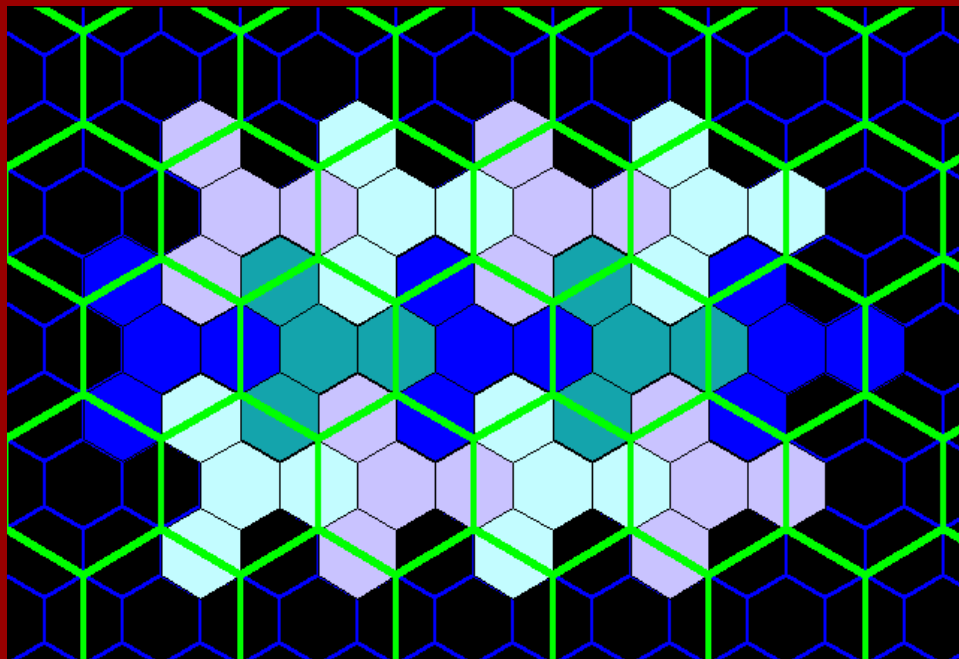**Figure 2.9a**. Green layer on tile from Figure 2.8 fits exactly to tile the plane (Theorem of Gauss).
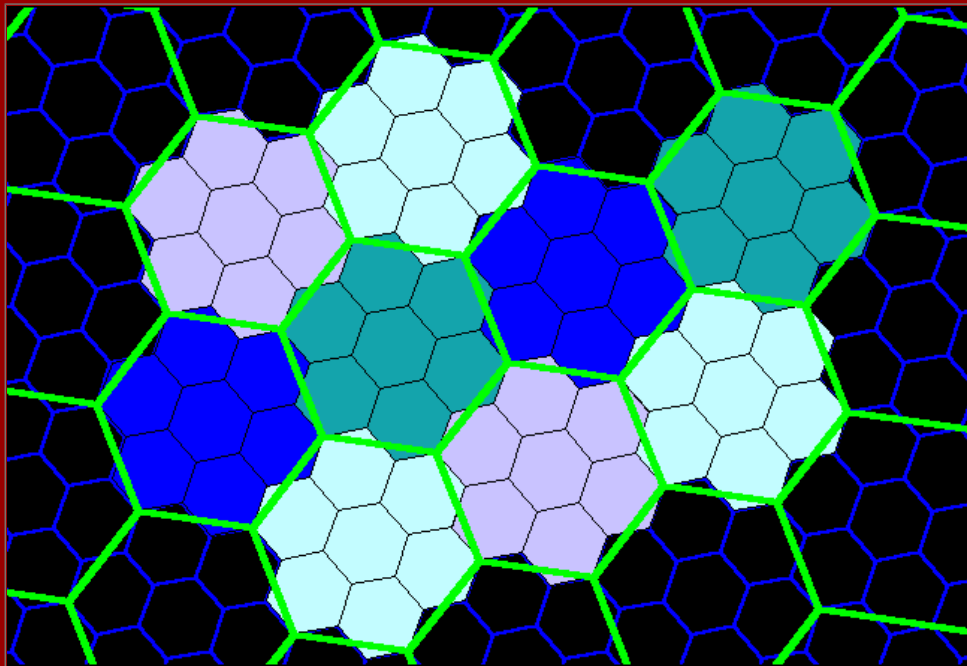
Figure 2.9b. Blue layer on tile from Figure 2.8 fits exactly to form classical *K*=7 landscape.

Figure 2.9c. Red layer on tile from Figure 2.8 fits exactly to form classical *K*=7 landscape.
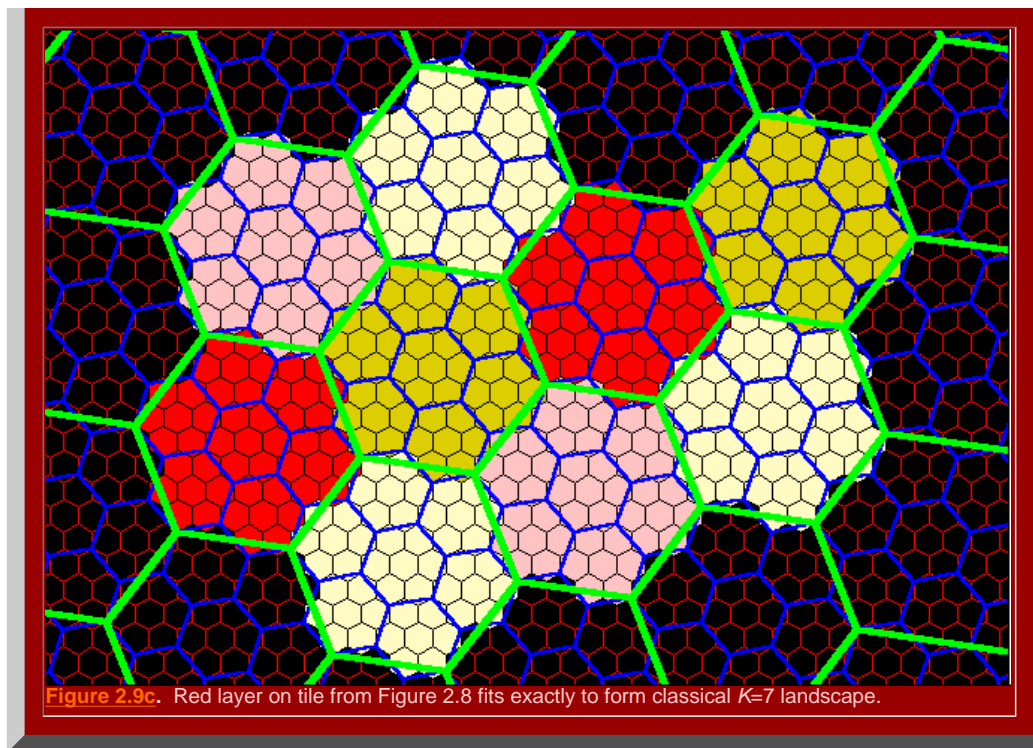
Thus, the complex mechanics of classical central place theory come alive as a single dynamic system when viewed using fractal geometry. The fit is exact.

The added role of the fractional dimension
    A fractal iteration sequence, such as those above but carried out infinitely, might be thought to increase the extent to which a line "fills" space. Mandelbrot captures this notion of space-filling with the concept of fractional dimension (hence "fractal"). He uses Hausdorff-Besicovitch dimension to measure the enduring mathematical concept of space-filling (see bibliography). We employ Mandelbrot's formulation for fractional dimension *D* as, *D*=log(number of generator sides)/log(square root of *K*). Thus, the following values for fractally-generated central place hierarchies emerge:

- *K*=3, *D*=log2/log $\sqrt{3}$ = 1.2618595
- *K*=4, *D*=log3/log 2   = 1.5849625
- *K*=7, *D*=log3/log $\sqrt{7}$ = 1.1291501

The idea with the space-filling is to pick an arbitrary point in the bounded space containing the curve. Place a circle of arbitrarily small radius around that point. Does that circle contain a point on the curve as the fractal iteration sequence goes to infinity? If that is the case for any point, then the curve is said to fill space and have dimension 2. If not, then there are holes or gaps (perhaps of infinitesimal size) in the space and the curve fails to fill space completely and has fractional dimension between 1 and 2 (as a sort of Swiss cheese with holes). Thus, the *K*=4 fractal iteration sequence, if permitted to repeat infinitely, has the highest fractional dimension of these three: this curve gets "closer" to arbitrary points in space than do the lines of the other hierarchies, as one might hope a hierarchy interpreted as a "transportation" hierarchy would. The fractional dimension of the fractal iteration sequence corresponds to the intuitive notion of scholars over time as to interpretation: another benchmark or field test of theory. The *K*=7 fractal iteration sequence, if permitted to repeat infinitely, has the lowest fractional dimension of these three, keeping control from the center optimized and hence supporting the "administrative" or "separation" interpretation often given to the classical *K*=7 hierarchy. Finally, the *K*=3 falls between: marketing needs greater spatial penetration than

does administration but less than does transportation. Here, the fit between classical interpretation and fractal calculation is reasonable (one could never say "exact" because the terms "marketing," "transportation," and "administrative" are inexact terms themselves).

   What is difficult with fractals is to visualize the infinite process. Graphic color display, including three dimensional display, offers exciting strategies for visualization. Very quickly, however, it becomes difficult to draw the fine lines required by repeating the process at more and more local scales: physical lines have width. Electronic lines can be controlled and made finer than can pen lines, but eventually the line-width limits the capability to produce graphic images. Eventually, the mind's eye must take over and extrapolate the visual infinite process.

   Another possibility might be to draw on the other human senses to aid in that extrapolation. Thus, Figure 2.10 shows figures generated by Fractal Music 1.9; click on the images and hear the associated music. The left figure shows the cellular automata base generated by default--it is bilaterally symmetric about a central vertical line and was generated using a symmetrically arranged initiator string of 64 digits ranging in value from 0 to 7 (one for each tone). The next figure, K=3, shows the cellular automata diagram (another sort of "bubble foam" in appearance) generated using the value for the fractional dimension of the K=3 hexagonal hierarchy carried out to 64 decimal places as the initiator string for the music. The next figure, K=4, shows the cellular automata diagram generated using the value for the fractional dimension of the K=4 hexagonal hierarchy carried out to 64 decimal places as the initiator string for the music. The final figure, K=7, shows the cellular automata diagram generated using the value for the fractional dimension of the K=7 hexagonal hierarchy carried out to 64 decimal places as the initiator string for the music. Click on each figure to hear the music. Each musical sequence, of over 1000 steps, was created from the default base, changing only the initiator string, so that the fractional dimension is what operates on a "seed" value of basic notes. The listener should hear the basic pattern in all characterizations: great symmetry in the base value; abrupt changes of state in the K=3 value; a smoother filling of musical space in the K=4 music; and, gaps in the K=7 musical characterization derived from the K=7 fractional dimension. The bilaterally symmetric bubble-foam figure associated with the base has been skewed by each of the K-values, as has the corresponding music. Thus, we extend visualization from two dimensional graphical images to three dimensional graphical images to the mind's eye, and finally, to the mind's ear: capturing hierarchical pattern through 1000 steps or more is easy in the musical clips. Such characterization offers added capability to those of us with all of our senses that are functional: for those with limited visual sensory function, it offers a way to an auditory "visualization" of the beauty of geometry.

| Base | K=3 | K=4 | K=7 |
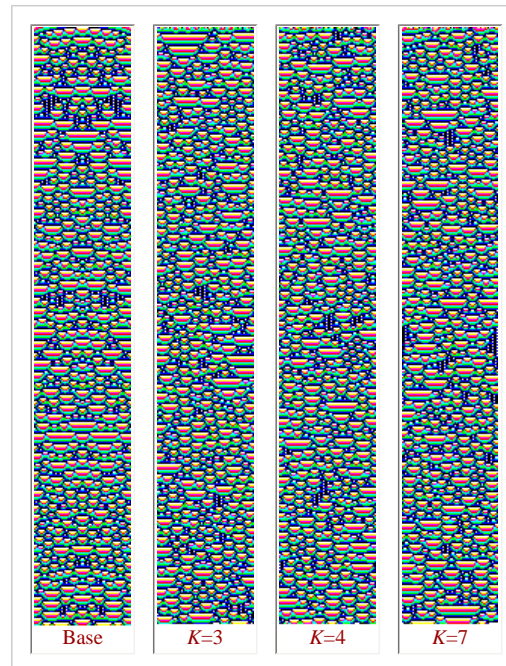
Figure 2.10. Fractal music connection. Click on the images generated by the fractional dimensions of the hexagonal hierarchies; compare these to the default base created by the software.

In subsequent chapters, we offer mathematical proof of these ideas and extensions of these ideas into new realms. The classical is used for alignment of new with the old: a strategy useful in a wide range of theoretical and applied research.

Chapter 3
Number Theory Background

Primes and Divisibility

Even in ancient times, people were fascinated by the idea of divisibility. This book is interested primarily in positive integers, just as Euclid was.

Definition 3.1. A positive integer *a* is said to be a divisor of another positive integer *b* if *b=ac* for some positive integer *c*. (If *a* is a divisor of *b*, we write *a|b* and say "*a* divides *b*," or "*b* is a multiple of *a*").

Definition 3.2. If an integer *p*>1 has only 1 and *p* as divisors, it is called prime (for example 2, 3, 4, 7, and 11 are primes).

Two elementary facts help illuminate the place of primes among the integers. First, if p_1, p_2, ..., p_n are primes, then $N=1+p_1p_2...p_n$ is not divisible by any of p_1, p_2, ..., p_n (the remainder when *N* is divided by any p_i is 1). Thus either *N* is prime or *N* has a prime divisor other than the p_i. Thus,

Theorem 3.3. (Euclid). There are infinitely many primes.

Also, if *n*>1 is not prime (such an integer is called composite), *n* must have a prime divisor $\leq \sqrt{n}$, since it must have a divisor $\leq \sqrt{n}$ (*n = ab* implies $a \leq \sqrt{n}$ or $b \leq \sqrt{n}$), and that divisor is either prime a or has a prime divisor $\leq \sqrt{n}$. Thus, one can determine if a number $\leq \sqrt{n}$ is prime by eliminating all multiples of the primes $\leq \sqrt{n}$. This method is known as the Sieve of Eratosthenes (Figure 3.1).

For example, all primes < 169=13^2 can be determined by crossing out the multiples of 2, 3, 4, 7, and 11. Indeed, given that every even integer > 2 is composite (since divisible by 2) and every integer >5 is composite (since divisible by 5), one need only consider integers with last digit 1, 3, 7, or 9 and cross out the multiples of 3, 7, and 11. That process is illustrated in the animated Figure 3.1.

2	3	5	7
11	13	17	19
	23		29
31		37	
41	43	47	
	53		59
61		67	
71	73		79
	83		89
		97	
101	103	107	109
	113		
		127	
131		137	139
			149
151		157	
	163	167	

Figure 3.1. Animated Sieve of Eratosthenes. Primes are sifted out that are less than $169 = 13^2$. Thus, only multiples of 2, 3, 5, 7, and 11 need be eliminated. The animation shows the successive elimination of these multiples to reveal the set of all primes less than 169. Click here to see a movie in which the reader can control the animation rate in order to study pattern.

The primes are the building blocks of the integers, since every positive integer can be written uniquely as a product of primes (Fundamental Theorem of Arithmetic). This uniqueness extends only to the primes involved and how many times they are involved; for example, the fact that 12 = 2·2·3 =2·3·2 = 3·2·2 does not violate uniqueness. By convention, we say that 1 is a product of no primes. It is the desire for unique factorization that led to the avoidance of 1 as a prime; obviously, 1 can be included in a factorization of a number as often as desired.

Take a side trip to an application that employs a strategy that is abstractly similar to the method of Eratosthenes. It does so, however, in the urban setting of downtown Ann Arbor, Michigan.

The Euclidean Algorithm

Almost as important as knowing what divisors an integer has is knowing what divisors it shares with other integers. For this allows the consideration of equations relating one integer to another.

Definition 3.4. Let *a, b* be two positive integers. The greatest common divisor (*a, b*) of these two integers is the largest positive integer *d* such that $d|a$ and $d|b$.

For example (12, 16) = 4 since 4|12 4|16, and no greater divisor of 12 (6, 12 are possibilities) is a divisor of 16.

The greatest common divisor is useful in reducing fractions to lowest terms, since if *a/b* is a fraction [a/(a,b)]/[b/(a,b)] is in lowest terms.

For example, 12/16 = [12/4]/[16/4] = ¾.

Definition 3.5. The above definition can be extended to any integer as follows
1. if *a* and *b* are integers, neither of which is equal to 0, then (*a, b*) = (|a|, |b|)
2. if $a \neq 0$, then (*a*, 0) = |a| ((0,0) is not defined).

If the prime factorizations of *a* and *b* are readily available, it is easy to find (*a, b*).

For example, if a = 360 = 2^3 · 3^2 · 5 and b = 756 = 2^2 · 3^3 · 7, then (a,b) = 2^2 · 3^2 =36, since the highest power of 2 which is a factor of (*a, b*) is the lowest power of 2

in the factorizations of a and b (*i.e.* the 2^2 in b).

Unfortunately, it is not always obvious what the prime factorizations of a and b are when the problem of finding (a, b) occurs. A method that is relatively quick and always successful is called the Euclidean Algorithm. It depends on some easy properties of divisibility, familiar from grade school arithmetic and high school algebra.

Suppose a and b are positive integers, $a > b$. Then there are integers q (quotient) and r (remainder) such that $a = bq + r$ and $0 \leq r < b$ (these were first encountered when learning long division in the fourth grade).

For example, $756 = 360(2) + 36$; in fourth grade terms, if we want to computer 756/360, the quotient is 2, the remainder 36.

This division algorithm is closely related to the idea of greatest common divisor, as the following mini-theorem demonstrates.

Mini-Theorem 3.6. Suppose a, b, r are positive integers with $a = bq + r$, $0 < r < b < a$. Then $(a,b) = (b, r)$.
Proof: It is only necessary to show that a, b, r share exactly the same divisors, since then they certainly have the same GREATEST common divisor.

1. First, suppose $n|a$ and $n|b$, say $a = nx$ and $b = ny$. Then $r = a - bq = nx - nyq = n(x - yq)$, so $n|r$.
2. Suppose $n|b$ and $n|r$, say $b = ny$ and $r = nz$. Then $a = bq + r = nyq + nz = n(yq + z)$, so $n|a$.

Mini-Fact 3.7. If $a = bq$, then $(a,b) = b$.

These two small facts are all we need to prove the famous

Euclidean Algorithm 3.8. Suppose a, b are positive integers with $a > b$. Suppose further that

$$a = bq_0 + r_1 \qquad\qquad 0 <$$
$$r_1 < b$$
$$b = r_1 q_1 +$$
$$r_2 \qquad\qquad 0 < r_2 <$$
$$r_1$$
$$r_1 = r_2 q_2 +$$

$$r_3 \qquad\qquad 0 < r_3 <$$

$$r_2$$

$$...$$

$$r_{n-1} = r_n q_n + r_n$$

$$+1 \qquad\qquad 0 < r_{n+1} <$$

$$r_n$$

$$r_n = r_{n+1} q_{n+1}$$

Then $(a, b) = r_{n+1}$, the last non-zero remainder in the process.

Proof: First note that the process defined above is a finite one, since each remainder is smaller than the previous one, with the result that eventually, the integer remainder must become 0. (Computer scientists might be interested in LamÃ©'s Theorem, which proves that this process can take at most $5n$ steps, where n is the number of decimal digits in b.)

By the mini-fact, $(r_n, r_{n+1}) = r_{n+1}$. But, by the mini-theorem, $(a, b) = (b, r_1) = (r_1, r_2) = ... = (r_{n-1}, r_n) = (r_n, r_{n+1})$. Therefore, $(a, b) = r_{n+1}$.

For example,

$$756 = 360(2) + 36$$
$$360 = 36(10)$$

so that $(756, 360) = 36$

It is always possible to express (a, b) as $ma + nb$ for some integers m and n. That this is true can be seen from the Euclidean Algorithm as follows:
$(a, b) = r_{n+1} = r_{n-1} - r_n q_n = r_{n-1} - (r_{n-2} - r_{n-1} q_{n-1}) q_n = ...$.

That is, one can work backwards through the equations until (a, b) is expressed in terms of a and b. But the computations appear quite difficult, and it appears that all the quotients and remainders are needed. But the computation can be done more easily if each remainder is expressed in terms of a and b as the Euclidean Algorithm is carried out. Note that

$$a = 1(a) + 0(b)$$
$$b = 0(a) + 1(b)$$

Then since

$$r_1 = a - bq_0,$$

$$a = 1(a) + 0(b)$$

$$-q_0 b = -q_0(a) - q_0(1)(b)$$

Subtracting

$$r_1 = a - q_0 b = 1a - q_0 b$$

This process can be continued for each remainder.

In fact, the *a* and *b* can be left understood and only their coefficients kept track of. A detailed example follows.

Example. Find d = (6888, 792), and find m, n such that 6888m + 792n = d.

First computation 6888 = 792(8) + 552.

Notice
6888 = 1(6888) + 0(792)
 792 = 0(6888) + 1(792)
  552 = 6888 - 8(792) = [1 - 8(0)]
6888 + [0 - 8(1)](792) = 1(6888) - 8
(792)

so we retain the following information

			6888
1	0		
			792
0	1		
6888 = 792(8) + 552		552	1
-8			

noting that 1 - 8(0) = 1 and 0 - 8(1) = -8 so row 3 above is obtained by subtracting 8(row 2) from row 1.

Second computation 792 = 552(1) + 240.

Notice
240 = 792 - 2(552)
   = [0 - 1(1)]6888 + [1 - 1(-8)]

$$(792) = -1(6888) + 9(792)$$

so we retain the following information

```
                                      6888
            1    0
                                       792
            0    1
             6888 = 792(8) + 552     552
            1   -8
             792 = 552(1) + 240       240   -
            1    9
```

noting row 4 = row 2 - 1(row 3) since 1 is the quotient in the second computation.

Full computation

```
                                      6888
            1    0
                                        792
            0    1
            6888 = 792(8) + 552       552
            1   -8
            792 = 552(1) + 240         240   -
            1    9
            552 = 240(2) + 72           72
            3   -26
            240 = 72(3) + 24            24   -
            10   87
             72 = 24(3)
```

In each case, an **arbitrary row** is obtained by subtracting the **quotient times the row above** from **the row two rows above**.
The result: (6888, 792) = 24, 24 = -10(6888) + 87(792).

This example is illustrated in the animation in Figure 3.2.

Find the **GCD** of 6888 and 792

$$6888 = 792(8) + 552$$
$$792 = 552(1) + 240$$
$$552 = 240(2) + 72$$
$$240 = 72(3) + 24$$
$$72 = \mathbf{24}(3)$$

6888	1	0
792	0	1
552	1	-8
240	-1	9
72	3	-26
24	-10	87
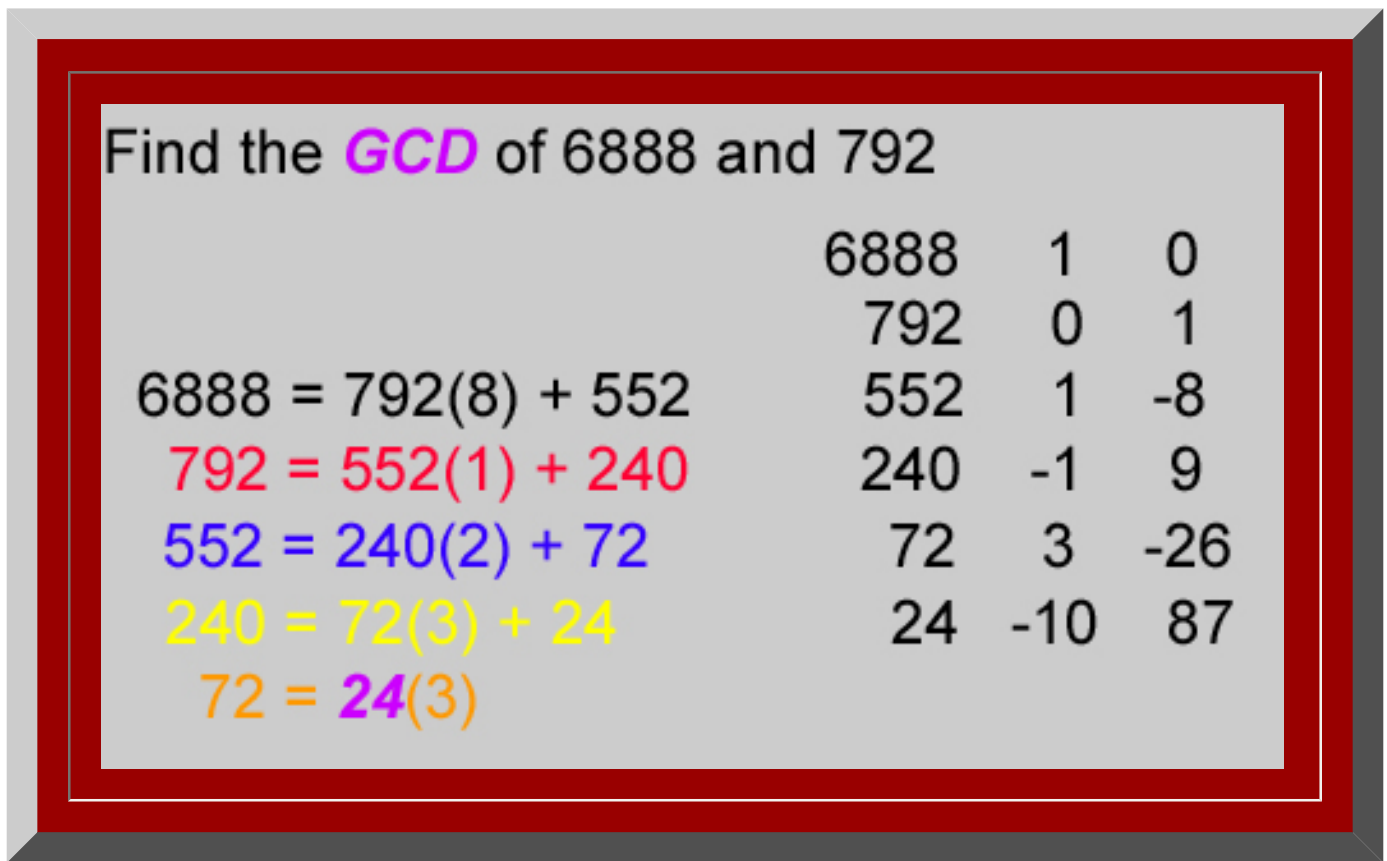
Figure 3.2. Animation of Euclidean Algorithm application. Click here to see a movie in which the reader can control the animation rate in order to study pattern.

The procedure of this section will be of great significance in solving congruences in the next section.

Number-theoretic congruence

One of the most powerful tools of number theory is the notion of congruence, which partitions the integers into finite sets of related integers.

Definition 3.9. Two integers x and y are said to be congruent modulo m (a positive integer) if m is a divisor of $x - y$. This is written $x \equiv y$ (mod m).

The most common place the everyday world uses congruence, albeit not consciously, is in telling time. Any time y a multiple of 12 hours after a time x is called by the same time as x.

For example, 60 hours after 3 o'clock, it is once more 3 o'clock, since $60 + 3 \equiv 3$ modulo 12.

Indeed, it is quite common to use a set of small representatives of all the possibilities modulo m. In telling time, 1, 2, ..., 12 are used for all possibilities. Military time uses 0, 1, ..., 23 for the hours in a day modulo 24. Mathematicians usually use 0, 1, ..., m-1 when they want representatives for the classes of numbers which are congruent modulo m, for the following reason.

Theorem 3.10. If $a = mb + r$, $0 \leq r < n$, then $a \equiv r \pmod{m}$.

Proof: $a - r = mb$, so m is a divisor of $a - r$. Thus the natural representative of a number modulo m is its remainder when divided by m.

In fact, any set of m integers, none of which is congruent to any of the others modulo m, is called a complete residue system modulo m. No doubt this name comes from thinking of remainders as residues (what's left over) after division by m. It is easy to create an addition and multiplication for these residues.

Theorem 3.11. Suppose $x \equiv y \pmod{m}$ and $s \equiv t \pmod{m}$. Then $x + s \equiv y + t \pmod{m}$ and $xs \equiv yt \pmod{m}$.

Proof: Suppose $x - y = am$ and $s - t = bm$. Then $(x + s) - (y + t) = (x - y) + (s - t) = am + bm = (a + b)m$. So $x + s \equiv y + t \pmod{m}$. Also $xs - yt = (xs - xt) + (xt - yt) = x(s - t) + (x - y)t = xbm + amt = m(xb + at)$ So $xs \equiv yt \pmod{m}$.

Telling time is an obvious example of the addition part of this theorem. For instance, 5 hours after 9 o'clock comes 2 o'clock, since $9 + 5 \equiv 2 \pmod{12}$.

Linear congruences

The first type of equation to investigate is the linear congruence $ax \equiv b \pmod{m}$. One needed fact is an easy consequence of the Euclidean Algorithm.

Lemma 3.12. If $a \mid bc$ and $(a, b) = 1$, then $a \mid c$.

Proof: Suppose $bc = ax$. Because $(a, b) = 1$, there are integers m, n such that $1 = ma + nb$. Then $c = cma + cnb = cma + nax = a(cm + nx)$. Thus $a \mid c$.

This allows proof of a limited cancellation theorem. In ordinary algebra, if $ax = ay$, then $x = y$. Such a general theorem is impossible for congruences.

For example, $6(4) \equiv 6(2) \bmod 12$, but 4 is not congruent to 2 mod 12.

However, if $(a, m) = 1$, cancellation is still possible.

Theorem 3.13. If $ax \equiv \pmod{m}$ and $(a, m) = 1$, then $x \equiv y \pmod{m}$.

Proof: Since $ax \equiv ay \pmod{m}$, $a(x - y) \equiv 0 \pmod{m}$. Thus $m \mid a(x - y)$. But, since $(a, m) = 1$, Lemma 3.12 assures $m \mid (x - y)$. Therefore, $x \equiv y \pmod{m}$.

This enables a complete analysis of $ax \equiv b \pmod{m}$ if $(a, m) = 1$.

Theorem 3.14. Suppose $(a, m) = 1$. Then

       a) $ax \equiv 1 \pmod{m}$ has a unique solution $x \equiv t \pmod{m}$
       b) $ax \equiv b \pmod{m}$ has a unique solution $x \equiv tb \pmod{m}$.

Proof:

       a) Since $(a, m) = 1$, there are integers s, t such that $ms + at = 1$, so $at - 1 = ms$. Therefore $at \equiv 1 \pmod{m}$. This is the only solution, since by Theorem 3.13 $at \equiv ay$ $\pmod{m}$ implies $x \equiv y \pmod{m}$.
       b) To solve $ax \equiv b \pmod{m}$, multiply through by this number t. Therefore $t(ax) \equiv tb$ mod m. Since $ta \equiv 1 \pmod{m}$, this gives $x \equiv tb$ mod m. As before, this solution is unique.

The solution of $ax \equiv 1 \pmod{m}$ is sometimes called the inverse a^{-1} of a modulo m, analogous to the fact that $a^{-1} = 1/a$ is the multiplicative inverse of a in ordinary arithmetic. Of course, a natural question arises: what happens if $(a, m) \neq 1$. There are two cases: $(a, m) \mid b$ and $(a, m) \nmid b$.

Theorem 3.15. Suppose $d = (a, m) \nmid b$. Then $ax \equiv b \pmod{m}$ has no solution.

Proof: If $ax \equiv b \pmod{m}$, then $ax - b = my$ for some integer y. Thus $b = ax - my$. But since $d \mid a$ and $d \mid m$, this means $d \mid b$, contrary to the theorem's hypothesis. (Note: $a = ds$, $m = dt$ means $b = dsn - dty = d(sx - ty)$.)

Theorem 3.16. Suppose $d = (a, m) \mid b$. Then $ax \equiv b \pmod{m}$ has a unique solution modulo $m \mid d$ and d solutions modulo m.

Proof: Let $b = dr$, $a = ds$, $m = dt$. Then $ax \equiv b \pmod{m}$ is and only if $ax - b = my$ for some integer y. Substituting for a, b, $cdsx - ds = dty$. Canceling $xs - r = ty$ or $sx \equiv r \pmod{t}$. By Theorem 3.14, this has a unique solution modulo $t = m/d$. Call this solution A (so $sA \equiv r \pmod{t}$). Then, A, $A + t$, ..., $A + (d-1)t$ are the d solutions (modulo m). Note that these are all congruent modulo t but incongruent modulo m, and notice that since $sA - r = tB$ for some B

      $s(A+kt) - r = t(B+sk)$, $k=0, 1, ..., d-1$
      $ds(A+kt) - dr = dt(B+sk)$, $k=0, 1, ..., d-1$
      $a(A+kt) - b = m(B+sk)$, $k=0, 1, ..., d-1$
      $a(A+kt) \equiv b \pmod{m}$, $k=0, 1, ..., d-1$

Fermat's Little Theorem and Euler's Theorem

The ability to solve congruences leads to some interesting results.

Theorem 3.17 (Fermat's Little Theorem) Suppose p is a prime, $(a, p) = 1$. Then $a^{p-1} \equiv 1$ (mod

p).

Proof: Consider the integers $a, 2a, 3a, ..., (p-1)a$. These $p-1$ integers are all incongruent mod p, since by <u>Theorem 3.13</u> $sa \equiv ta$ (mod p) implies $s \equiv t$ (mod p). Since none of them is divisible by p (by Lemma 3.12, if $p \mid ka$, then $p \mid k$, which is false). Thus these $p - 1$ integers are congruent to the integers $1, 2, ..., p-1$ in some order. Therefore, $a(2a)...(p-1)a \equiv 1(2)...(p-1)$ (mod p). By <u>Theorem 3.13</u>, cancellation of $2(3)...(p-1)$ gives $a^{p-1} \equiv 1$ (mod p).

Fermat's Little Theorem can be used to perform some amazing computations. For example, it can be used to compute the remainder when 3^{2460} is divided by 113, certainly a computation unlikely by direct computation. But <u>Theorem 3.17</u> assures $3^{112} \equiv 1$ (mod 113). Simple division gives $2460 = 112(13) + 4$. Therefore $3^{2460} = 3^{112(13)+4} = (3^{112})^{13} 3^4 \equiv 3^4 \equiv 81$ mod 113. So the remainder when 3^{2460} is divided by 113 is 81.

The situation of <u>Theorem 3.17</u> can be generalized.

Definition 3.18. Let m be a positive integer. A complete reduced residue system modulo m is the set of numbers obtained from a complete residue system by removing all the integers which have a factor in common with m.

For example, the integers $1, 2, ..., p-1$ are a reduced residue system modulo a prime p. Also, the integers 1, 3, 7, 11, 13, 17, 19 for a reduced residue system modulo 20.

Definition 3.19. The Euler ϕ - function (phi-function) $\phi(m)$ (or, phi(m) in subscripts or superscripts) is the number of integers in a complete reduced residue system modulo m.

For example $\phi(p) = p-1$, $\phi(20) = 8$.

The Euler ϕ - function has been studied extensively. The interested reader should consult any of the numerous number theory texts listed in the references. <u>Fermat's Little Theorem</u> can be generalized as follows:

Theorem 3.20.(Euler's Theorem) Suppose $(a, m) = 1$. Then $a^{\text{phi}(m)} \equiv 1$ (mod m).

Proof: Let $1, x_2, x_3, ..., x_{\text{phi}(m)}$ be a reduced residue system modulo m. As in <u>Theorem 3.17</u>, a, $a_2, ..., ax_{\text{phi}(m)}$ are all incongruent modulo m; also, since each has no factor in common with m, they form a complete reduced residue system and are congruent to $1, x_2, ..., x_{\text{phi}(m)}$ in some order.

Therefore $a(ax_2) ... (ax_{\text{phi}(m)}) \equiv x_2 x_3 ... x_{\text{phi}(m)}$ mod m, so by cancellation $a^{\text{phi}(m)} \equiv 1$ (mod m).

Again, by way of example, it is easy to compute the remainder when 13^{8059} is divided by 20. By Euler's Theorem, $13^{phi(20)} = 13^8 \equiv 13^3 \pmod{20}$. But $13^2 = 169 \equiv 9 \pmod{20}$. Therefore $13^3 = 13^2(13) \equiv 9(13) \equiv 117 \equiv 17 \pmod{20}$. Thus the remainder is 17.

Wilson's Theorem and Quadratic Residues

Definition 3.21. Let m be a positive integer, $(a, m) = 1$; a is said to be a quadratic residue modulo m if the congruence $x^2 \equiv a \pmod{m}$ has a solution.

A great deal of discussion about quadratic residues centers on prime moduli. The case $p = 2$ is not very interesting, since a is a quadratic residue if and only if $a \equiv 1 \pmod 2$. So odd primes are of the most interest.

Theorem 3.22. Let p be an odd prime. Then the congruence $x^2 \equiv a \pmod p$ has either 0 or 2 solutions modulo p.

Proof: If $s^2 \equiv a \pmod p$, then $(-s)^2 \equiv a \pmod p$, and since p is odd, s and $-s$ are incongruent $\pmod p$. ($s \equiv -s \pmod p$ implies $2s \equiv 0 \pmod p$.) Thus, if there is one solution, there are two solutions. If t is another solution, then $t^2 \equiv a \equiv s^2 \pmod p$. Then $t^2 - s^2 \equiv 0 \pmod p$, so $(t - s)(t + s) \equiv 0 \pmod p$. Thus p is a divisor of either $t - s$ or $t + s$, so either $t \equiv s \pmod p$ or $t \equiv -s \pmod p$. So there are no other solutions.

A surprising consequence of this simple fact is

Theorem 3.23 (Wilson's Theorem) If p is a prime, then $(p - 1)! \equiv -1 \pmod p$.

Proof: If $p = 2$, this just says $1 \equiv -1 \pmod 2$, which is true. If p is an odd prime, the congruence $x^2 \equiv 1 \pmod p$ has the two solutions $x \equiv 1 \pmod p$ and $x \equiv -1 \equiv p - 1 \pmod p$. If a is an integer between 2 and $p - 2$, then the congruence $ax \equiv 1 \pmod p$ has a unique solution by Theorem 3.14, and that solution is not congruent to a modulo p, or a would satisfy $a^2 \equiv 1 \pmod p$, not possible by Theorem 3.22. Thus the integers $2, ..., (p - 2)$ can be grouped into $(p-3)/2$ pairs (a_i, a_i^{-1}), $1 \leq i \leq (p-3)/2$ such that for each i, $(a_i, a_i^{-1}) \equiv 1 \pmod p$. Thus the product $(p-1)! \equiv 1(p-1)(a_i, a_i^{-1})...(a_k, a_k^{-1}) \equiv p - 1 \equiv -1 \pmod p$, where $k = (p-3)/2$.

Quadratic Residues and Euler's Criterion

Suppose p is an odd prime. Clearly $1^2, 2^2, ..., ((p-1)/2)^2$ are all quadratic residues. Further, if $1 \leq x, y \leq (p-1)/2$, then x^2 and y^2 are incongruent modulo p, since $x^2 \equiv y^2 \pmod p$ implies $(x-y)(x+y) \equiv 0 \pmod p$; but then either $p|(x-y)$ and $x = y$ or $p|(x+y)$, which is impossible since $2 \leq x+y \leq p - 1$. So there are $(p-1)/2$ quadratic residues accounted for. But

$(-1)^2$, $(-2)^2$, ..., $(-(p-1)/2)^2$ give the same numbers as 1^2, 2^2, ..., $((p-1)/2)^2$; so since $-(p-1)/2$, ..., -1, 1, ..., $(p-1)/2$ is a complete reduced residue system modulo p, there are exactly $(p-1)/2$ quadratic residues mod p and hence there are $(p-1)/2$ quadratic non-residues modulo p.

Definition 3.24 Legendre symbol. The symbol (a/p), called the Legendre symbol, is defined by $(a/p) =$

> 1 if a is a quadratic residue mod p
> (-1) if a is not a quadratic residue mod p.

Some number theorists write $(0/p)=0$. Clearly $0^2 \equiv 0 \pmod{p}$, but quadratic residues are defined to be relatively prime to the modulus.

Now suppose a is a quadratic residue. Then there is an x with $x^2 = a$. But by <u>Fermat's Little Theorem</u> $x^{p-1} \equiv 1 \pmod{p}$, so $a^{(p-1)/2} = x^2 \equiv 1 \pmod{p}$. On the other hand, suppose a is not a quadratic residue. Then, if $(r, p)=1$, the equation $rx \equiv a \pmod{p}$ has a unique solution $s \pmod{p}$ by <u>Theorem 3.14</u>, and s is not congruent to $r \pmod{p}$ (otherwise a would be a quadratic residue). Thus the elements of the set 1, 2, ..., $p-1$ can be grouped into $(p-1)/2$ pairs, where the product of each pair is $\equiv a \pmod{p}$. Thus $a^{(p-1)/2} \equiv 1(2)...(p-1) \equiv -1$ by <u>Wilson's Theorem</u>. Thus we have proved

Theorem 3.25 Euler's Criterion $(a/p) \equiv a^{(p-1)/2} \pmod{p}$

This enables one to prove some interesting facts about quadratic residues

Theorem 3.26

> a) $(a^2/p) = 1$
> b) $(a/p)=(b/p)$ if $a \equiv b \pmod{p}$
> c) $((ab)/p) = (a/p)(b/p)$
> d) $(-1/p)=(-1)^{(p-1)/2}$

Proof:

a) and b) are obvious, d) is a restatement of <u>Euler's Criterion</u> for $a = 1$, and c) follows since $(ab)^{(p-1)/2} = a^{(p-1)/2} b^{(p-1)/2}$

So -1 is a quadratic residue of primes $p \equiv 1 \pmod 4$, since then $(p-1)/2$ is even but not of primes $p \equiv 3 \pmod 4$, since then $(p-1)/2$ is odd. The product of quadratic residues is a quadratic residue, but so is the product of quadratic non-residues. The product of a residue and a non-residue is a non-residue.

For example, if $p = 7$, the quadratic residues are congruent to 1^2, 2^2, 3^2 (mod 7); that is congruent to 1, 2, 4. Note that -1 is not a residue. Since 2 and 4 are residues, so is $2(4) \equiv 1$(mod 7). Since 3 and 6 are non-residues, $3(6) \equiv 4$(mod 7) is a residue. But $4(6) \equiv 5$(mod 7), the product of a residue and a non-residue, is a non-residue.

Similarly, for $p = 13$ the residues are 1, 3, 4, 9, 10, 12 and the non-residues are 2, 5, 6, 7, 8, 11; -1 $\equiv 12$ (mod 13) is a residue, $4(9) \equiv 10$ (mod 13) is a residue, $5(6) \equiv 4$ (mod 13) is a residue, and $4(7) \equiv 2$(mod 13) is a non-residue.

For $p=11$, the residues are 1, 3, 4, 5, 9; the non-residues 2, 6, 7, 8, 10.

Quadratic Reciprocity

The most famous theorem relating quadratic residues, the Law of Quadratic Reciprocity, was first proved by Gauss.

Theorem 3.27. Gauss's Law of Quadratic Reciprocity.

If p, q are odd primes $(p/q)(q/p) = (-1)^{((p-1)/2)((q-1)/2)} = (-1)^{((p-1)(q-1))/4}$

This theorem has been proved many times in many ways. An example illustrates its power. There are many proofs available on the Internet. Take a look at the linked paper to see one contemporary strategy. Compare the proof of Wilson's Theorem in the linked material to the proof of Wilson's Theorem above in order to gain insight into the strategy in the linked paper. Then, consider the example below and then the proof of the Quadratic Reciprocity law that appears in that link. (Click here, if the link at the beginning of this paragraph fails).

$(p/3)(3/p) = (-1)^{(p-1)(3-1)/4} = (-1)^{(p-1)/2} = (-1/p)$
Therefore, $(p/3)(3/p)(3/p) = (-1/p)(3/p) = (-3/p)$
Therefore $(p/3) = (-3/p)$
But $(p/3) = (1/p)=1$ if $p \equiv 1$ (mod 3) and $(p/3) = (2/3) = -1$. Thus -3 is a quadratic residue of the primes $p \equiv 1$ (mod 3) but not of the primes $p \equiv 2$ (mod 3).

Spatial Synthesis: Centrality and Hierarchy, Volume I, Book 1.
Sandra Lach Arlinghaus and William Charles Arlinghaus

Chapter 4
Geometric Representations for Arbitrary Hierarchies

In the last chapter, we saw the complex mechanics of classical central place theory come alive as a single dynamic system when viewed through the lens of fractal geometry. The fit of the classical and fractal geometric hierarchies is exact. Thus, as one might use a carefully surveyed topographic map, with field-checked spot elevations, as a guide into dense jungle or other unsurveyed landscapes, so too we use our carefully field checked alignment of the classical and the fractal as a guide into unseen or unproven areas of theoretical geography. The difference is that the "field" tests in one case occur in "terrestrial space" while in the other the "field" tests occur in "geometry, number theory, and pure mathematics."

We saw hexagonal hierarchies, of different orientation, cell size, and stacking characteristics, arise from the same base of unit hexagons. These were associated with three integers: 3, 4, and 7. The thoughtful reader might naturally ask a number of questions, such as:

- are there other numbers that would serve as K values or are 3, 4, and 7 the only such values?
    - are 5 or 6 possible K values?
    - are there K values larger than 7?
    - how many K values are there?
    Dacey considered these issues.
- How does one determine the number of sides in a fractal generator that will generate a correct hierarchy for arbitrary K values?
- How does one determine fractal generator shape that will generate a correct hierarchy for arbitrary K values?

In this chapter we offer geometric representations for higher numerical K values. Subsequent chapters will develop the number theory required to execute these constructions.

Coordinatization of the triangular lattice

Previous chapters employed a lattice of points to represent central places as a synthetic (coordinate-free) system. It is straightforward to assign a coordinate system, as well. If a point is given the usual Euclidean coordinate (x,y), based on perpendicular axes, its distance from the origin is easily calculated to be $(x^2 + y^2)^{1/2}$. Thus, there is a natural association of the quadratic expression $x^2 + y^2$ with the point (x,y). Such an expression is sometimes called a quadratic form. Quadratic forms have been studied extensively and material about them will appear in Chapter 5.

When the plane is occupied by a set of hamlets, each equidistant from its nearest neighbors, it seems

more reasonable to pick a coordinate system which gives coordinates (0,0), (1,0), and (0,1) to three hamlets which are vertices of an equilateral triangle. Thus it is natural to have a horizontal *x*-axis and a *y*-axis at angle 60Â° to the *x*-axis, as illustrated in Figure 4.1. Now, however, the calculation of distance between a point with coordinates (*x,y*) and the origin (0,0) is more complicated. Figure 4.1 illustrates the situation when *x* and *y* are both positive. The right triangle whose hypotenuse has length this distance now has vertical side of length $\sqrt{3}\, y/2$ and horizontal side of length *y*/2+*x*. Thus the distance, *d*, is

$$\sqrt{(\sqrt{3}y/2)^2 + (y/2+x)^2} = \sqrt{3y^2/4 + y^2/4 + yx + x^2} = \sqrt{x^2 + xy + y^2}$$

The quadratic form *x*² + *xy* + *y*² is thus associated with the vertex (*x,y*) as both <u>Dacey</u> and <u>Loeb</u> had suggested earlier.
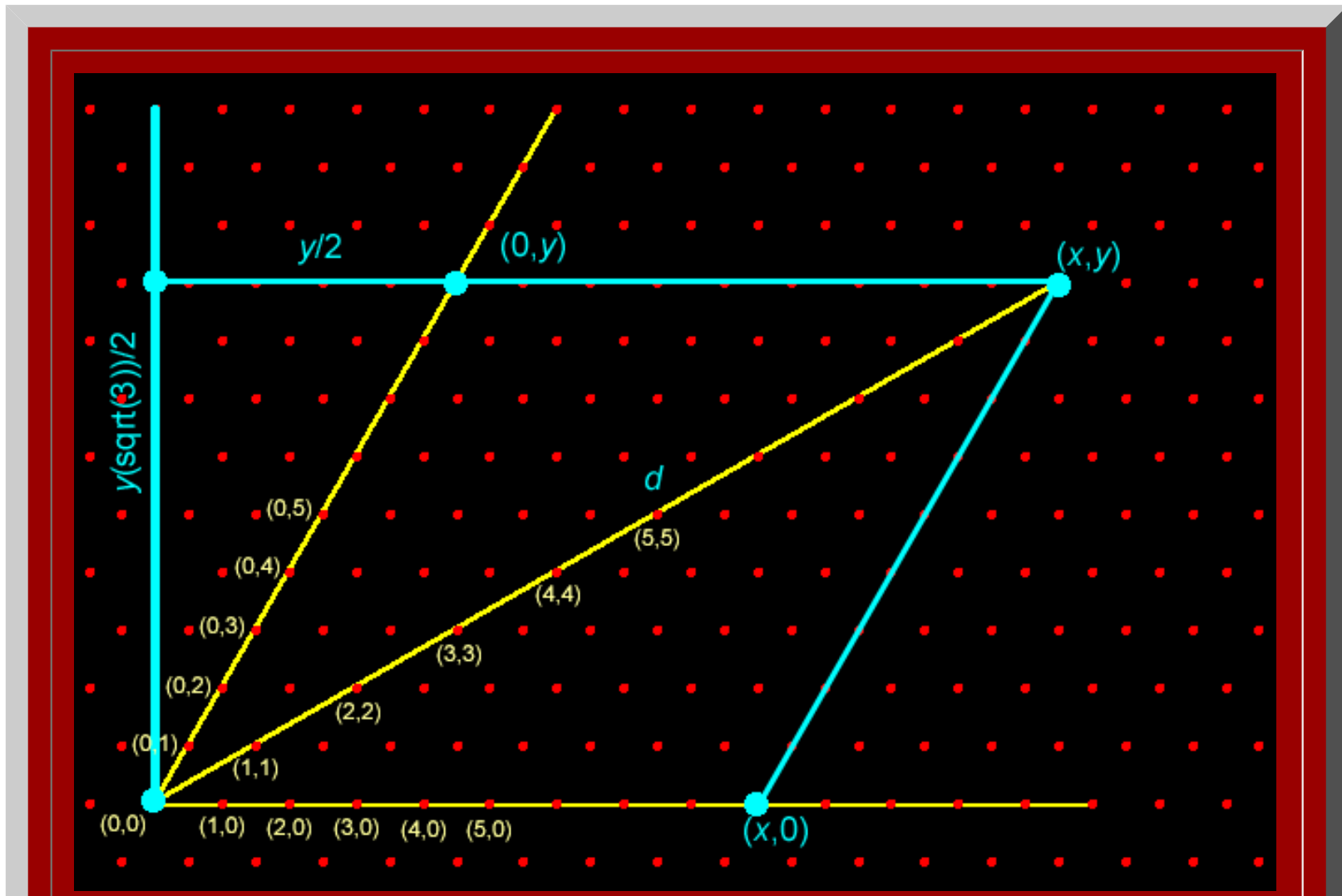
Figure 4.1. The standard *y*-axis of Cartesian coordinates is shown in cyan (turquoise). The yellow lines show the oblique axes. The value *d* represents the distance between the origin and an arbitrary point, (*x*,*y*), drawn in this case on the line *y* = *x* of the oblique axes.

The illustration in Figure 4.1 shows both values as positive. Thus, it must be established that this distance is the same even when *x* and *y* are not both positive. When *x* and *y* are both negative. |*x*| must be substituted for *x*, and |*y*| must be substituted for *y*, but the calculation remains the same.

When exactly one of *x* or *y* becomes negative, the geometry is different. Now the vertical side of the relevant right triangle has side of length

$$\sqrt{3}\,|y|/2$$

but the horizontal side is now of length x-|*y*|/2.

Thus the appropriate distance is

$$\sqrt{(-\sqrt{3}y/2)^2 + (x-(-y)/2)^2} = \sqrt{x^2 + xy + y^2}$$

When *x* is negative and *y* is positive, a similar calculation results.

Thus the form $x^2 + xy + y^2$ is indeed associated with the vertex (*x*,*y*) in this coordinate system. Any positive integer that is equal to $x^2 + xy + y^2$ for some integers *x* and *y* is called Löschian, after August Lösch. One mathematical question that then occurs is: what integers are Löschian? The next chapter (Chapter 5) develops the number theory necessary to answer that question. Other issues involve values of *K* greater than 7 as well as questions involving number of generator sides and generator shape mentioned above. The rest of this chapter deals with these items.

Higher *K*-values: An Infinite Number

Earlier research, by August Lösch, Michael Dacey, and others shows illustrations of *K*-values greater than 7. Indeed, research by Arthur Loeb, in crystallography, and Dacey, in geography, led to independent discovery that the Diophantine equation, $x^2+xy+y^2 = K$ would generate all *K* values when pairs of positive integers were substituted for *x* and for *y*. Thus, when (*x*,*y*)=(1,1) the equation $x^2+xy+y^2 = K$ yields a value of *K*=3; when (*x*, *y*)=(0,2), it follows that *K*=4; and, when (*x*,*y*)=(1,2), it follows that *K*=7. Pairs such as (0,0) and (1,0) yield only trivial results so that the values of 3, 4, and 7 are the three smallest *K*-values. There are no other *K* values less than 7.

The result of Loeb/Dacey is important because it shows

- that there is an infinite number of possible *K* values
- that this infinity of values is in one-to-one correspondence with the integral lattice points in the plane
- that one can give a numerical generating function to create *K* values

Thus, a graph of lattice points in the plane offers a convenient method of visualizing *K*-values larger than 7 (Figure 4.2).

Figure 4.2. The coordinatized lattice points in yellow transform into *K*-values in cyan using the Diophantine equation $K=x^2+xy+y^2$
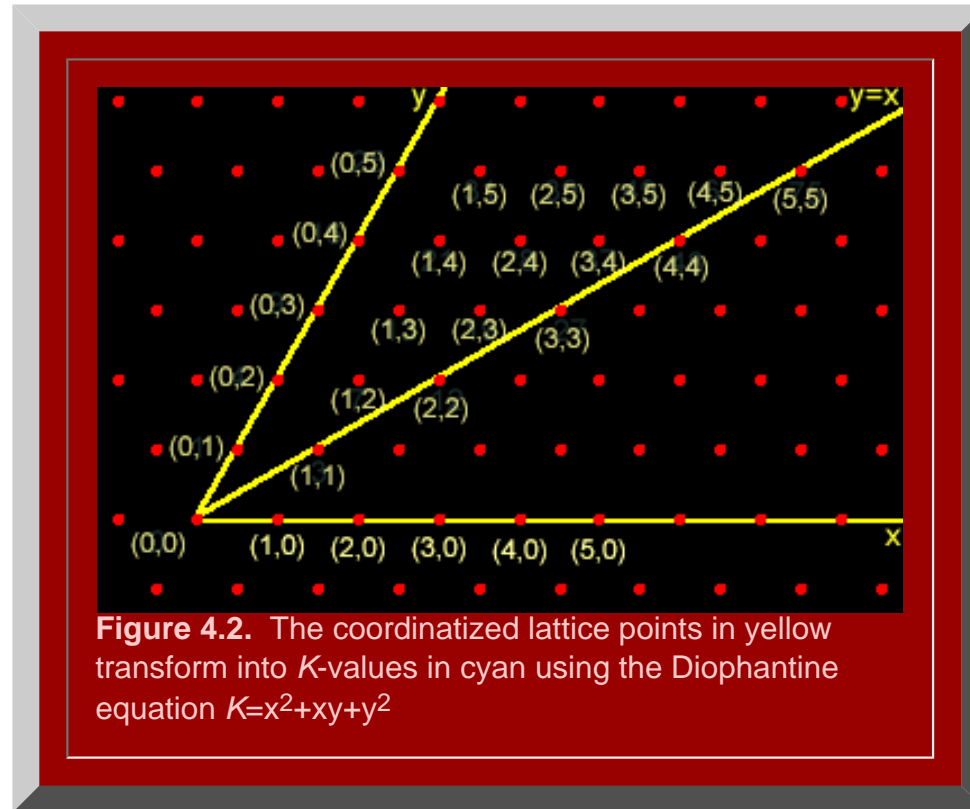
The Diophantine equation, $x^2+xy+y^2 = K,$ is symmetric: the points (1,2) and (2,1) represent different locations in the plane. They both generate the same *K* value. Thus, it suffices to consider only a portion of the available lattice points: those in the first quadrant on one side of the line y=x. Because the pattern of points associated with central place hierarchies is based on a triangular lattice, the graph of lattice points displayed in Figure 4.2 is based on an oblique, rather than on a rectangular, coordinate system with angles at the origin of 60 and 120 degrees. Combining considerations of symmetry and oblique coordinates led to Figure 4.2. In that figure, both coordinate pairs, and corresponding *K*-value generated by the Diophantine equation, are shown.

With an infinite number of *K*-values available, it is a daunting consideration to try to figure out how to create a nested hierarchy of hexagonal trade areas suited to each value of *K*. Simple drawing skills do not suffice.

One needs a formal strategy that can be replicated at will. Fractal geometry will offer that capability.

In the previous chapter, fractal generators appear simply to be plucked out of thin air: there is art in generator selection. Actually, the generator for the *K*=7 hierarchy suggested itself naturally with observations of overfit/underfit of the six small hexagons in relation to the boundary of the next larger one (Figure 4.3). From there, it was simply a matter of educated guessing and trial and error to find generators for *K*=3 and *K*=4 hierarchies. Someone with considerable experience working with this approach might, for example, figure out a fractal generator for a *K*=76 hierarchy, associated with the lattice point (4,6) (Figure 4.4). For replication by arbitrary individuals to be successful, however, one needs to capture the art in the formalized theory and language of mathematics: to transform art into science.
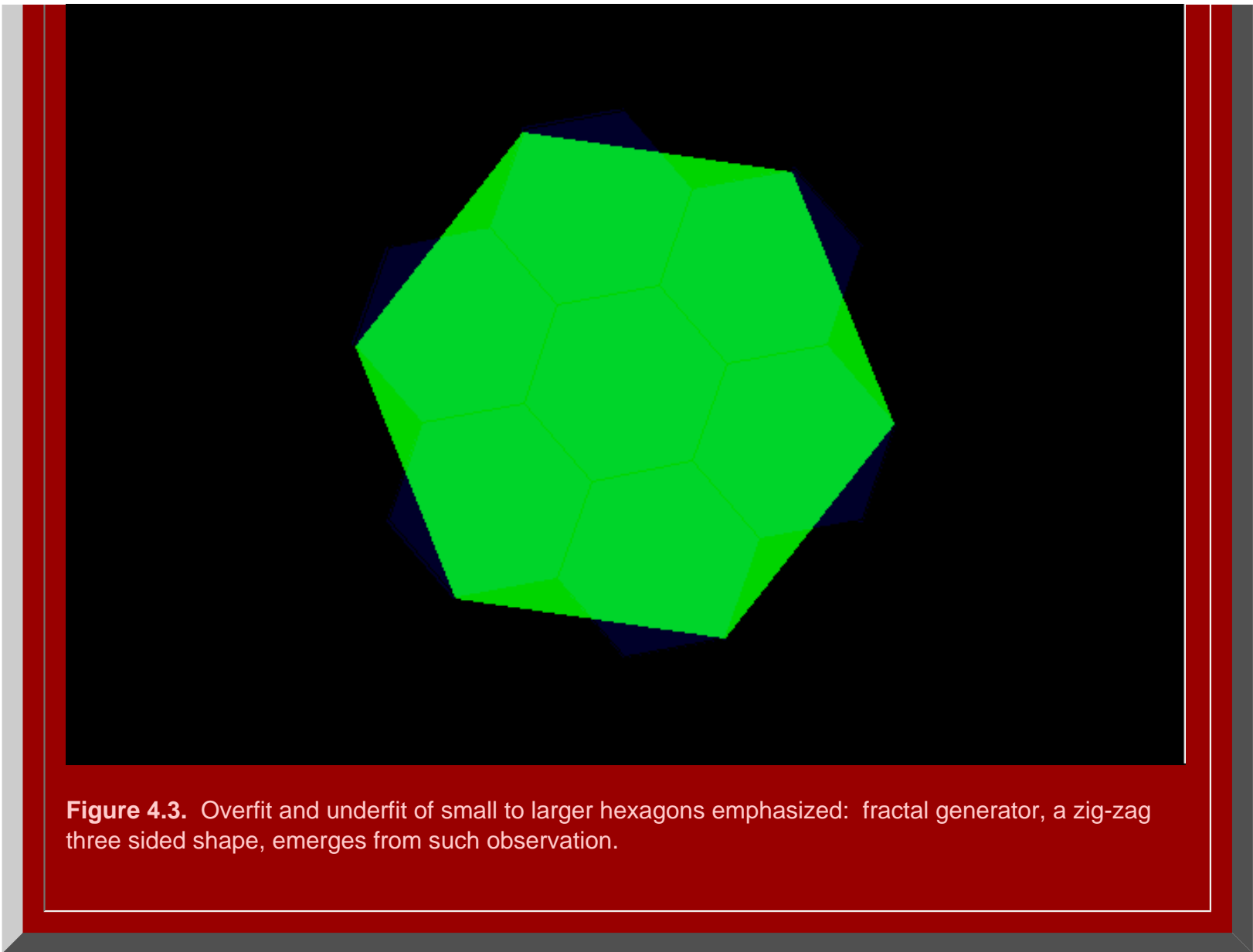
Figure 4.3. Overfit and underfit of small to larger hexagons emphasized: fractal generator, a zig-zag three sided shape, emerges from such observation.

Figure 4.4. *K*=76 fractal generation; corresponding lattice point has coordinates (4,6). The generator shape appears at the edge.
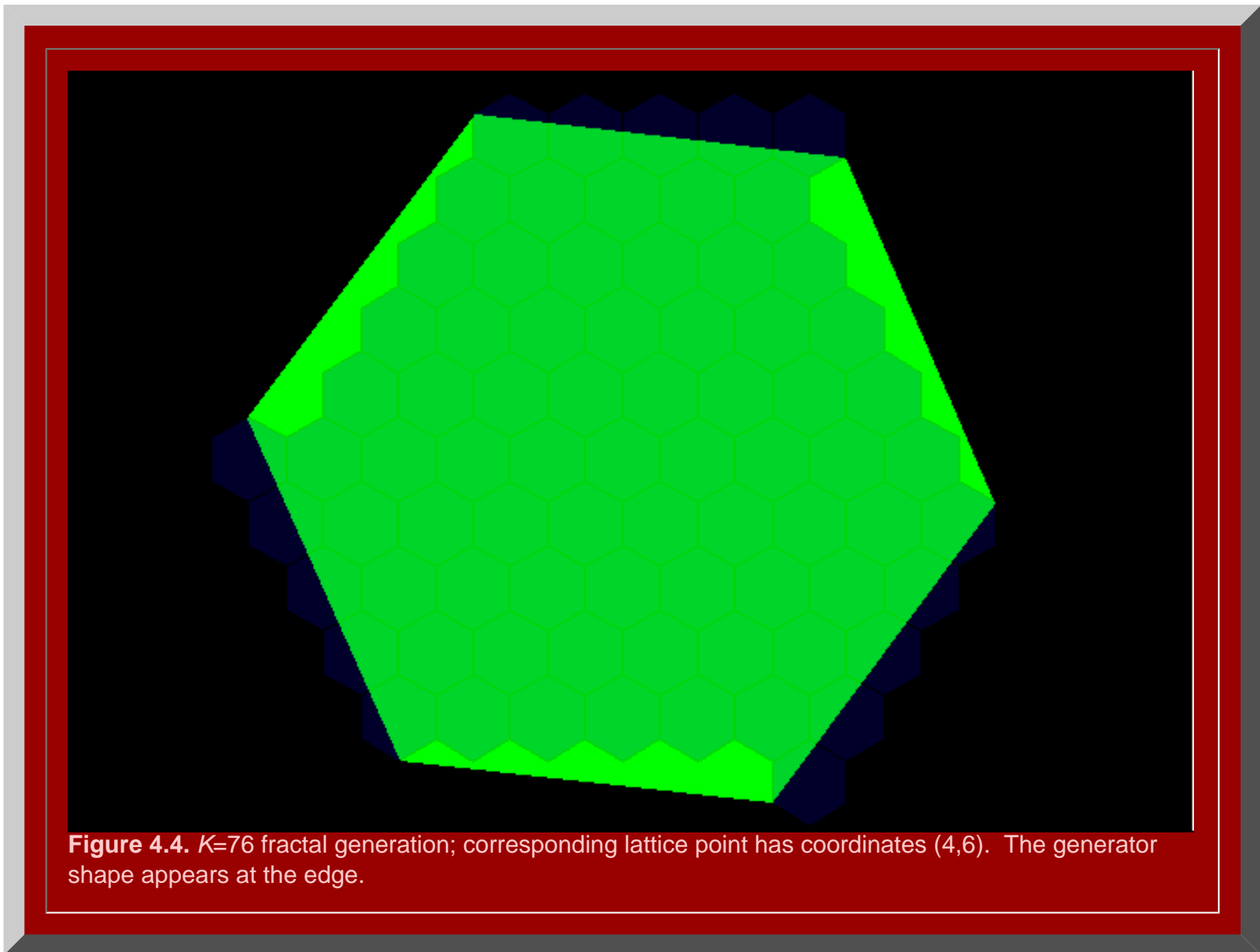
Fractal Generation of Arbitrary K-Values: Geometric Evidence

Once one generator shape is known, can it be used to determine other generator shapes? The answer is yes. The table in Table 4.1 illustrates that the *K*=3 generator, with a half a "hexstep" added, leads to the *K*=7 generator.
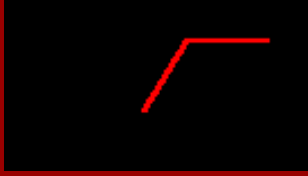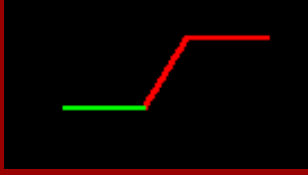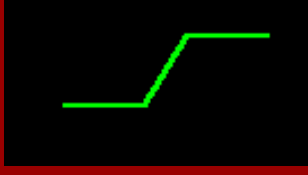
Table 4.1. The K=3 generator leads to the K=7 generator.

 To try to uncover pattern useful in creating fractal generators for arbitrary K values, we begin by looking at a subset of K values: those along the y-axis, only. In that case, because $x^2+xy+y^2 = 0 + 0 + y^2 = K$, it follows that the square root of K is an integer and that the lattice points $(0,y)$ on the y-axis may be rewritten as $(0,$

$\sqrt{K}$). Trial and error with finding fractal generators for selected values along the y-axis produced the table of generators shown in Figure 4.5. The trivial value of K=1, associated with the point $(0,1)$ is not shown in this figure. Within that "trial and error" process a pattern emerged, demonstrated in the animated Figure 4.5.

- Begin with the K=4 generator (lowest value on the y-axis): generator in red.
  - To the previous generator, add a full hexstep to the left of it and a half hexstep, curled under, to the right: generator in green. This new generator produces the K=9 hierarchy.
  - To the previous generator, add a half hexstep to the left (flat portion of the step): generator in blue. This new generator produces the K=16 hierarchy.
- Add two full hexsteps, one on each side, to the K=4 generator, creating a symmetric generator that produces the K=25 hierarchy.
  - To the previous generator, add a full hexstep to the left of it and a half hexstep, curled under, to the right:

generator in green. This new generator produces the *K*=36 hierarchy.

- ○ To the previous generator, add a half hexstep to the left (flat portion of the step): generator in blue. This new generator produces the *K*=49 hierarchy.

- Add two full hexsteps, one on each side, to the *K*=25 generator, creating a symmetric generator that produces the *K*=64 hierarchy.
  - ○ To the previous generator, add a full hexstep to the left of it and a half hexstep, curled under, to the right: generator in green. This new generator produces the *K*=81 hierarchy.
  - ○ To the previous generator, add a half hexstep to the left (flat portion of the step): generator in blue. This new generator produces the *K*=100 hierarchy.
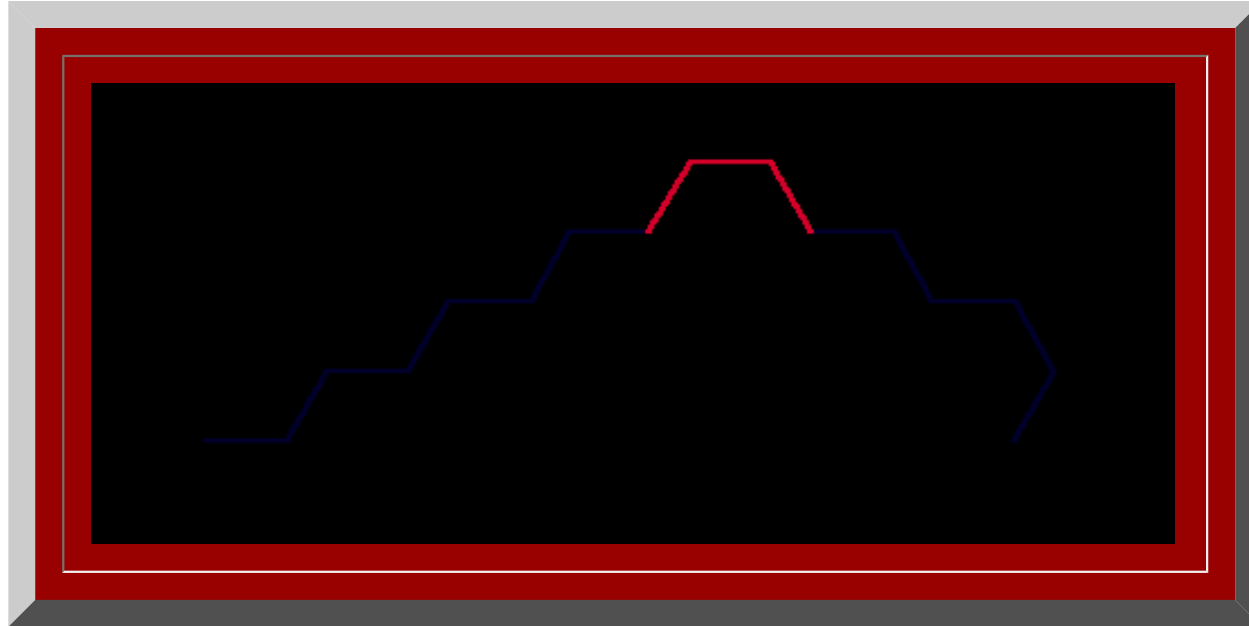
Lattice Coordinate	*K*-value (y-axis values)	Generator Shape	Hierarchy Type

| (0,2) | *K*=4 | | 4 |
| (0,3) | *K*=9 | | 3 |
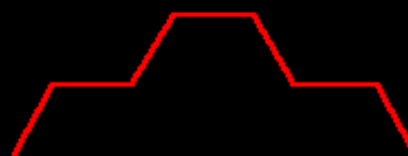
(0,4)	*K*=16		7
(0,5)	*K*=25		4
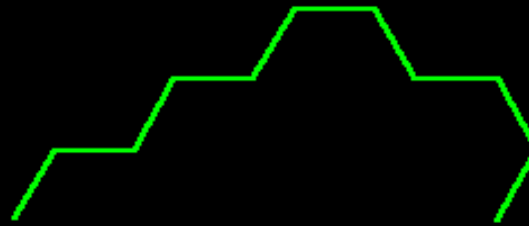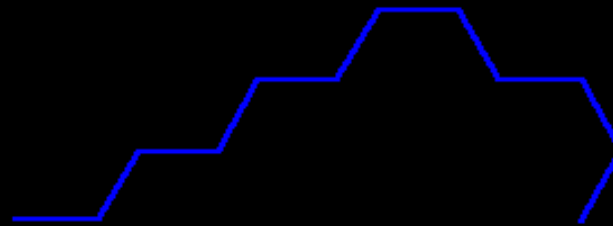
| (0,6) | *K*=36 | | 3 |
| (0,7) | *K*=49 | | 7 |

| (0,8) | *K*=64 | | 4 |
| (0,9) | *K*=81 | | 3 |
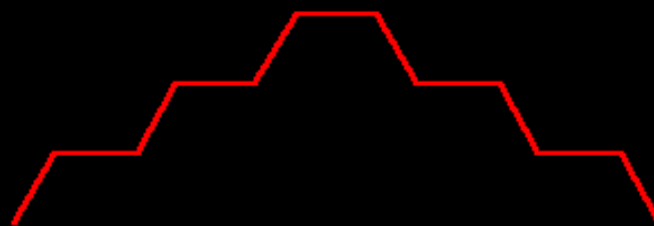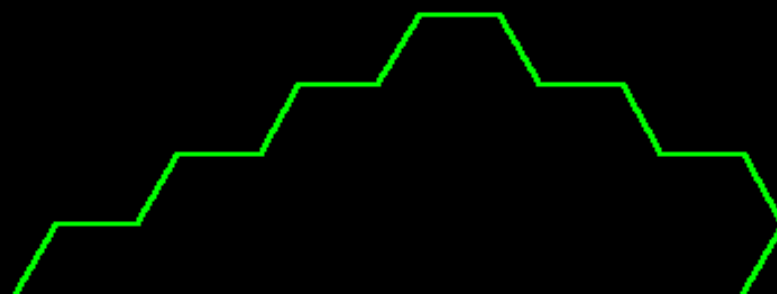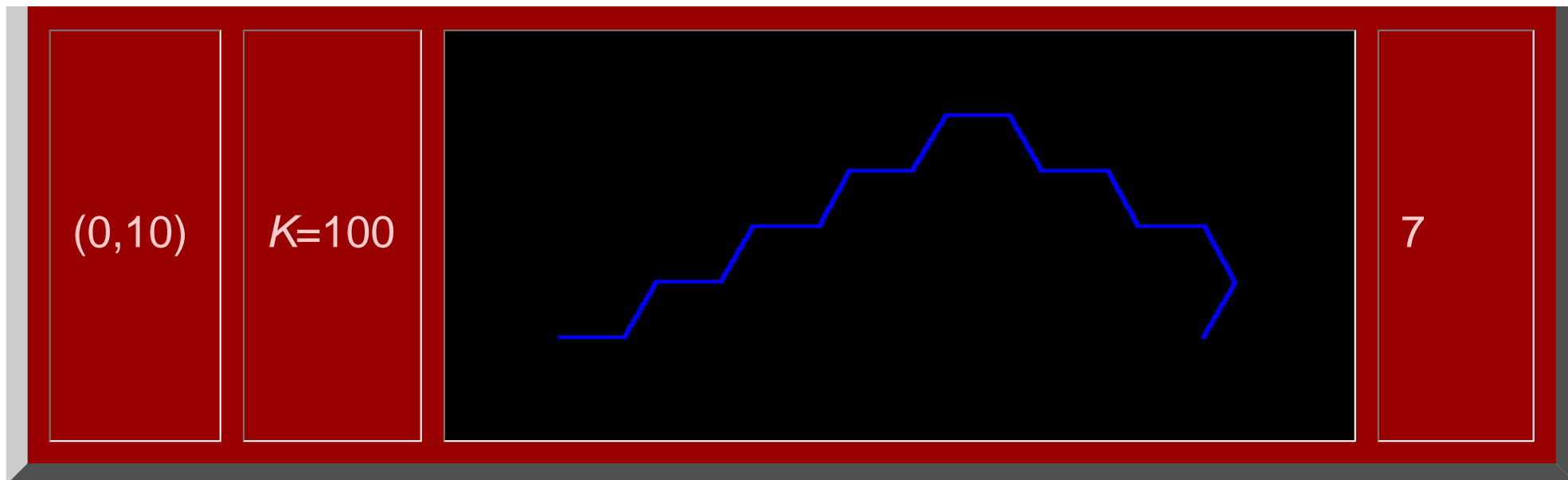
Figure 4.5. Fractal generators for selected values on the y-axis of lattice points generated by $x^2+xy+y^2 = K$. Animation and static versions.

Broadly speaking, we observe the following pattern (refer for this discussion to the static portion of Figure 4.5; the colors match).

- **(0,2), K=4.** Begin with the isosceles trapezoidal shape of the K=4 hierarchy.
  - Note its bilateral symmetry about a vertical line.
  - Note that it takes two sides to climb the right side to the top of the generator
- **(0,3), K=9.** For K=9, begin with the K=4 generator and
  - add one full hex-step to the left
  - add one half hex-step to the right, tucked under at 120 degrees
  - note that it takes three sides to climb the right side to the top of the generator, one more than it did for the "begin" value
- **(0,4), K=16.** For K=16, begin with the K=9 generator and
  - add one half level part of a hex-step to the left
  - note that it takes the same number of sides to climb the right side to the top of the generator as it did in the previous case.
- **(0,5), K=25.** For K=25, begin with the K=4 generator and
  - add a full hex-step to the left
  - add a full hex-step to the right
  - note that it takes four sides to climb the right side to the top of the generator
  - note the bilateral symmetry about a vertical line
- **(0,6), K=36.** For K=36, begin with the K=25 generator and

- - add one full hex-step to the left
  - add one half hex-step to the right, tucked under at 120 degrees
  - note that it takes one more side to climb the right side to the top of the generator than it did for the "begin" value
- **(0,7), K=49.** For K=49, begin with the K=36 generator and
  - add one half level part of a hex-step to the left
  - note that it takes the same number of sides to climb the right side to the top of the generator as it did in the previous case.
- **(0,8), K=64.** For K=64, begin with the K=25 generator and
  - add a full hex-step to the left
  - add a full hex-step to the right
  - note that it takes six sides to climb the right side to the top of the generator
  - note the bilateral symmetry about a vertical line
- **(0,9), K=81.** For K=81, begin with the K=64 generator and
  - add one full hex-step to the left
  - add one half hex-step to the right, tucked under at 120 degrees
  - note that it takes one more side to climb the right side to the top of the generator than it did for the "begin" value
- **(0,10), K=100.** For K=100, begin with the K=81 generator and
  - add one half level part of a hex-step to the left
  - note that it takes the same number of sides to climb the right side to the top of the generator as it did in the previous case.

continue, using the pattern without Figure 4.5

- **(0,11), K=121.** For K=121, begin with the K=64 generator and
  - add a full hex-step to the left
  - add a full hex-step to the right
  - note that it takes eight sides to climb the right side to the top of the generator
  - note the bilateral symmetry about a vertical line
- **(0,12), K=144.** For K=144, begin with the K=121 generator and
  - add one full hex-step to the left
  - add one half hex-step to the right, tucked under at 120 degrees
  - note that it takes one more side to climb the right side to the top of the generator than it did for the "begin" value

After a number of cases, there appears to be a clear pattern, color-coded as red-green-blue. If that pattern is correct, then the reader could, through successive (but perhaps tedious) application of this pattern, produce a fractal generator for an arbitrary value on the y-axis. We will show a more systematic procedure later in

this Chapter for finding generator size and shape; it will, however, be based on the observations above, so it is important that the reader have a clear understanding of them.

To produce generators for K-values not on the y-axis is also a simple matter of examining pattern. Figure 4.6 shows how to form generators for all other *K*-values (not on the *y*-axis) simply by adding hex-steps to the *y*-axis *K*-value generators as one moves to the right across lines of lattice points parallel to the line *y=x* (cyan lines in Figure 4.7). Thus, the reader could then form a fractal generator for an arbitrary *K*-value.

Y-axis value and line position	Fractal generators off the *y*-axis as determined by *y*-axis generator shape.
(0,0): the first generator appears for *K*=3 (not on the *y*-axis; *K*=0, on the *y*-axis, is disregarded) and subsequent generators appear for *K*-values of 12, 27, and 48 as one moves to the right across the line *y=x*.	
(0,1): the first generator appears for *K*=7 (not on the *y*-axis; *K*=1, on the *y*-axis, is disregarded) and subsequent generators appear for *K*-values of 19, 37, and 61 as one moves to the right across the line displaced by 1 from, and parallel to, the line *y=x*.	
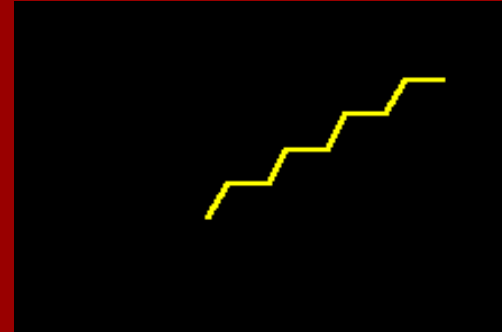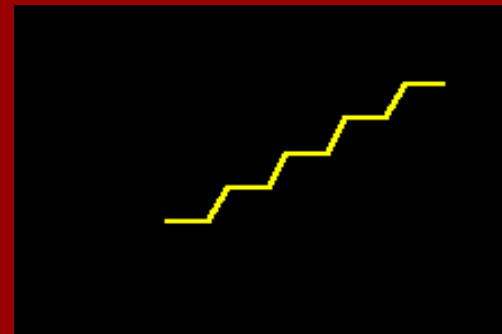
(0,2): the first generator appears for *K*=4 and subsequent generators appear for *K*-values of 13, 28, 49, and 76 as one moves to the right across the line displaced by 2 from, and parallel to, the line *y*=*x*.
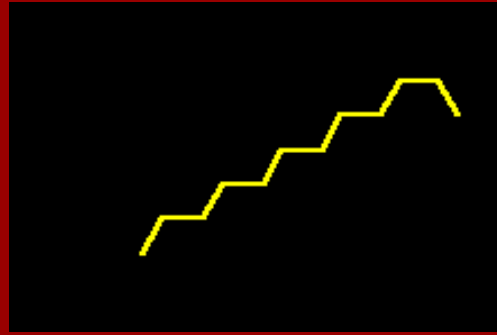
(0,3): the first generator appears for *K*=9 and subsequent generators appear for *K*-values of 21, 39, 63, and 93 as one moves to the right across the line displaced by 3 from, and parallel to, the line *y*=*x*.
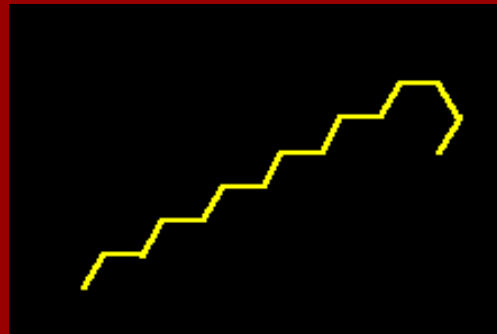
Figure 4.6. Fractal generators are produced for arbitrary *K*-values from *y*-axis *K*-values. See the cyan lines in Figure 4.7.

Fractal Generation of Arbitrary K-Values: the Cross-cut Equation as a Systematic Characterization of Generator Size and Shape

In Figure 4.5, the "red" category corresponds to a generator type similar to the *K*=4 generator: an isosceles trapezoid with some number of hex-steps on either side, producing a bilaterally symmetric form. The "blue" category corresponds to a generator type similar to the *K*=7 category, identical to the previous case but with one half level hex-step added to the left. If one looks at the trivial cases of *K*=0 and *K*=1 in Figure 4.6, this style of pattern is evident in moving from *K*=3 to *K*=7. Thus, it appears that there are really only three basic, or primitive, styles of generator type: *K*=3 (green), *K*=4 (red), and *K*=7 (blue). Because generator shape on the *y*-axis determines generator shape off the axis along rays parallel to the line *y*=*x* (cyan lines in Figure 4.7), we next consider partitioning the set of all *K* values according to these three categories using a set of parallel rays (cyan lines in Figure 4.7) to create that partition. Thus, we seek another equation to represent that partition with the intent of using it to cut across the Diophantine equation and provide straightforward solution to finding the number of sides and the shape of fractal generators for arbitrary *K*-values.

The pattern of numerical K values along rays parallel to $y=x$, shown as cyan lines, is captured in Figure 4.7. Thus,

- along $y=x$, we have $K=3x^2$: the K values along that ray, only, are generated exactly by substituting 0, 1, 2, 3, 4,... into that equation yielding K values of 0, 3, 12, 27, 48, ...
- along the ray displaced 1 unit from the line $y=x$, we have $K=3x^2+3x+1$: the K values along that ray, only, are generated exactly by substituting 0, 1, 2, 3, 4,... into that equation yielding K values of 1, 7, 19, 37, 61,...
- along the ray displaced 2 units from the line $y=x$, we have $K=3x^2+6x+4$: the K values along that ray, only, are generated exactly by substituting 1, 2, 3, 4,... into that equation yielding K values of 4, 13, 28, 49, 76,...
- along the ray displaced 3 unit from the line $y=x$, we have $K=3x^2+9x+9$: the K values along that ray, only, are generated exactly by substituting 0, 1, 2, 3, 4,... into that equation yielding K values of 9, 21, 39, 63, 93,...
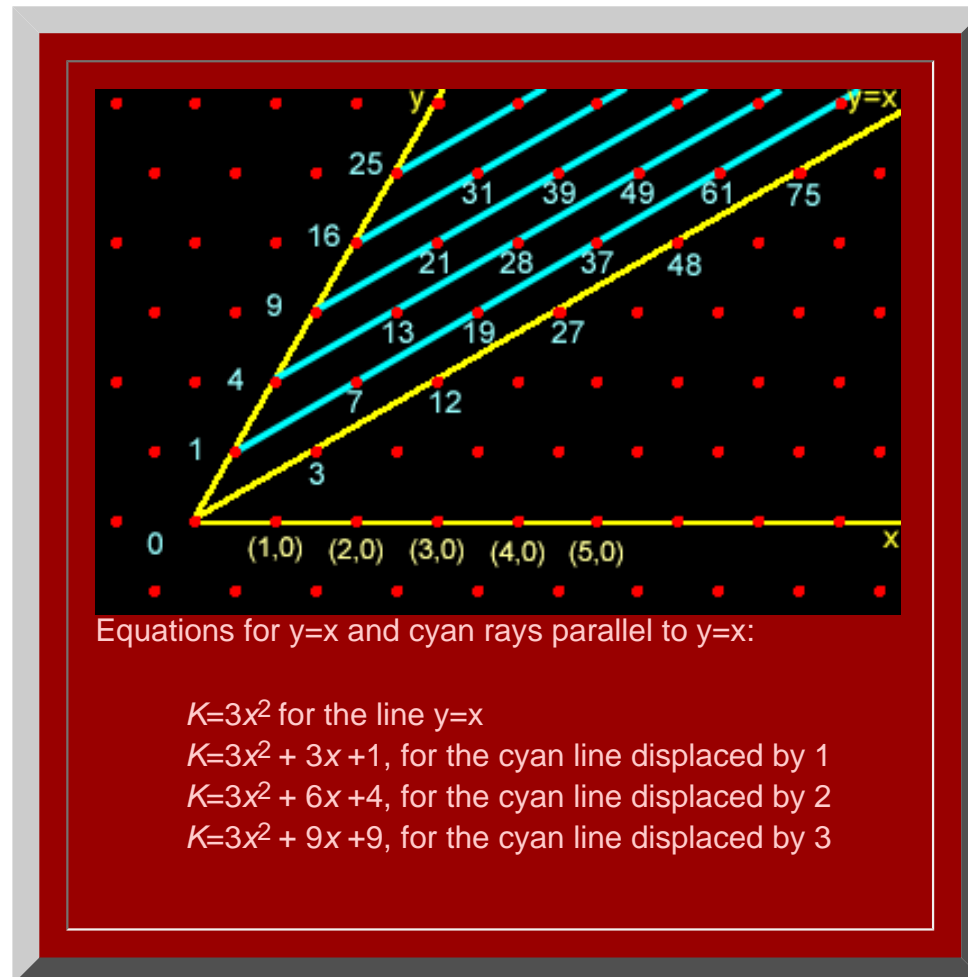
Figure 4.7. Pattern suggesting cross-cut equation. The equation for the cyan rays, parallel to $y=x$, generate exactly the K-values associated with lattice points along that ray (when integers are substituted into

those equations..

Generalizing from the observed pattern, it appears that the equation $K=3x^2 + 3bx +b^2$, where b counts the number of units the ray is displaced from $y=x$, will serve to capture all the K-values associated with the lattice points along a single horizontal ray parallel to $y=x$ (cyan, Figure 4.7), and to capture no others elsewhere. This idea is stated in the following theorem; the next chapter will present some of the number theoretic infrastructure behind it.

Fundamental Theorem (S. Arlinghaus, <u>1985</u>, and S. Arlinghaus in S. and W. Arlinghaus, <u>1989</u>).

> In a triangular central place lattice, the central place K-values, lying along any single one of the rays parallel to the line $y=x$, are generated by substituting non-negative integral values into a quadratic equation $K=3x^2 + 3bx +b^2=3x^2+3(\sqrt{K})x+(\sqrt{K})^2$, where $b=0, 1, ..., n,...$ counts the number of units the ray is translated from $y=x$.

Thus, any single K value has two quadratic equations that represent it. We now proceed to use properties of these quadratic equations to extract information from them sufficient to determine the number of fractal generator sides and number of hex-steps for arbitrary K values from algebraic information, alone. Thus, an informed reader will have the capability to replicate the results, independent of relative position on any image. As an analogy, this process is similar to using latitude and longitude as numerical measures to determine absolute position on the earth-sphere rather than using parallels and meridians as geometric measures to determine relative position on the earth-sphere.

Number of Generator Sides

The patterns observed appear often to involve partitions related to the number 3. Thus, we consider a value based on divisibility by 3 as one index.

Define an integral value j, using K-values along the y-axis, only, as:

- If K is <u>congruent</u> to 0(mod 3), then $j=(\sqrt{K}) / 3$;

- If K is not congruent to 0(mod 3), then $j=((\sqrt{K})-1)/3$ or $j=((\sqrt{K})-2)/3$, which ever is an integer (clearly, both cannot be integers--K leaves either a remainder of 1 or of 2 when divided by 3).

As some examples:

- **when $K=4$**, then 4 is not evenly divisible by 3 so that K is not congruent to 0(mod 3). Thus, one of $j=((\sqrt{K})-1)/3$

or $j=((\sqrt{K})-2)/3$ is an integer. Indeed, $j=((\sqrt{K})-2)/3 = (2-2)/3=0$ is an integer.

- **when K=9**, then 9 is evenly divisible by 3 so that K is congruent to 0(mod 3). Thus, $j=(\sqrt{K})/3 = 3/3 = 1$.
- **when $K = 16$**, then 16 is not evenly divisible by 3 so that K is not congruent to 0(mod 3). Thus, one of $j=((\sqrt{K})-1)/3$ or $j=((\sqrt{K})-2)/3$ is an integer. Indeed, $j=((\sqrt{K})-1)/3 = (4-1)/3=1$ is an integer.
- **when K=25**, then 25 is not evenly divisible by 3 so that K is not congruent to 0(mod 3). Thus, one of $j=((\sqrt{K})-1)/3$ or $j=((\sqrt{K})-2)/3$ is an integer. Indeed, $j=((\sqrt{K})-2)/3 = (5-2)/3=1$ is an integer.
- **when K=36**, then 36 is evenly divisible by 3 so that K is congruent to 0(mod 3). Thus, $j=(\sqrt{K})/3 = 6/3 = 2$.
- **when K=49**, then 49 is not evenly divisible by 3 so that K is not congruent to 0(mod 3). Thus, one of $j=((\sqrt{K})-1)/3$ or $j=((\sqrt{K})-2)/3$ is an integer. Indeed, $j=((\sqrt{K})-1)/3 = (7-1)/3=2$ is an integer.
- **when K=64**, then 64 is not evenly divisible by 3 so that K is not congruent to 0(mod 3). Thus, one of $j=((\sqrt{K})-1)/3$ or $j=((\sqrt{K})-2)/3$ is an integer. Indeed, $j=((\sqrt{K})-2)/3 = (8-2)/3=2$ is an integer.
- **when K=81**, then 8 is evenly divisible by 3 so that K is congruent to 0(mod 3). Thus, $j=(\sqrt{K})/3 = 9/3 = 3$.
- **when K=100**, then 100 is not evenly divisible by 3 so that K is not congruent to 0(mod 3). Thus, one of $j=((\sqrt{K})-1)/3$ or $j=((\sqrt{K})-2)/3$ is an integer. Indeed, $j=((\sqrt{K})-1)/3 = (10-1)/3=3$ is an integer.
- **when K=121**, then 121 is not evenly divisible by 3 so that K is not congruent to 0(mod 3). Thus, one of $j=((\sqrt{K})-1)/3$ or $j=((\sqrt{K})-2)/3$ is an integer. Indeed, $j=((\sqrt{K})-2)/3 = (11-2)/3=3$ is an integer.
- **when K=144**, then 144 is evenly divisible by 3 so that K is congruent to 0(mod 3). Thus, $j=(\sqrt{K})/3 = 12/3 = 4$.

The examples above are color-coded using the scheme of the geometric table to suggest pattern in the output of j-values. What the pattern suggests is, for K-values on the y-axis only,

- when K is congruent to 0(mod 3), then the number of sides for a fractal generator is given by $2+4j$
- when K is not congruent to 0(mod 3), then the number of sides for a fractal generator is given by $3+4j$.

Number of Generator Hex-steps: Generator Shape
    To count the number of hex-steps for an arbitrary K-value on the y-axis, we employ not only the j-value calculated in the previous section, but also the well-known discriminant (square root of ($B^2 - 4AC$) in $Ax^2 +$

$Bx + C$) of a <u>quadratic form</u>. Once again, we begin by considering a number of examples in order to study pattern and to piece it together with other pattern that is known. From the Fundamental Theorem, we know that $K = 3x^2 + 3(\sqrt{K})x + (\sqrt{K})^2$. The discriminant of this equation is $D = (3(\sqrt{K}))^2 - 4\cdot3(\sqrt{K})^2 = 9K - 12K = -3K$. To count the number of hex-steps for a fractal generator for a y-axis K-value, follow the strategy below:

- if K is congruent to 0(mod 3) and
    - if D is congruent to 1(mod 4), then the number of generator hex-steps is equal to the greatest integer in $(2+4j)/2 = 1+2j$.
    - if D is congruent to 0(mod 4), then the number of generator hex-steps is equal to the greatest integer in $(2+4j)/2 = 1+2j$.
- if K is not congruent to 0(mod 3) and
    - if j is even (divisible by 2) then
        - if D is congruent to 1(mod 4), then the number of generator hex-steps is equal to the greatest integer in $(3+4j)/2$.
        - if D is congruent to 0(mod 4), then the number of generator hex-steps is equal to the greatest integer in $(5+4j)/2$.
    - if j is odd (not divisible by 2) then
        - if D is congruent to 1(mod 4), then the number of generator hex-steps is equal to the greatest integer in $(5+4j)/2$.
        - if D is congruent to 0(mod 4), then the number of generator hex-steps is equal to the greatest integer in $(3+4j)/2$.

Looking at some examples, again, the color-coding of red-green-blue shows that the number theoretic patterns provide an exact fit with the geometric pattern and they do so without requiring seeing previous cases: the number theoretic patterns offer absolute measures, replicable independent of examination of previous cases.

Thus, for K-values on the y-axis,

- **when $K=4$**, then $D = -3K = -12$ which is evenly divisible by 4. In addition, K is not congruent to 0(mod 3) and $j=0$ from above, which is even. Thus, the number of hex-steps is the greatest integer in $(5+4j)/2$ which is 2.
- **when $K=9$**, then $D = -3K = -27$ which is not evenly divisible by 4 and leaves a remainder of 1. In addition, K is congruent to 0(mod 3) and $j=1$ from above. Thus, the number of hex-steps is the greatest integer in $1+2j$ which is 3.
- **when $K = 16$**, then $D = -3K = -48$ which is evenly divisible by 4. In addition, K is not congruent to 0(mod 3) and $j=1$ from above, which is odd. Thus, the number of hex-steps is the greatest integer in $(3+4j)/2$ which is 3.
- **when $K=25$**, then $D = -3K = -75$ which is not evenly divisible by 4 and leaves a remainder of 1. In addition, K is not congruent to 0(mod 3) and $j=1$ from above, which is odd. Thus, the number of hex-steps is the greatest integer in $(5+4j)/2$ which is 4.
- **when $K=36$**, then $D = -3K = -108$ which is not evenly divisible by 4 and leaves a remainder of 1. In addition, K is congruent to 0(mod 3) and $j=2$ from above. Thus, the number of hex-steps is the greatest integer in $1+2j$ which is 5.
- **when $K=49$**, then $D = -3K = -147$ which is not evenly divisible by 4. In addition, K is not congruent to 0(mod 3) and $j=2$ from above, which is even. Thus, the number of hex-steps is the greatest integer in $(3+4j)/2$ which is 5.

- **when $K=64$**, then $D = -3K = -192$ which is evenly divisible by 4. In addition, K is not congruent to 0(mod 3) and $j=2$ from above, which is even. Thus, the number of hex-steps is the greatest integer in $(5+4j)/2$ which is 6.
- **when $K=81$**, then $D = -3K = -243$ which is not evenly divisible by 4 and leaves a remainder of 1. In addition, K is congruent to 0(mod 3) and $j=3$ from above. Thus, the number of hex-steps is the greatest integer in $1+2j$ which is 7.
- **when $K=100$**, then $D = -3K = -300$ which is evenly divisible by 4. In addition, K is not congruent to 0(mod 3) and $j=3$ from above, which is odd. Thus, the number of hex-steps is the greatest integer in $(3+4j)/2$ which is 7.
- **when $K=121$**, then $D = -3K = -363$ which is not evenly divisible by 4 and leaves a remainder of 1. In addition, K is not congruent to 0(mod 3) and $j=3$ from above, which is odd. Thus, the number of hex-steps is the greatest integer in $(5+4j)/2$ which is 8.
- **when $K=144$**, then $D = -3K = -432$ which is not evenly divisible by 4 and leaves a remainder of 1. In addition, K is congruent to 0(mod 3) and $j=4$ from above. Thus, the number of hex-steps is the greatest integer in $1+2j$ which is 9.

■ ■ ■ ■ ■ ■ ■ ■ .....

Use of the Fundamental Theorem

The following example shows how to determine the b-value corresponding to an arbitrary Löschian number and therefore create a second Diophantine expression of that number. Suppose it has been determined, using the sufficient condition given in the Fundamental Theorem, that the number 397 is a Löschian number. Express 397 as $3x^2 + 3bx + b^2$, for some b. To do so, consider values of b from 0 to $397^{1/2}$. The greatest integer in this square root is 19. Thus, possibilities for b range from 0 to 19. Because $3x^2 + 3bx = 397 - b^2$, it follows that $397 - b^2$ must be divisible by 3. This fact eliminates from further consideration, as b, any integer between 0 and 19 for which $397 - b^2$ is not a multiple of 3. These values are shown in the central column of Table 4.2. Additionally, the material associated with the Fundamental Theorem states that the discriminant of the quadratic form, $3x^2 + 3bx + b^2$ must be an integer. Thus, in the right-hand column of Table 4.2 we calculate these discriminants for each of the candidate b-values singled out in the central column. The only candidate b value that remains is $b=1$ and therefore the correct quadratic form to also associate with 397 is $3x^2 + 3x + 1$. Geometrically, the ordered pair that generates 397 is represented as a lattice point that lies along the line $b=1$, displaced one unit from the line $y=x$ in the oblique coordinate system.

b	$(397-b^2)/3$	Square root of discriminant
0	132.333	
1	132	$4761^{1/2}=69$
2	131	$4752^{1/2}=68.934$
3	129.333	

4	127	$4716^{1/2}=68.673$
5	124	$4689^{1/2}=68.476$
6	120.333	
7	116	$4617^{1/2}=67.948$
8	111	$4572^{1/2}=67.616$
9	105.333	
10	99	$4464^{1/2}=66.813$
11	92	$4401^{1/2}=66.340$
12	84.333	
13	76	$4257^{1/2}=65.245$
14	67	$4176^{1/2}=64.621$
15	57.333	
16	47	$3996^{1/2}=63.213$
17	36	$3897^{1/2}=62.425$
18	24.333	
19	12	$3681^{1/2}=60.671$

Table 4.2. This table shows candidate values for b for K=397 in the left-hand column. It shows values of $(397-b^2)/3$ for each of those candidate values in the center column. The right-hand column shows the square root of the discriminant of the quadratic expression $3x^2 + 3bx + b^2$ for different values of b (from 0 to 19) that produce an integral value in the center column.

Now we have two quadratic equations to solve simultaneously to obtain the ordered pair that gives rise to the Löschian value of 397.

$$397 = 3x^2 + 3x + 1$$
$$397 = x^2 + xy + y^2$$

Solving the first equation using standard techniques from high school algebra, and choosing the positive value, gives $x = 11$. Use that value of x to find $y = 12$ in the second equation. There are no other lattice points that give rise to this particular Löschian number because there is no other integral discriminant of the quadratic form $3x^2 + 3bx + b^2$.

The geometric characterization of the central place lattice as a set of integral lattice points lying along a set of lines parallel to $y = x$ resulted, after some work, in a Fundamental Theorem that permits the algebraic determination of a quadratic form, $3x^2 + 3bx + b^2$, to generate a set of lattice points lying along a single line. When this second quadratic form was applied to the Diophantine equation, $K= x^2 + xy + y^2$,

easy calculations permit the determination of the lattice coordinates associated with an arbitrary Löschian number and of whether or not those coordinates are unique.

Uniqueness of Löschian numbers: solutions to previously unsolved problems.

Solving the K-value Twin Hierarchy Problem
  Dacey noticed that some *K*-values have more than one central place hierarchy associated with them. Using classical methods, however, it is difficult to determine what these hierarchies might look like. Indeed, Dacey noted this issue as an unsolved problem in the classical geometry of central place theory. The fractal approach, when extended to arbitrary *K*-values, permits solution of this unsolved problem using the Fundamental Theorem and associated constructions.
      Suppose it has been determined that the number 49 is a Löschian number. Express 49 as $3x^2 + 3bx + b^2$, for some *b*. To do so, consider values of *b* from 0 to $49^{1/2}$. The greatest integer in this square root is 7. Thus, possibilities for *b* range from 0 to 7. Because $3x^2 + 3bx = 49 - b^2$, it follows that $49 - b^2$ must be divisible by 3. This fact eliminates from further consideration, as *b*, any integer between 0 and 7 for which $49 - b^2$ is not a multiple of 3. These values are shown in the central column of Table 4.3. Additionally, the material associated with the Fundamental Theorem states that the discriminant of the quadratic form, $3x^2 + 3bx + b^2$ must be an integer. Thus, in the right-hand column of Table 4.3 we calculate these discriminants for each of the candidate *b*-values singled out in the central column. The only candidate *b* values that remains are *b*=2 and *b*=7 and therefore the correct quadratic forms to also associate with 49 are $3x^2 + 6x + 4$ and $3x^2 + 21x$ +49. Geometrically, the ordered pairs that generate 49 are represented as a lattice points that lies along the line *b*=2, displaced two units from the line *y*=*x* in the oblique coordinate system, and along the line *b*=7, displaced seven units from the line *y*=*x* in the oblique coordinate system.

b	$(49 - b^2)/3$	Square root of discriminant
0	16.333	
1	16	$585^{1/2} = 24.186$
2	15	$576^{1/2} = 24$
3	13.333	
4	11	$540^{1/2} = 23.237$
5	8	$512^{1/2} = 22.627$
6	4.333	
7	0	$441^{1/2} = 21$

Table 4.3. This table shows candidate values for *b* for *K*=49 in the left-hand column. It shows values of (49-b^2)/3 for each of those candidate values in the center column. The right-hand column shows the square root of the discriminant of the quadratic expression $3x^2 + 3bx + b^2$ for different values of *b* (from 0 to 7) that produce an integral value in the center column.

Now we have two sets of two quadratic equations each to solve simultaneously to obtain the ordered pairs that gives rise to two different hexagonal hierarchies associated with the Löschian value of 49.

$$49 = 3x^2 + 6x + 4$$
$$49 = x^2 + xy + y^2$$

$$49 = 3x^2 + 21x + 49$$
$$49 = x^2 + xy + y^2$$

In the first set of equations, *x*=3 and *y*=5. In the second set, *x*=0 and *y*=7. There are no other lattice points that give rise to this particular Löschian number because there is no other integral discriminant, beyond these two, of the quadratic form $3x^2 + 3bx + b^2$. Thus, *K*=49 is produced either from the lattice point (0,7) on the *y*-axis or from the lattice point (5,3) not on the *y*-axis. Figure 4.8 illustrates the two different fractal generators that give rise to the two different hierarchies using the procedure based on the Fundamental Theorem in associating fractal generators with lattice points.
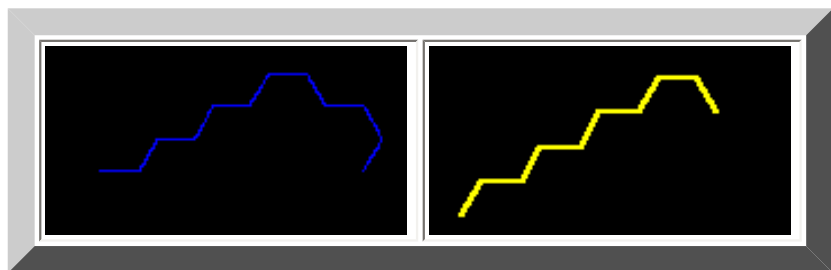
Figure 4.8. Geometric solution of the *K*=49 twin hierarchy puzzle. The left frame shows an 11-sided generator formed from the ordered pair (0,7) on the *y*-axis, yielding a *K*=7 type of hierarchy. The right frame shows a 9-sided generator formed from the ordered pair (5,3), not on the *y*-axis, yielding a *K*=4 type of hierarchy.

This example illustrates the fact that the Fundamental Theorem solves, completely, the previously unsolved problem involving uniqueness, and its lack, in calculating hexagonal hierarchies. The geometric characterization of the central place lattice as a set of integral lattice points lying along a set of lines parallel to *y* = *x* resulted, after some work, in a Fundamental Theorem that permits the algebraic

determination of a quadratic form, $3x^2 + 3bx + b^2$, to generate a set of lattice points lying along a single line. When this second quadratic form was applied to the Diophantine equation, $K = x^2 + xy + y^2$, easy calculations permit the determination of the lattice coordinates associated with an arbitrary Löschian number and also the determination of whether those coordinates are unique.

Putting the Pieces Together

The material in the previous sections indicates a plausible strategy for producing appropriate fractal generators that will create, through iteration, exact central place hierarchies for arbitrary K-values. It does so using only number theoretic properties of two quadratic forms. Thus, process is replicable and independent of previous cases. In the next chapter we consider some of the number theoretic infrastructure on which these methods rest and in a final chapter we present some real world considerations.

Chapter 5
Binary Quadratic Forms and the Löschian Diophantine Equation

One proof of Gauss's Law of Reciprocity, using contemporary techniques was linked to at the end of the previous chapter. There are also numerous classical proofs, some of which rest on the Chinese Remainder Theorem (link to one of them). Because such proofs often assume that the reader already knows the Chinese Remainder Theorem, and because it has been our experience that readers often do not know this theorem, we present it here in detail.

The Chinese Remainder Theorem

At the time the greatest common divisor was defined, it would have been possible to define a related number, the least common multiple.

Definition 5.1. Suppose a and b are two positive integers. The least common multiple $[a, b]$ is the smallest positive integer which is a multiple of both a and b. The relationship between them is illustrated in the following lemma.

Lemma 5.2. Let a and b be two positive integers. Then

  a) $(a, b) [a, b] = ab$
  b) If $d \mid a$ and $d \mid b$, then $d \mid (a, b)$
  c) If $a \mid m$ and $b \mid m$, then $ab \mid m$.

Proof:

  a) Consider the prime factorizations of a, b. Let

$$a = p_1^{a_1} p_2^{a_2} ... p_k^{a_k}$$
$$b = p_1^{b_1} p_2^{b_2} ... p_k^{b_k}$$

  (in this case, some exponents may be 0; a prime is included in the list if it is a divisor of either a or b).

  Then

$$(a, b) = p_1^{c_1} ... p_k^{c_k} \text{ where } c_i = \min \{a_i, b_i\}$$
$$[a, b] = p_1^{d_1} ... p_k^{d_k} \text{ where } d_i = \max (a_i, b_i)$$

  Since $a_i + b_i = c_i + d_i$ for each i, $(a, b) [a, b] = ab$.

  b) There are integers s, t such that $(a, b) = as + bt$. If $a = dx$, $b = dy$, $(a, b) = d(xs) + d(yt) = d(xs + yt)$. So $d \mid (a, b)$.

  c) Let $m = [a, b]q + r, 0 \leq r < [a, b]$. As in b), since $a \mid m$ and $a \mid [a, b]$, $a \mid r$. Similarly $b \mid r$. Since $r < [a, b]$, this contradicts the fact that $[a, b]$ is the LEAST common multiple of a and b. So $r = 0$. If $(a, b) = 1$, $[a, b] = ab$ by part a), so $ab \mid m$.

The least common multiple is used in arithmetic to add fractions, where it is called the least common denominator. For example, since $[15, 21] = 15(21)/(15,21) = 15(21)/3 = 105$

$$4/15 + 5/21 = (4/15)((21/3)/(21/3)) + (5/21)((21/3)/(21/3)) = (4(7) + 5(5))/105 = 53/105.$$

The least common multiple arises when it is desired to solve several congruences (with different moduli) simultaneously. The process below appears to have been known in first century China. Hence it has come to be known as the Chinese Remainder Theorem.

Theorem 5.3. The Chinese Remainder Theorem
Let m_1, m_2, ..., m_r be positive integers such that $(m_i, m_j) = 1$ if $i \neq j$. Let a_1, ..., a_r be any integers. Then the system of congruences

$$x \equiv a_1 \ (\text{mod } m_1)$$
$$x \equiv a_2 \ (\text{mod } m_2)$$
....
$$x \equiv a_r \ (\text{mod } m_r)$$

has a common solution of x, and if x, y are two such solutions $x \equiv y (\text{mod } m = m_1 m_2 ... m_r)$.

Proof:
For each j, let $k_j = m / m_j$. Thus $(k_j, m_j) = 1$, since m_j has no factors in common with any m_i if $i \neq j$.
Thus there is an integer b_j with $k_j b_j \equiv 1 (\text{mod } m_j)$. Also, if $i \neq j$ $k_j b_j \equiv 0 (\text{mod } m_i)$. Let $x = S k_j b_j a_j$ $1 \leq j \leq r$. Then, for each i, $x \equiv k_i b_i a_i \equiv a_i \ (\text{mod } m_i)$. Further, if x and y are two solutions $x \equiv y (\text{mod } m_i)$. Thus $m_i \mid (x - y)$ for each i. By Lemma 5.2c) $m \mid (x - y)$. So $x \equiv y (\text{mod } m)$.

Here is a classic example. A man has a basket of eggs. He doesn't know how many eggs there are, but when he counts them by twos, there is one left over. Similarly, when he counts by threes or fives, there is one remaining. When he counts by sevens, there are two left over. What is the least number of eggs he could have in his basket? If x is the number of eggs, the system of congruences is

$$x \equiv 1 (\text{mod } 2)$$
$$x \equiv 1 (\text{mod } 3)$$
$$x \equiv 1 (\text{mod } 5)$$
$$x \equiv 2 (\text{mod } 7)$$

So $m = 210$, $k_1 = 105$, $k_2 = 70$, $k_3 = 42$, $k = 30$. To find b_1, b_2, b_3, b_4 solve

$$105 b_1 \equiv 1 (\text{mod } 2) \text{ or } b_1 \equiv 1 (\text{mod } 2)$$
$$70 b_2 \equiv 1 (\text{mod } 3) \text{ or } b_2 \equiv 1 (\text{mod } 3)$$
$$42 b_3 \equiv 1 (\text{mod } 5) \text{ or } 2 b_3 \equiv 1 (\text{mod } 5)$$
$$30 b_4 \equiv 1 (\text{mod } 7) \text{ or } 2 b_4 \equiv 1 (\text{mod } 7)$$

One set of solution is $b_1 = 1$, $b_2 = 1$, $b_3 = 3$, $b_4 = 4$. Thus $x = 105(1)(1) + 70(1)(1) + 42(3)(1) + 30(4)(1) = 541$.
The smallest positive integer congruent to $541 (\text{mod } 210)$ is 121. Thus the least number of eggs the man has is 121.

While computations such as those of the above example are fascinating, the theoretical consequences are more important.

Theorem 5.4. Suppose $(m_1, m_2) = 1$. Then the equation $f(x) \equiv 0 (\text{mod } m = m_1 m_2)$ has a solution if and only if both $f(x) \equiv 0 (\text{mod } m_1)$, and $f(x) \equiv 0 (\text{mod } m_2)$ have solutions (here $f(x)$ is a polynomial with integer coefficients).

Remark: In fact if $f(x) \equiv 0 (\text{mod } m_1)$ has n_1 solutions and $f(x) \equiv 0 (\text{mod } m_2)$ has n_2 solutions, then $f(x) \equiv 0 (\text{mod } m)$ has $n_1 n_2$ solutions. See Niven, Zuckerman, and Montgomery, Theorem 2.20, for a proof. In the book, the

theorem will be used to see if $x^2 \equiv a$ has solutions for certain composite moduli.

Proof: If $f(x) \equiv 0 (\text{mod } m)$, then for some integer k, $f(x) \equiv km = km_1 m_2$. Thus $f(x) \equiv 0 (\text{mod } m_1)$ and $f(x) \equiv 0 (\text{mod } m_2)$. On the other hand, suppose $f(x) \equiv 0 (\text{mod } m_1)$ and $f(x) \equiv 0 (\text{mod } m_2)$ both have solutions. Suppose $f(a_1) \equiv 0 (\text{mod } m_1)$ and $f(a_2) \equiv (\text{mod } m_2)$. By the Chinese Remainder Theorem, there is an integer x (mod m), $x \equiv a_1$ (mod m_1) and $x \equiv a_2 (\text{mod } m_2)$. Then $f(x) \equiv f(a_1) \equiv 0 (\text{mod } m_1)$ and $f(x) \equiv f(a_2) \equiv 0 (\text{mod } m_2)$. Thus $m_1 \mid f(x)$, $m_2 \mid f(x)$. Thus since $(m_1, m_2) \equiv 1$, by Lemma 5.2 $m = m_1 m_2 \mid f(x)$, so $f(x) \equiv 0 (\text{mod } m)$.

The Chinese Remainder Theorem can also be used to help calculate the value of Euler's ϕ-function.

Theorem 5.5.

    a) If p is a prime, $\phi(p^n) = p^n - p^{n-1}$

    b) If $(m_1, m_2) = 1$, $\phi(m_1, m_2) = \phi(m_1) \phi(m_2)$.

Proof:

    a) Suppose p is a prime. Then, consider the complete residue system 1, 2, ..., p^n. The only integers in this list NOT relatively prime to p are p_1, $2p$, ..., $(p^{n-1})p$. Thus $\phi(p^n) = p^n - p^{n-1}$.

    b) The goal is to establish a one-to-one correspondence between integers a in the set $\{1, 2, ..., m\}$ which are relatively prime to m and pairs of integers (a_1, a_2), where

        a_1 is in $\{1, 2, ..., m_1\}$, relatively prime to m_1
        a_2 is in $\{1, 2, ..., m_2\}$, relatively prime to m_2.

First, suppose $(a, m) = 1$. Then $(a, m_1) = 1$ and $(a, m_2) = 1$. Let a_i be the remainder when a is divided by m_i, $i = 1, 2$. Second, suppose a_1, a_2 are as above. Then the Chinese Remainder Theorem assures there is a unique a in $\{1, 2, ..., m\}$ with $a \equiv a_1 (\text{mod } m_1)$ and $a \equiv a_2 (\text{mod } m_2)$. Since $(a, m_1) = 1$ and $(a, m_2) = 1$, it follows that $(a, m_1 m_2) = 1$. Thus, since this one-to-one correspondence exists, $f(m) = f(m_1) f(m_2)$.

For example, since $\phi(4) = 4 - 2 = 2$ and $\phi(5) = 4$, $\phi(20) = 8$. Since $\phi(8) = 8 - 4 = 4$ and $\phi(9) = 9 - 3 = 6$, $\phi(72) = 4(6) = 24$. One of the pairings of part b) of the theorem is of $(1, 2)$, where $(1, 8) = 1$ and $(2, 9) = 1$ with 65, a number relatively prime to 72 with $65 \equiv 1 (\text{mod } 8)$ and $65 \equiv 2 (\text{mod } 9)$. This is the solution of the system

        $x \equiv 1 (\text{mod } 8)$
        $x \equiv 2 (\text{mod } 9)$

determined by the Chinese Remainder Theorem ($k_1 = 9$, $k_2 = 8$; $b_1 = 1$, $b_2 = 8$) since $x \equiv 9(1)(1) + 8(8)(2) = 137 \equiv 65$ (mod 72).

Binary Quadratic Forms

In order to find which integers are of the form $x^2 + xy + y^2$ for integers x, y (as desired by Loeb and Dacey), it is first necessary to study binary quadratic forms in general.

Definition 5.6.

    a) A function $f(x, y) = ax^2 + bxy + cy^2$ is called a binary quadratic form. If $n = f(x_0, y_0)$ for some integers x_0, y_0, then the form f represents n properly if $(x_0, y_0) = 1$, improperly if $(x_0, y_0) \neq 1$.

    b) The points (x, y) where x, y are integers are called lattice points.

c) The discriminant d of a quadratic form is $d = b^2 - 4ac$.
d) A form is called

positive definite if it takes on only positive values when $(x, y) \neq (0, 0)$.
negative definite if it takes on only negative values when $(x, y) \neq (0, 0)$.
semidefinite if it takes on only non-negative values or non-positive values.

Theorem 5.7.

a) $d \equiv 0$ or $1 \pmod 4$
b) A form with $d = 0$ is semidefinite but not definite. A form with positive discriminant is indefinite. A form with negative discriminant is definite (positive if $a>0$, negative if $a<0$)

Theorem 5.8. Let $M = [m_{11} m_{12}; m_{21}, m_{22}]$. Let $[u; v] = M[x; y]$, that is $u = m_{11}x + m_{12}y$, $v = m_{21}x + m_{12}y$. Then this transformation is a permutation of the lattice points in the plane if and only if $\det M = +/- 1$.

Definition 5.9. Two quadratic forms $f(x, y) = ax^2 + bxy + cy^2$ and $g(x, y) = Ax^2 + Bxy + Cy^2$ are said to be equivalent if there is a matrix M of determinant 1, $M = [m_{11}, m_{12}; m_{21}, m_{22}]$, such that $g(x, y) = f(m_{11}x + m_{12}y, m_{21}x + m_{22}y)$.

Theorem 5.8 suggests that matrices of determinant -1 could have been allowed in Definition 5.9. Indeed, some number theory texts allow this. Still others use the term "properly equivalent" if $\det M = 1$, "improperly equivalent" if $\det M = -1$. Niven, Zuckerman, and Montgomery use the approach of Definition 5.9.

Theorem 5.9.

a) Equivalence of forms partitions the set of quadratic forms into sets of forms all of which are equivalent to each other.
b) Equivalent forms represent the same integers n, and represent the same integers properly.
c) Equivalent forms have the same discriminant.

Definition 5.10. Let f be a binary quadratic form whose discriminant is not a perfect square; f is called reduced if $-|a| < b \leq |a| < |c|$ or if $0 \leq b \leq |a| = |c|$.

Theorem 5.11. If d is not a perfect square, each equivalence class of binary quadratic forms of discriminant d contains at least one reduced form.

Theorem 5.12. Suppose f is a reduced positive definite quadratic form of discriminant d. The $0 < a \leq (-d/3)^{0.5}$.

Corollary 5.13. There is only one reduced form with discriminant -3.

Proof: By Theorem 5.12 $a = 1$; $b = 0$ is impossible since $d \equiv b^2 \pmod 4$. Therefore, Definition 5.10 assures $b = 1$, $c = 1$.

Theorem 5.14. Let n and d be given integers with $n \neq 0$. There is a binary quadratic form of discriminant d which represents n properly if and only if $x^2 \equiv d \pmod{4|n|}$ has a solution.

Corollary 5.15. Suppose $a \equiv 0$ or $1 \pmod 4$. If p is an odd prime, there is a binary quadratic form of discriminant which represents p if and only if $(d/p) = 1$.

Application to Löschian Numbers

Definition 5.16. A positive integer n is called Löschian if there are integers x and y such that $n = x^2 + xy + y^2$.

Since there is only one reduced form of discriminant -3, namely $x^2 + xy + y^2$, and since if n is representable by

a form of discriminant -3 if and only if it is representable by an equivalent reduced form, <u>Theorem 5.14</u> assures that n is properly representable by $x^2 + xy + y^2$ if and only if $x^2 \equiv -3 \pmod{4n}$ or $x^2 + 3 \equiv 0 \pmod{4n}$ has a solution.

By <u>Theorem 5.4</u>, $x^2 + 3 \equiv 0 \pmod{4n}$ has a solution if and only if $x^2 + 3 \equiv 0 \pmod{p_i^{a_i}}$ has a solution for every i.

1) If $p \mid n$ and $p \equiv 1 \pmod 3$, then by <u>quadratic reciprocity</u> $(-3/p) = (p/3) = 1$ and also $(-3/p^n) = (p^n/3) = (p/3)^n = 1$, so $x^2 + 3 \equiv 0 \pmod{p^n}$ has a solution for every n.

2) However suppose $p \equiv 2 \pmod 3$. Then $(-3/p) = 1$, and so $x^2 + 3 \equiv 0 \pmod p$ has no solution. But $x^2 + 3 \equiv 0 \pmod{p^n}$ implies $p^n \mid (x^2 + 3)$ which in turn implies that $p \mid (x^2 + 3)$, which is impossible.

3) Of course $x^2 + 3 \equiv 0 \pmod 3$ has a solution (x = 0) but $x^2 + 3 \equiv 0 \pmod{3^n}$ has no solution for $n > 1$ since $9 \mid (x^2 + 3)$ implies $3 \mid x^2$ implies $3 \mid x$, say $x = 3a$; but then $x^2 + 3 = 3(3a^2 + 1) \equiv 3 \pmod 9$, a contradiction.

Thus N is properly representable by $x^2 + xy + y^2$ if and only if $N = 3^a p p^b$, where every $p \equiv 1 \pmod 3$ and a = 0 or 1. Of course if $N = x^2 + xy + y^2$, $c^2 N = (cx)^2 + (cx)(cy) + (cy)^2$ so the square of any properly representable integer is improperly representable. Thus an integer N is Löschian if and only if $N = 3^a p p^b p q^{2g}$ where every $p \equiv 1 \pmod 3$, every $q \equiv 2 \pmod 3$. Of course, sometimes, it is not necessary to find the prime factorization of N to see if it is Löschian. Since always $x^2 + xy + y^2 \equiv 0$ or $1 \pmod 3$ [try the nine cases $x \equiv a$, $y \equiv b \pmod 3$; if $a = b$, $x^2 + xy + y^2 \equiv 0 \pmod 3$; otherwise $x^2 + xy + y^2 \equiv 1 \pmod 3$].

So if $N \equiv 2 \pmod 3$, N is non-Löschian.

For example, $N = 32759$ is non-Löschian (it is not immediately obvious that $N = 17(41)(47)$.

Similarly, suppose $N = p^n M$, where $(M, p) = 1$, $p \equiv 0, 1 \pmod p$. If $M \equiv 2 \pmod 3$, N is non-Löschian, since the sum of the exponents of the primes $\equiv 2 \pmod 3$ in the prime factorization of M must be odd.

For example, $N = 8073 = 3^3(299)$, and $299 \equiv 2 \pmod 3$. So 8073 is non-Löschian. In fact, $8073 = 3^3(13)(23)$.

In summary,
Theorem 5.17. Let N be a positive integer. Then

a) N is properly representable as $x^2 + xy + y^2$ for integers x, y if and only if $N = 3^a M$, where a = 0,1 and every prime factor of M is $\equiv 1 \pmod 3$.
b) N is Löschian if $N = 3^a M T^2$, where every prime factor of M is $\equiv 1 \pmod 3$ and every prime factor of T is $\equiv 2 \pmod 3$.
c) N is non-Löschian if $N \equiv 2 \pmod 3$
d) N is non-Löschian if $N = p^n M$, $(M, p) = 1$, $M \equiv 2 \pmod 3$.

Löschian numbers: examples of Theorem usage
In this chapter, we have proved a theorem that lets anyone determine exactly which numbers are Löschian and which numbers are not Löschian. The formal mechanics of proof drew on a variety of earlier theorems and on facts from number theory. The creative effort involved the recasting of Marshall's earlier work in a form that would lead to the desired conclusion of a sufficient condition. Readers wishing to examine the history of this development are referred to articles published by <u>Marshall</u> (1975), <u>S. Arlinghaus</u> (1985), and <u>S. Arlinghaus and W. Arlinghaus</u> (1989). So that one might see how the results of Theorem 5.17 can be implemented, we offer several examples below.

- $K = 175$ is Löschian, since $K = 5^2 \times 7$.
- $K = 125 = 5^3$ is not Löschian
- $K = 245 = 5 \times 7^2$ is not Löschian
- $K = 85$ is not Löschian, even though 85 is congruent to $1 \pmod 3$, since $K = 5 \times 17$, and both 5 and 17 are congruent to $2 \pmod 3$
- $K = 49$ is Löschian as 49 may be generated using the Diophantine equation on either the ordered pair (0, 7) or on (3, 5): representation is not unique.

Theorem 5.17 offers an easy way to check whether a given number is Löschian. It does not give the geometric characterization of the associated hierarchy. For that characterization, the reader then needs to return to the material in Chapter 4 and the <u>Fundamental Theorem</u> offered there.

Chapter 6
Back to the Real World: Eratosthenes in Ann Arbor

eHighlights of this Chapter
Application of Eratosthenes sieve to parcel map of Ann Arbor
Virtual reality of downtown Ann Arbor: used in work on a maximum height in the downtown

Back to the Real World
The synthetic approach to central place geometry, in earlier chapters, has found application (by S. Arlinghaus and others as noted) in the usual and the unusual. The articles below have all appeared in *Solstice* and links to those articles are given below (*Solstice*, itself, is a Pirelli INTERNETional Award Semi-Finalist (top 80), 2001).

- 1990, June. "Beyond the Fractal, pages 17-35" suggests a transformation of the geometry presented in this work aligned with earlier work of Hagerstrand on the diffusion of an innovation. (Link is to scanned images of hardcopy printed from original TeX files sent as e-mail transmissions with instructions to the user to print out the file on a TeX enabled printer. See link in Bibliography for access to TeX code.)
- 1990, December. "Fractal Geometry of Infinite Pixel Sequences: "Super-definition" Resoultion? pages 98-103" offers an application of this geometry to the cathode ray tube, followed up on with queries from the business world. (Link is to scanned images of hardcopy printed from original TeX files sent as e-mail transmissions with instructions to the user to print out the file on a TeX enabled printer. See link in Bibliography for access to TeX code.)
- 1993, June. "Micro-cell Hex-nets" explores the use of this geometry in association with systems of relay towers on the geographic landscape. (Link is to scanned images of hardcopy printed from original TeX files sent as e-mail transmissions with instructions to the user to print out the file on a TeX enabled printer. See link in Bibliography for access to TeX code.)
- 1996, December. "Web Fractals: An Overview"
- 2002, December. "Spatial Synthesis: Research Program" with W. C. Arlinghaus.
- 2004, June. "Spatial Synthesis Sampler. Geometric Visualization of Hexagonal Hierarchies: Animation and Virtual Reality" with W. C. Arlinghaus, a Pirelli INTERNETional Award Semi-Finalist (top 80), 2003.
- 2004, December. "Spatial Synthesis: A 3D Atlas of Ann Arbor"
- 2005, June. "Spatial Synthesis. The Evidence of Cartographic Example: Centrality and Hierarchy." Serves as a lead-in to this book.

Communication of these ideas, an important part of real-world use of information, has appeared in a number of other locales, as well. A few links are given below to work by S. Arlinghaus (and others as noted).

- 1985. "Fractals Take A Central Place." *Geografiska Annaler, Series B*.
- 1986. "Steiner Transformations" in *Essays on Mathematical Geography*, Monograph 3, pages 55-70, Institute of Mathematical Geography.
- 1987. "Fractals: Constructions, Speculations, and Concepts" in *Essays on Mathematical Geography--II*, Monograph 5, pages 54-66, Institute of Mathematical Geography.
- 1989. "The Fractal Theory of Central Place Geometry: A Diophantine Analysis of Fractal Generators for Arbitrary Loschian Numbers" with W. C. Arlinghaus. *Geographical Analysis*.
- 1990 (January). "Geometry of boundary exchanges: Compression patterns for boundary dwellers" with John D. Nystuen. *The Geographical Review*, American Geographical Society of New York.
- 1991. "Table for Central Place Fractals" in *Essays on Mathematical Geography--III,* Monograph 14, pages 6-15, Institute of Mathematical Geography.
- 1991. "Tiling According to the Administrative Principle" in *Essays on Mathematical Geography--III*, Monograph 14, pages 16-25, Institute of Mathematical Geography.
- 1993. *Fractals in Geography* edited by Nina Siu-Ngan Lam and Lee De Cola, Chapter 10, "Central Place Fractals: Theoretical Geography in an Urban Setting." Prentice-Hall.
- 1993. "Electronic Geometry," The Geographical Review April, 1993. Vol. 83, No. 2, pp. 160-169.

Eratosthenes in Ann Arbor
Ann Arbor is a small city in southeastern Michigan. It is home to the main campus of The University of Michigan, a state university with over 35,000 students on the Ann Arbor campus. The student population composes about

1/3 of the population of the city. Much of the rest of the population works at the university in some capacity or in research industry, businesses, or institutions that locate near the campus. Most cities in the US have shapes that are topologically equivalent to a circle, in terms of paying taxes to the city: land parcels that lie within the city boundaries pays taxes to the city. There are, of course, cities that contain enclaves within their boundaries that are not part of the city itself: Detroit, for example, contains the small (in area) towns of Hamtramck and Highland Park totally within its borders. However, in the case of Ann Arbor and other small cities that contain large state universities, the city is more of an annulus (doughnut) in shape. A large hole, containing the university is cut out of the city: lands in this hole do NOT pay taxes to the city. Hence, a disproportionately large property tax burden is placed on owners of non-university parcels within the city.

For the city to offer a fine quality of life to all its residents (taxpayers and others) there need to be mechanisms to create continuing economic development within the city. One way to do this is to increase the stock of housing and space for commercial and other establishments in support of that housing. This path is all the more attractive in light of enduring interests in reducing "sprawl" and in preserving open space in the more rural surrounding lands. In a city with few remaining empty buildable lots, this approach seems to offer few alternatives, the most obvious of which is to increase the density of dwelling units within the city. When density increases are proposed in established residential neighborhoods there is often loud and long public objection from residents of those neighborhoods. There may also be serious environmental considerations, as well. Few residents, however, seem to object to increasing density in the downtown: many who already live there moved in with an acceptance of taller buildings and those who do not live there often do not care about the idea of increasing density in the downtown. What people do seem to care about, however, is what an increase in downtown residential density may mean to the character, appearance, and feeling of the downtown. To some, an 18 story building is a visual blight on the skyline that provokes negative comment everytime it is viewed; yet, others note that they have become accustomed to it and view it as an old, familiar friend. Building height can be a source of substantial dispute.

The problem of where to locate tall buildings, with sensitivity to existing building types on adjacent and nearby lots, is a difficult one. In Ann Arbor, building height is currently limited by "floor area ratio" (FAR). The FAR is calculated as the ratio of floor area in a building divided by parcel area, times 100. If a given parcel has an FAR of 100 assigned to it, then a building footprint built lot line to lot line may have a height of 1 story. If a parcel has an FAR of 200 assigned to it, then a building footprint built lot line to lot line may have a height of 2 stories. Similarly, an FAR of 300, assigned to a parcel, yields a building of height 3 stories covering the entire parcel.   Thus, on a parcel with an FAR of 300, one might, instead, build a building on half of the lot area but of height six stories, or on a third of the lot area but of height 9 stories. On the same parcel, a 30 story building could be built only if its footprint covered one-tenth of the land area of the parcel.

The FAR provides a height limit based on the size of foundation needed to support a tall building. It also offers subtle encouragement for preserving some amount of open space and visual variation in the region to which it applies. The drawback is that a tall building may get built with no regard to the broader context of how a new building will fit in with existing buildings on the surrounding parcels. A possible side effect of using FAR (alone) to limit height is that it might encourage parcel amalgamation by large developers, thereby driving out desired local small business owners.
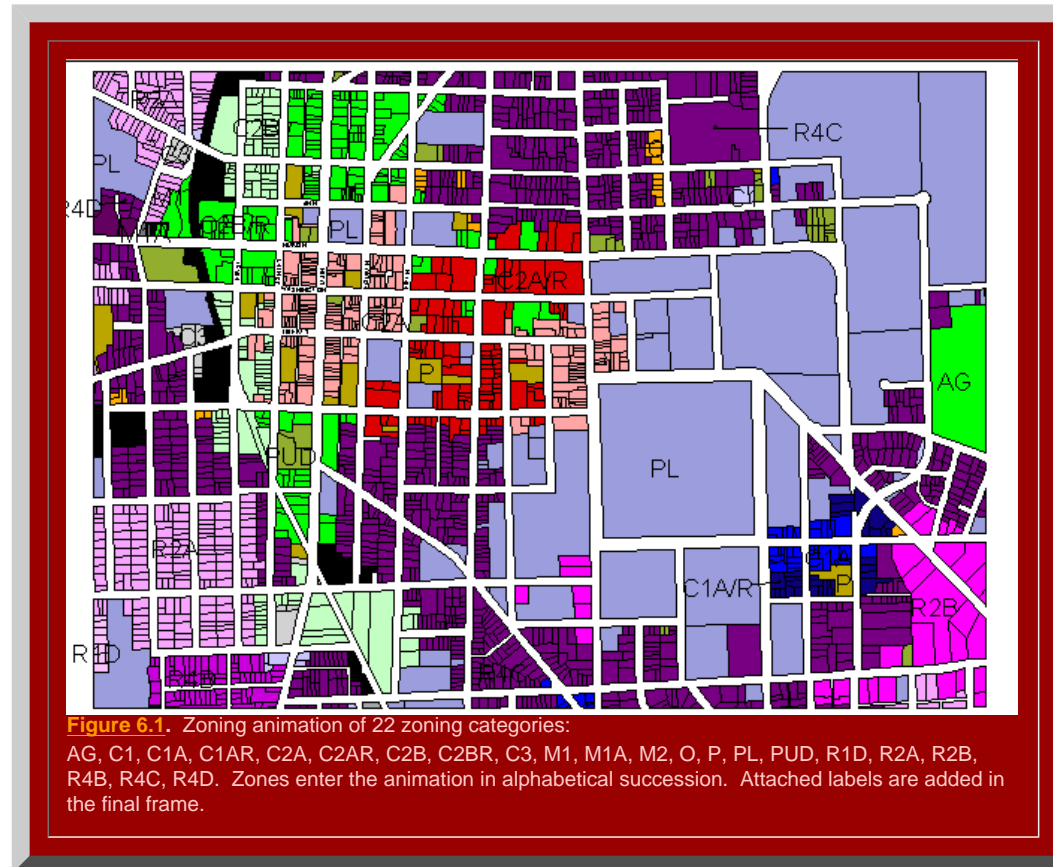
The issue of creating greater height in the downtown is a complex one. In 2003, Mayor John Hieftje and the Ann Arbor City Council established, in conjunction with the Downtown Development Authority, DDA, (Susan Pollay, Executive Director) a Taskforce to study increasing residential land use in the downtown. Some of the materials studied by that group was created by the first author, in collaboration with others (Fred J. Beal, President Beal Construction, and Douglas S. Kelbaugh, Dean Taubman College of Architecture and Urban Planning, The University of Michigan). The material that follows highlights the use of concepts from this book that were used in that context. It, and associated materials were used in public hearings and by City Council in passing the recommendations of that Taskforce. A more complete story of the policy and 3D modeling aspects is available elsewhere (link to Arlinghaus, Beal, and Kelbaugh).

A Prime Parcel Sieve.
The FAR is assigned by zoning type. In the downtown, there are currently parcels assigned to each of 22 different zoning categories (AG, C1, C1A, C1AR, C2A, C2AR, C2B, C2BR, C3, M1, M1A, M2, O, P, PL, PUD, R1D, R2A, R2B, R4B, R4C, R4D). Roughly speaking, any category beginning with C is a commercial category; M is for manufacturing; R is for residential. The AG category is for agricultural zoning, O is for office, P (except for PUD) is for Public Land (as for the University of Michigan), and PUD is for Planned Unit Development.

Enumeration of parcels via geometric partition

In Figure 6.1, the animated map shows the downtown area of the City of Ann Arbor parcel map colored as a thematic map by zoning category: the broad PL zoning is part of the central campus of the University of Michigan. The curved line near the left side of the map. representing the Ann Arbor Railroad corridor, has most of the manufacturing parcels adjacent to it. Separate categories enter the picture in sequence, arranged according to alphabetical ordering of zoning category. The coloring scheme is exhaustive: every parcel is covered. It is also mutually exclusive: no parcel has more than one color. Thus, the zoning classification serves as a geometric partition of the parcels. It offers a way to enumerate all the parcels: to order them in some logical fashion and to assign some quality to them as well, in much the way that we assign both cardinal and ordinal properties to numbers.

Figure 6.1. Zoning animation of 22 zoning categories: AG, C1, C1A, C1AR, C2A, C2AR, C2B, C2BR, C3, M1, M1A, M2, O, P, PL, PUD, R1D, R2A, R2B, R4B, R4C, R4D. Zones enter the animation in alphabetical succession. Attached labels are added in the final frame.

The casting out of parcels

With an enumeration of all parcels in hand, groups of parcels will be removed in accordance with various ideas. The goal is to select targets of opportunity for taller projects. The mechanism for such selection is similar to the mechanism for the selection of prime numbers employed by Eratosthenes (link back to Eratosthenes's Sieve). In the case of the downtown, parcels meeting certain criteria are cast out from further consideration as prime parcels much as numbers meeting certain criteria (multiples of 2, multiples of 3, multiples of 5, and so forth) were cast out from further consideration as prime numbers. What remains, are "primes": prime numbers or prime parcels. These prime parcels will then be viewed as possible targets of opportunity. Local considerations of various sorts might then be superimposed on them, such as design standards, spacing of tall buildings, or whatever constraints are within the legal code of the city.

Animated maps are useful for showing change; static maps are useful when one wishes to take a longer look
at pattern without regard to change in pattern. Thus, Figure 6.2 shows the final frame of the animated map
in Figure 6.1 along with a layer showing the boundary of the Downtown Development Authority (DDA) in yellow,
the railline in black/yellow, the floodway (channel) outline of Allen's Creek in blue, and the floodplain outline
of Allen's Creek in cyan. We begin the process of casting out parcels according to some replicable logic (not
as 'multiples' but according to some logical scheme). (In Ann Arbor, the "downtown" generally refers to the DDA:
a state-enabled authority that can capture increases in taxable value to pay for improvements within the
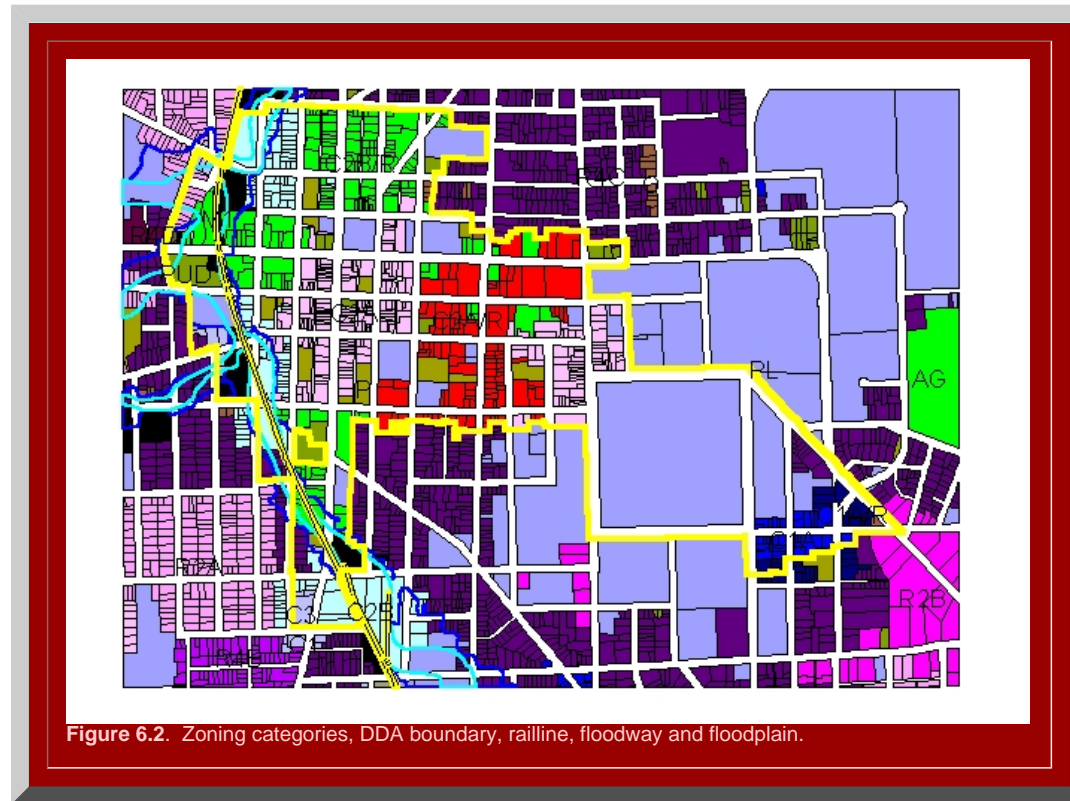defined boundaries.)

Figure 6.2. Zoning categories, DDA boundary, railline, floodway and floodplain.

CASTING OUT:

- **All zoning categories that cannot support height in excess of FAR are cast out.**
  Consider only zoning categories, as the downtown "core," of C1A, C1AR, C2A, C2AR, C2BR as those
  categories that might contain parcels that are targets of opportunity for building structures of height greater
  than that permitted by FAR. Thus, all parcels of zoning type other than those 5 are cast out from
  further consideration. This process opens up quite a bit of land within the DDA as possibilities for tall
  buildings (shown in white in Figure 6.3). As in the prime number seive, the first step removes a substantial
  set, parcels in color, from further consideration. Subsequent steps remove smaller subsets from
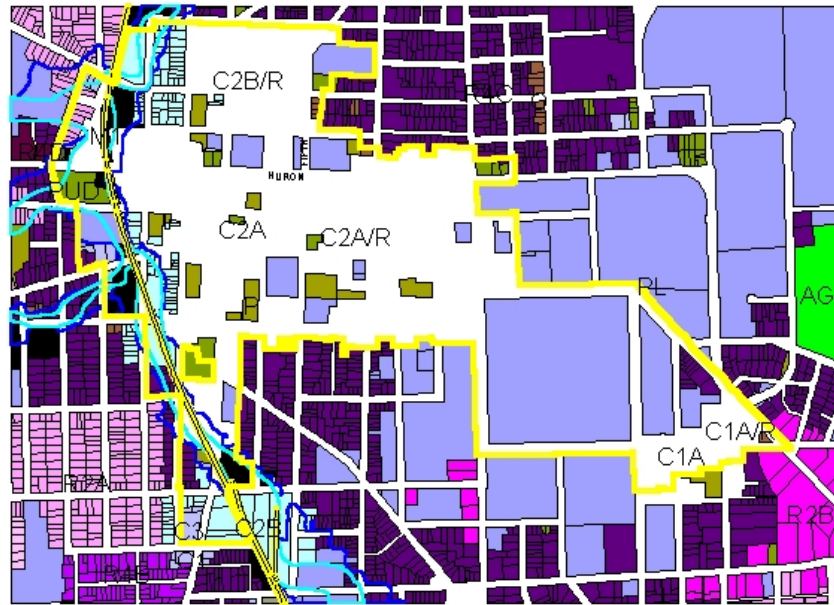 further consideration.

Figure 6.3. All zoning categories other than C1A, C1AR, C2A, C2AR, C2BR zoning categories are cast out from further consideration. Those 5 zoning categories cover the lands represented in white (as in open for further consideration). The parcels assigned a color other than white have been removed from consideration.

- **All historic district parcels are cast out.**

  When parcels containing historic district designation (and often relatively short buildings) are superimposed on the pattern in Figure 6.3, further limitation of targets of opportunity is the result (in Figure 6.4, historic district parcels are red). In this step, all historic district parcels are cast out, further limiting the number of parcels eligible to be considered for "prime" parcel status (Figure 6.4). The white area, targets of opportunity for tall buildings within the DDA, remains large but not as large as in Figure 6.3. Successive casting out of other parcels continues in the steps to follow.
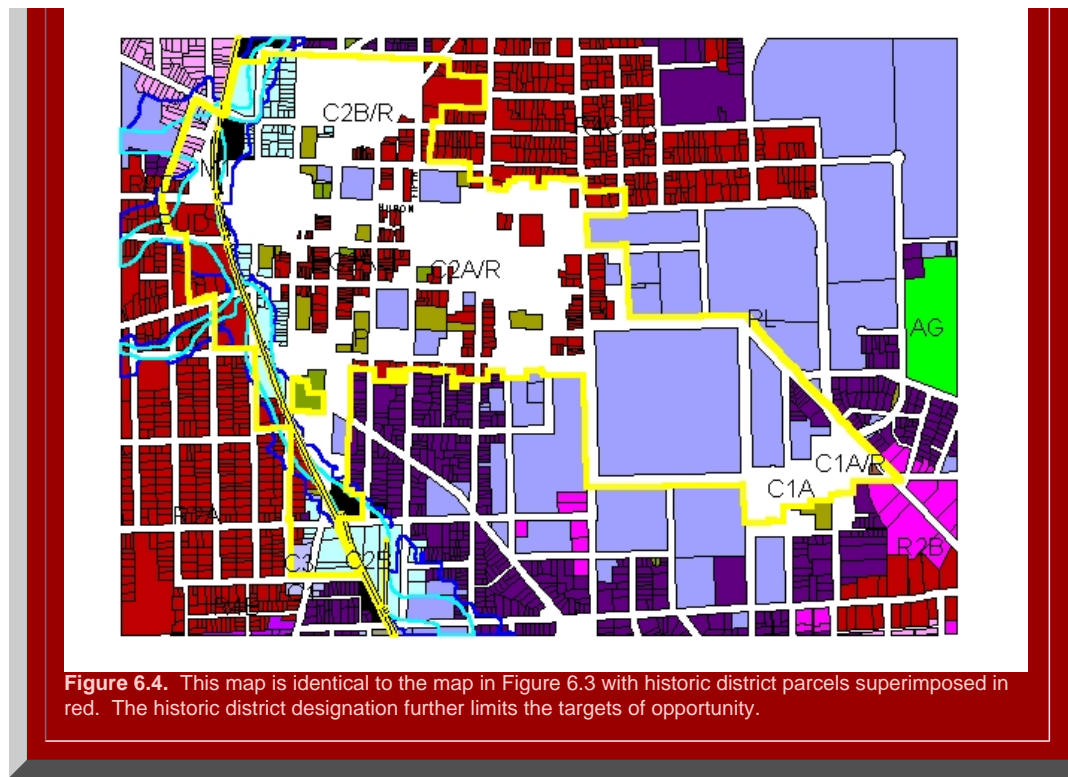
Figure 6.4. This map is identical to the map in Figure 6.3 with historic district parcels superimposed in red. The historic district designation further limits the targets of opportunity.

- **Floodplain parcels are cast out.**

    All parcels whose centroids lie within the floodplain of Allen Creek are cast out as possible prime parcels. Parcels that intersect the floodplain, but whose centroid does not lie in the floodplain remain. The reason to use the centroid analysis is that public benefit might come from having a building erected on the part of the parcel not in the floodplain and saving the part of the parcel in the floodplain as part of a greenway or other broad environmental amenity.

- **All parcels containing "steep slopes" are cast out.**

    Many of these are also floodplain parcels, as above. Elsewhere, the definition of "steep slope" is problematic. Generally, the DDA is fairly flat, away from the creek valley.
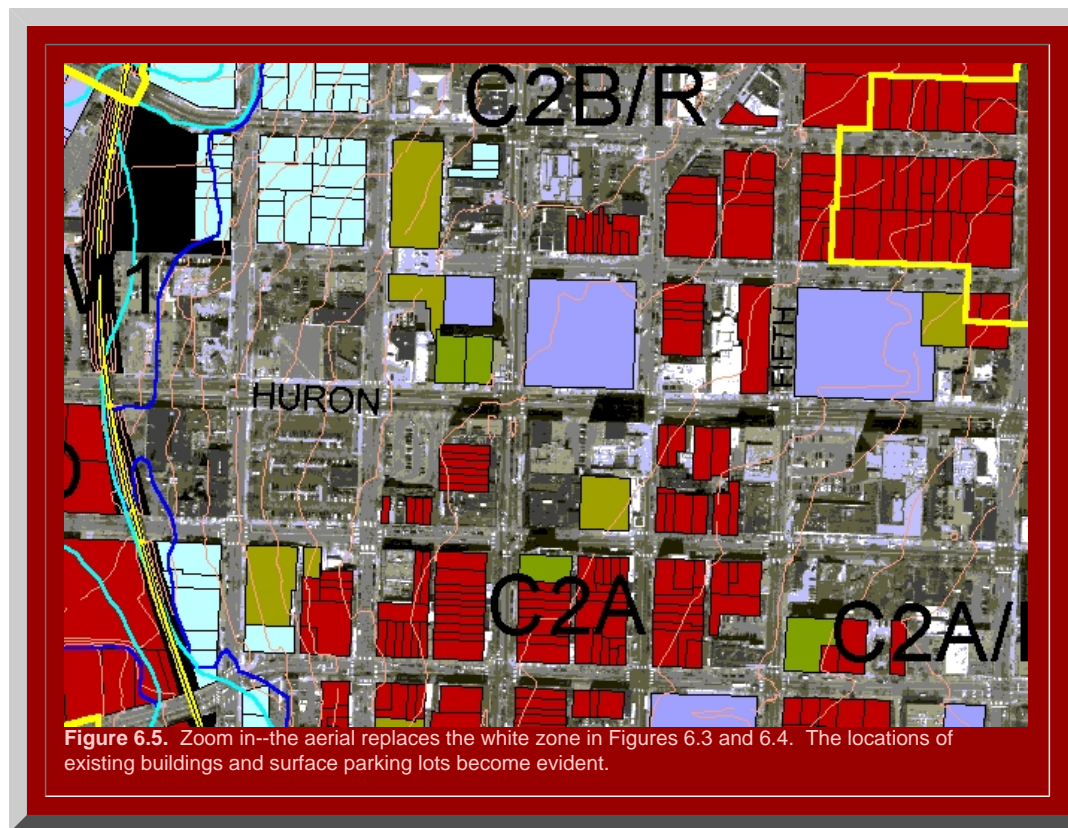
- **Church parcels are cast out.**

    Parcels containing churches, as listed in published official records, are cast out.

All possible prime parcels, as targets for opportunity to support buildings of height in excess of the FAR, are those that pass through this sieve: those that are not cast out based on zoning, environmental, and cultural factors above.

Zooming in

To take a closer look at the area, zoom in on a portion of it. One idea is to use the street hierarchy to select general target areas: wider streets support taller nearby structures. Thus, the zoom-in of Figure 6.5 is on Huron Street, the widest street in the DDA. Insert an aerial photo behind the map: the "white" area of earlier maps has been replaced with aerial so that one can see directly the current content of all potential prime parcels. With the aerial replacing the white zone, one can see what is currently located on each parcel. Thus, identification of immediate targets is easy: note the surface parking lots (with clearly underutilized existing infrastructure). Parcels already containing buildings might, or might not, become targets.

Figure 6.5. Zoom in--the aerial replaces the white zone in Figures 6.3 and 6.4. The locations of existing buildings and surface parking lots become evident.

The map in Figure 6.5 shows each parcel from lot line to lot line. Building footprints were digitized from aerials provided by the City. Associated databases gave estimates of building height. Interactive maps offered a constructive way to link a variety of two dimensional sets of information (as in Maps 6.1, 6.2, and 6.3).

- **I-Map 6.1:** Click here for a link to an interactive map showing building footprints and height (on mouse-over) as well as building address and street names (on mouse-over). Parcel boundaries are shown on the underlying aerial and on the green Downtown Development Authority (DDA) area. The Allen Creek floodway (underground) and flood plain are shown, shaded, respectively in blue and turquoise. Click on a building or a street to see associated entries in the underlying database.
- **I-Map 6.2:** Click here for a link to an interactive aerial showing parcel boundaries, zoning, building height (on mouse-over), and street name. DDA outline, only, is shown in light yellow so the user may zoom in to get a closer view of the aerial within the DDA (up to 800% enlargement--can see cars clearly). The Allen Creek floodway (underground) and flood plain are shown, outlined, respectively in blue and light blue; again, because the shading is removed, the viewer may look at the content of the floodway/floodplain in greater detail than above. Click on a building or a street to see associated entries in the underlying database.
- **I-Map 6.3:** Click here for a link to an interactive aerial showing zoning boundaries in the downtown, zoning type (on mouse-over), building height (in the "zoneht" record of the database), and street name. Click on a building or a street to see associated entries in the underlying database.

Designing the Vertical City: the Use of Virtual Reality Models

Once the parcels that could serve as targets of opportunity for tall buildings were agreed upon by the Taskforce, the prime parcels, a series of several hundred virtual reality models were developed to visualize alternatives for the DDA. The reader interested in the detail of the planning process, local policy matters, and the

mechanics involved in model construction are referred to the following materials in the references. The focus here is on the use of a concept identical to Erastosthenes prime number seive to sift out parcels elegible for further consideration, as above, and the subsequent application of virtual reality to visualize complex geometric situations, as in the case of Christaller nets, in order to facilitate scientific communication and eventual policy decisions by official municipal bodies.

The set of buildings that currently exist within the DDA was used as a base on which to build alternative scenarios of what might be done. Figure 6.6a shows a screen-capture of a virtual reality model built by extruding building footprints according to height records from the City of Ann Arbor Planning Department (Figure 6.6b is the virtual reality model; try driving around in it).
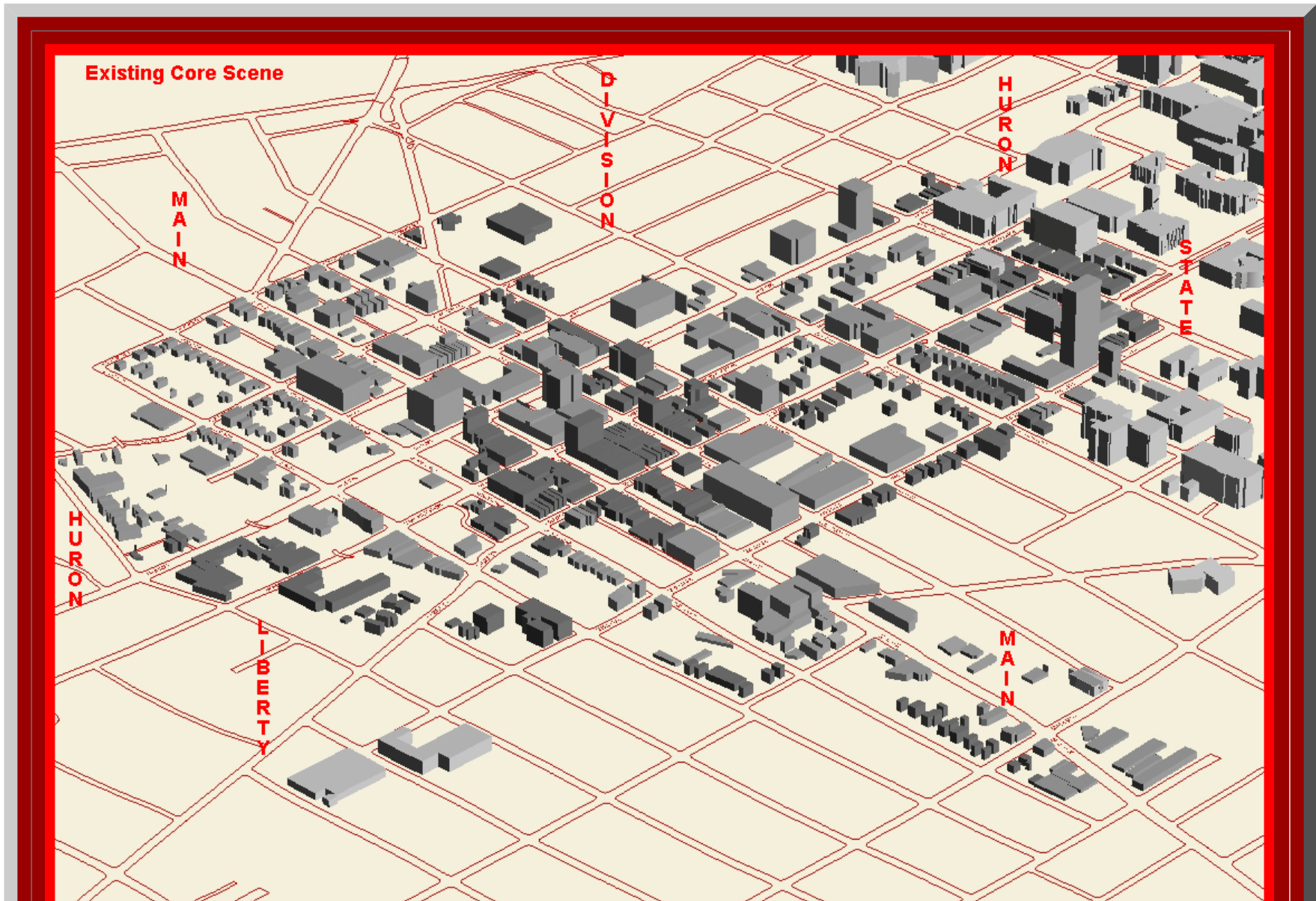

Existing Core Scene

Figure 6.6a. Downtown Ann Arbor buildings extruded from footprints digitized from aerial.
Figure 6.6b: link to virtual reality model from which Figure 6.6a was taken.

Figures 6.7a and b, 6.8a and b suggest how that model was used: colored buildings are added, only on prime parcels, according to numbers of residential units to be added and to guidelines suggested by Taskforce members (selected for expertise in construction, urban planning, architecture, and so forth). Different building colors respond to different particular suggestions. This set of four models represents merely one possible scenario; input from numerous sources was important in creating a variety of alternatives for policy makers to consider.
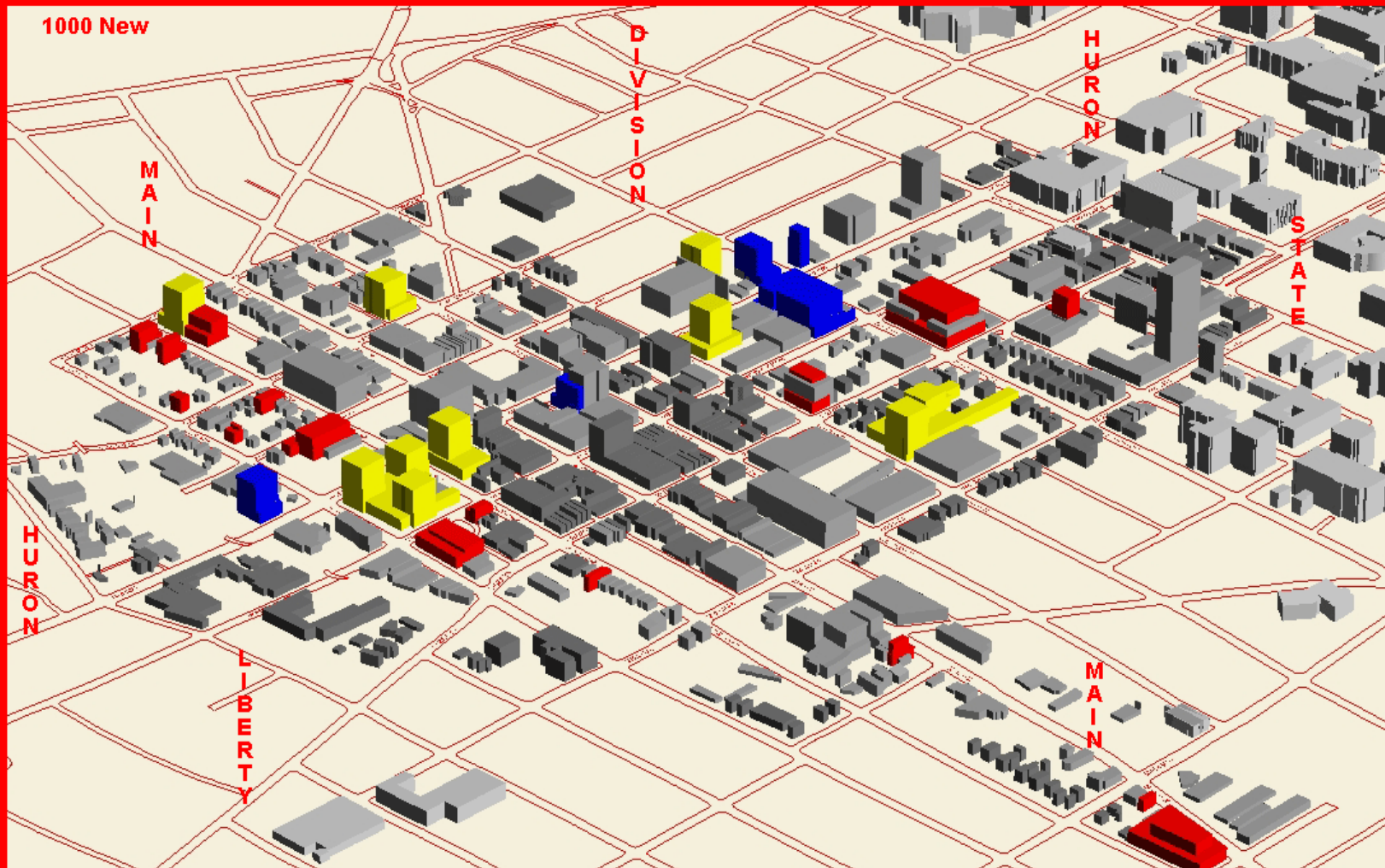
Figure 6.7a. Downtown Ann Arbor buildings extruded from footprints digitized from aerial. Gray buildings are existing buildings. Yellow buildings are built on empty lots or on surface parking lots. Blue buildings are built along Huron Street (possibly as replacements for, or on top of, existing buildings). Red buildings are built with upper story setbacks on a subset of streets identified by the Taskforce. The number of new buildings is sufficient to support 1000 new residential units. All non-gray buildings are built on prime parcels.
Figure 6.7b: link to virtual reality model from which Figure 6.7a was taken.
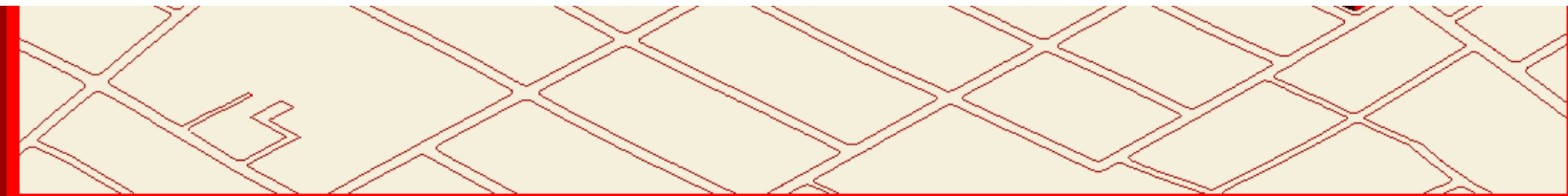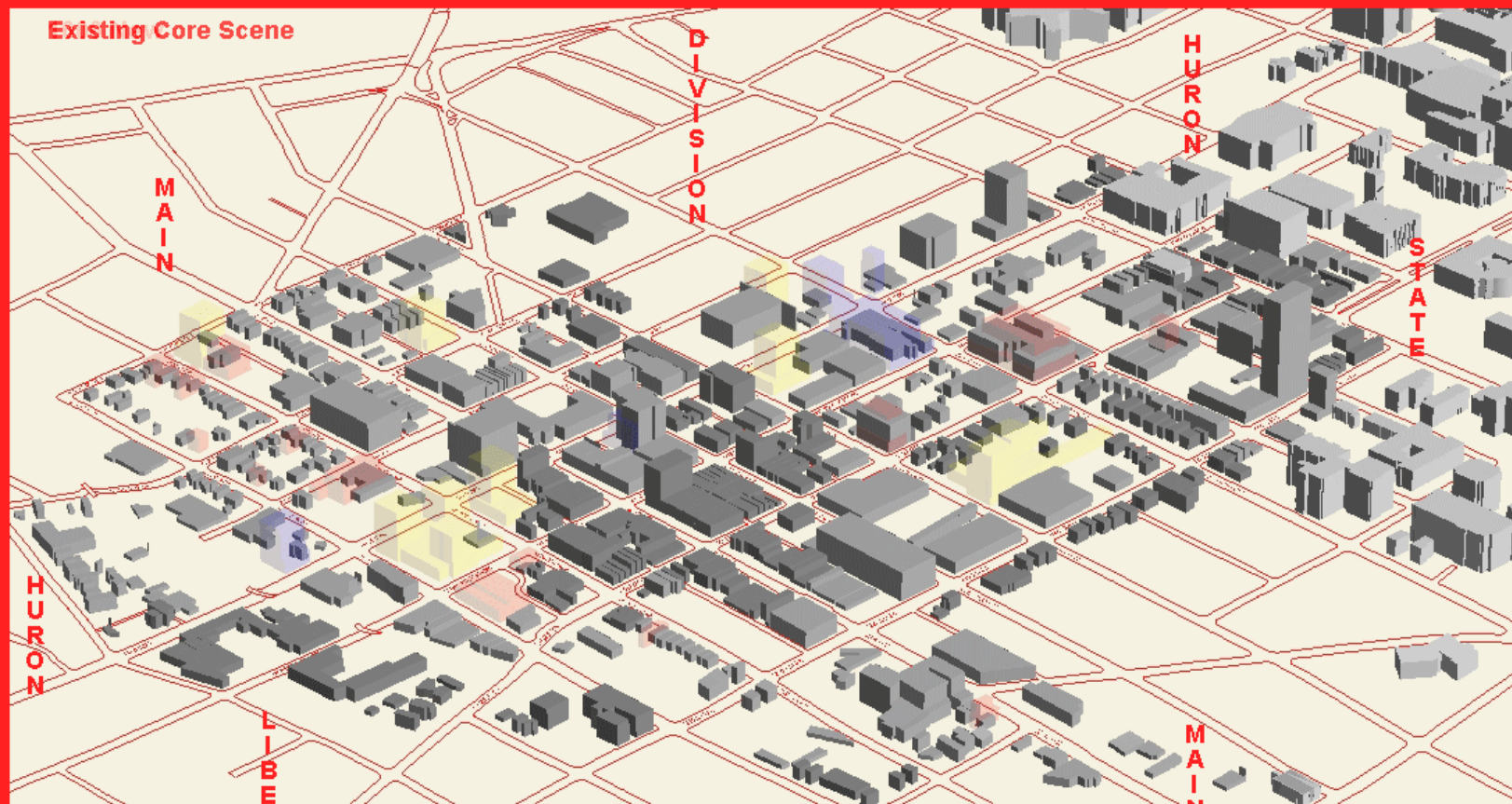
Figure 6.8a. Downtown Ann Arbor buildings extruded from footprints digitized from aerial. Gray buildings are existing buildings. Yellow buildings are built on empty lots or on surface parking lots. Blue buildings are built along Huron Street (possibly as replacements for, or on top of, existing buildings). Red buildings are built with upper story setbacks on a subset of streets identified by the Taskforce. The number of new buildings is sufficient to support 2500 new residential units. All non-gray buildings are built on prime parcels.
Figure 6.8b: link to virtual reality model from which Figure 6.8a was taken.

Virtual reality models served to pique conversations and help Taskforce members to visualize alternatives. Eventually, they saw a need to compare one virtual reality model to another. For that purpose, "viewpoints" were inserted into the VR models (find the "viewpoints" pull down in Figures 6.6b, 6.7b, 6.8b, so that different models could each be viewed from exactly the same vantage point (guided by the computer). While the insertion of viewpoints was helpful, direct comparison still required retention of a great deal of visual information in one's memory. Animation of the models of the DDA, as in Figure 6.9 offered a way to look at multiple global alternatives.

Existing Core Scene

Figure 6.9. Animation of various alternative screen captures from multiple VR models permits consistent visual comparison of models from one vantage point.

Thus, the solution for local views was also to take screen captures from the same viewpoint of different VR models and stack them in an animation. The 3D VR models above were built on May 27, 2004. Earlier models were shown to the public on April 27; public reaction was used to create a responsive model on May 3. The May 3 model was used in conjunction with the April 27 model as a stacked animation built from the taller April 27 model fading into the shorter response model. The results were presented to the Taskforce, May 10. as in Figures 6.10, 6.11, 6.12, and others. These exemplify the idea of using animation to make clear visual comparisons by taking screen captures from VR models from the same viewpoint: the VR models might all be from the same time, as in Figure 6.9, or they might be from different times as well, as in Figures 6.10, 6.11, and 6.12.

Figure 6.10. Animation of various alternative screen captures from multiple VR models permits consistent visual comparison of models from one vantage point.

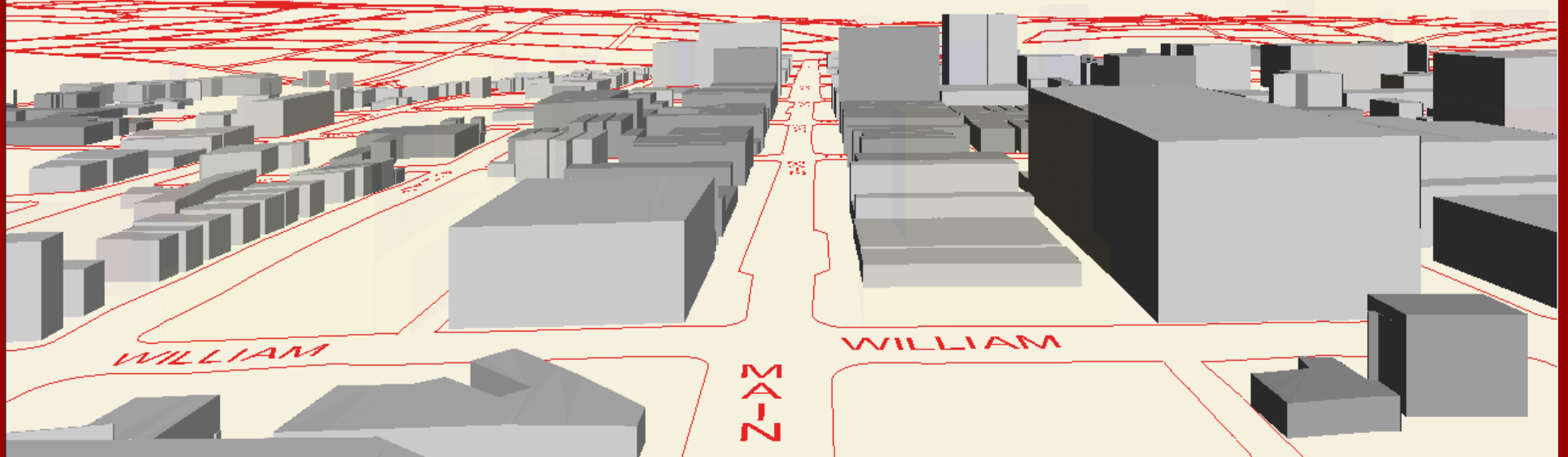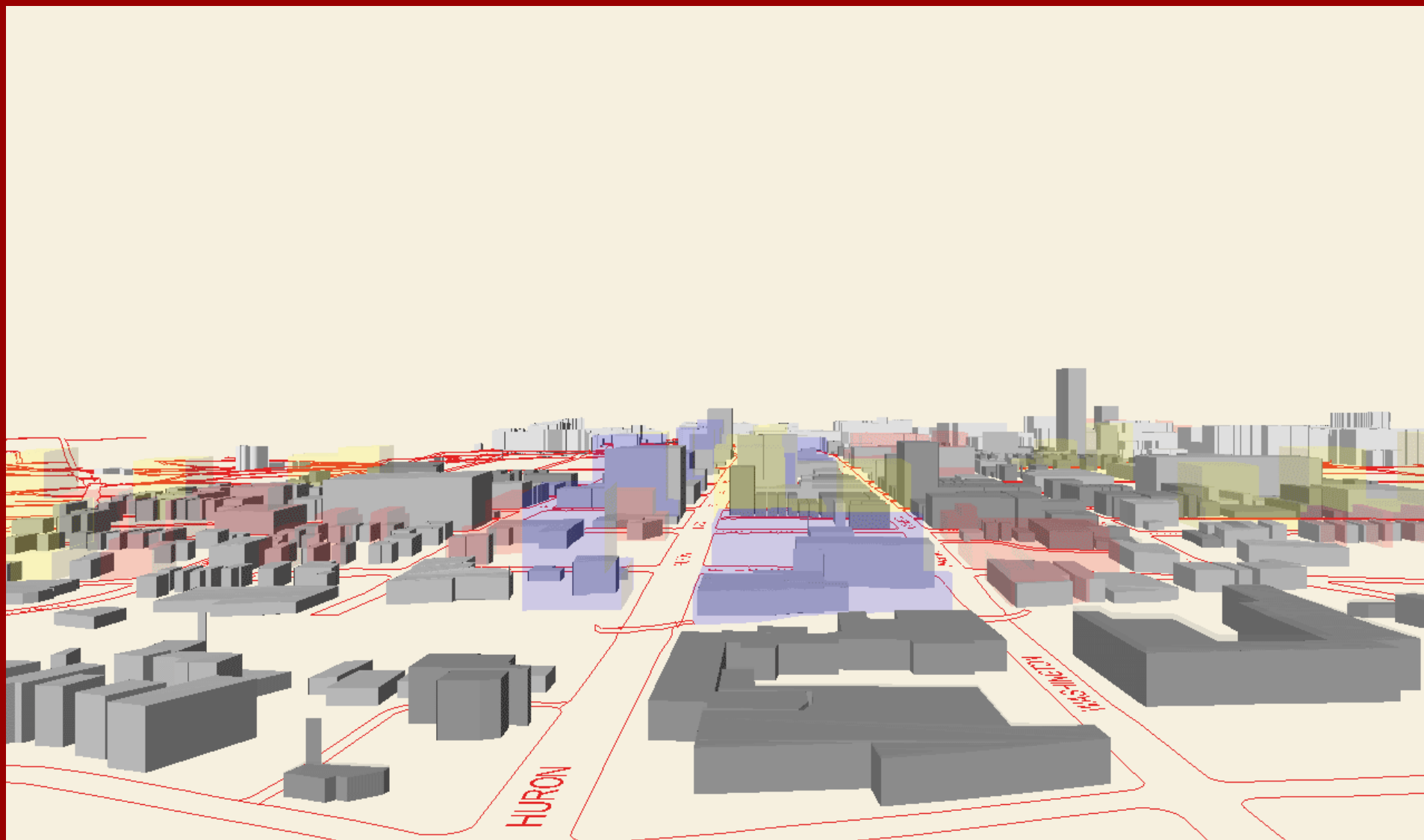Figure 6.11. Animation of various alternative screen captures from multiple VR models permits consistent visual comparison of models from one vantage point.

Figure 6.12. Animation of various alternative screen captures from multiple VR models permits consistent visual comparison of models from one vantage point.

These models, and results from hundreds of others, were presented to the Taskforce in 11 different meetings in the spring of 2004. They were presented in a public hearing to the citizens of Ann Arbor on April 27, 2004 as chronicled in a front page story in The Ann Arbor News with a picture of a model on the front page. They were presented to the Mayor and City Council on June 7, 2004. A previous article in Solstice describes this activity in detail. On July 19, 2004, the resolution derived in part from these models was approved by City Council with a request for a special session in September subsequent to the opportunity for City Council to analyze the mass of materials. From sieve to virtual reality, the strategy employed in one local study condensed time across millennia.

Bibliography

Includes references cited in the main work as well as others consulted or thought to be of use. Note: Links to external online files have been downloaded so that they will continue to work.

Agarwal, Pragya. Walter Christaller: Hierarchical Patterns of Urbanization

Alao, Nurudeen; Dacey, Michael F.; Davies, Omar; Denike, K. G.; Huff, James; Parr, John B.; Webber, M. J. 1977. *Christaller Central Place Structures: An Introductory Statement.* Northwestern University Studies in Geography, 22, Evanston.

Allen, P. M. and Sanglier, M.

- 1979. "A dynamic model of growth in a central place system--I", *Geographical Analysis.*
- 1981. "A dynamic model of growth in a central place system--II", *Geographical Analysis.*

American Scientist, Online

Ann Arbor Zoning Ordinance, Chapter 55, Ann Arbor City Code, pp. 36-38.

Archer, J. C. 1981. "Public choice paradigms in political geography. In Burnett, A. D. and Taylor, P. J., eds. *Political Studies from Spatial Perspectives*. New York: Wiley.

Archer, J. C. and Shelley, F. M. 1985. Theory and methodology in political geography. In Pacione, M., ed. *Progress in Political Geography*, London: Croom Helm.

Arlinghaus, Sandra Lach

- 1985. "Fractals take a central place," *Geografiska Annaler*, 67B, (1985), pp. 83-88. Journal of the Stockholm School of Economics.
- 1986. "Steiner Transformations" in *Essays on Mathematical Geography*, Monograph 3, pages 55-70, Institute of Mathematical Geography.
- 1987. "Fractals: constructions, speculations, and concepts," *Essays on Mathematical Geography--II*. IMaGe Monograph 5, pages 54-66, Ann Arbor, 1987.
- 1990. "Beyond the fractal." *Solstice: An Electronic Journal of Geography and Mathematics*, Institute of Mathematical Geography. Previous link is to original TeX code sent around via e-mail; click on the next link to see scanned images of typeset printout made from the TeX file: Beyond the Fractal, pages 17-35
- 1990. "Fractal Geometry of Infinite Pixel Sequences: "Super-definition" Resoultion?" *Solstice: An Electronic Journal of Geography and Mathematics*, Institute of Mathematical Geography. Previous link is to original TeX code sent around via e-mail;

click on the next link to see scanned images of typeset printout made from the TeX file: Fractal Geometry of Infinite Pixel Sequences: "Super-definition" Resoultion? pages 98-103

- 1991. "Table for Central Place Fractals" in *Essays on Mathematical Geography--III,* Monograph 14, pages 6-15, Institute of Mathematical Geography.
- 1991. "Tiling According to the Administrative Principle" in Essays on Mathematical Geography--III, Monograph 14, pages 16-25, Institute of Mathematical Geography.
- 1993 "Micro-cell Hex-nets" *Solstice: An Electronic Journal of Geography and Mathematics*, Institute of Mathematical Geography Previous link is to original TeX code sent around via e-mail; click on the next link to see scanned images of typeset printout made from the TeX file: Micro-cell Hex-nets
- 1993. "Electronic Geometry," *The Geographical Review* Vol. 83, No. 2, pp. 160-169.
- 1993, "Central Place Fractals"--Chapter 10 in *Fractals in Geography*, edited by Nina Lam and Lee DeCola, Prentice-Hall.
- 1996. "Web Fractals: An Overview" *Solstice: An Electronic Journal of Geography and Mathematics*, Institute of Mathematical Geography.
- 1996. "A Path Through Recent GIS Literature. Record Note." *The Geographical Review*, published by the American Geographical Society. Volume 86, No. 1.
- 1998. " Animated Four Color Theorem: Sample Map." *Solstice: An Electronic Journal of Geography and Mathematics*, Institute of Mathematical Geography, Ann Arbor, MI.
- 1998. " Animaps, II." *Solstice: An Electronic Journal of Geography and Mathematics*, Institute of Mathematical Geography, Ann Arbor, MI.
- 2000.   "Animaps, IV: Of Time and Place" *Solstice: An Electronic Journal of Geography and Mathematics*, Institute of Mathematical Geography, Ann Arbor, MI.
- 2001. " Base Maps, Buffers, and Bisectors" *Solstice: An Electronic Journal of Geography and Mathematics*, Institute of Mathematical Geography, Ann Arbor, MI.
- 2001. "The Lights Are On, All Over the World" *Solstice: An Electronic Journal of Geography and Mathematics*, Institute of Mathematical Geography, Ann Arbor, MI.
- 2003. "Ann Arbor, Michigan: Virtual Height Experiments" *Solstice: An Electronic Journal of Geography and Mathematics*, Institute of Mathematical Geography.
- 2003. Ann Arbor, Michigan: Virtual Height Experiments, Part II, *Solstice: An Electronic Journal of Geography and Mathematics*, Institute of Mathematical Geography.
- 2004. "Spatial Synthesis: A 3D Atlas of Ann Arbor" *Solstice: An Electronic Journal of Geography and Mathematics*, Institute of Mathematical Geography, Ann Arbor, MI.
- 2005. "Spatial Synthesis. The Evidence of Cartographic Example: Centrality and Hierarchy." *Solstice: An Electronic Journal of Geography and Mathematics*, Institute of Mathematical Geography, Ann Arbor, MI.
- 2005. "Kioskland: A Strategy for Linking Hierarchical Levels of Virtual Reality Maps." *Solstice: An Electronic Journal of Geography and Mathematics*, Institute of Mathematical Geography, Ann Arbor, MI.

Arlinghaus, William C. 1985. *The Classification of Minimal Graphs with Given Abelian Automorphism Group.* Memoirs, American Mathematical Society, 57.

Arlinghaus, Sandra L. and Arlinghaus, William C.

- 1989. "The fractal theory of central place hierarchies: a Diophantine analysis of fractal generators for arbitrary Löschian numbers," *Geographical Analysis: an International Journal of Theoretical Geography*. Ohio State University Press. Vol. 21, No. 2; pp. 103-121.
- 1999. Animaps III: Color Straws, Color Voxels, and Color Ramps. *Solstice: An Electronic Journal of Geography and Mathematics*, Institute of Mathematical Geography, Ann Arbor, MI.
- 2002. "Spatial Synthesis: Research Program." *Solstice: An Electronic Journal of Geography and Mathematics*, Institute of Mathematical Geography, Ann Arbor, MI.
- 2004. "Spatial Synthesis Sampler. Geometric Visualization of Hexagonal Hierarchies: Animation and Virtual Reality." *Solstice: An Electronic Journal of Geography and Mathematics*, Institute of Mathematical Geography, Ann Arbor, MI.

Arlinghaus, Sandra L.; Arlinghaus, William C.; and, Harary, Frank.

- 1993. "Sum Graphs and Geographic Information," Volume IV, No. 1. *Solstice: An Electronic Journal of Geography and Mathematics*, Institute of Mathematical Geography, Ann Arbor, MI. Previous link is to original TeX code sent around via e-mail; click on the next link to see scanned images of typeset printout made from the TeX file: Sum Graphs and Geographic Information
- 2002. *Graph Theory and Geography: An Interactive View* (Ebook). John Wiley and Sons, New York.

Arlinghaus, S., Beal, F., and Kelbaugh, D. The View from the Top: Visualizing Downtown Ann Arbor in Three Dimensions, *Solstice: An Electronic Journal of Geography and Mathematics*, Volume XV, No. 1, 2004, Institute of Mathematical Geography.

Arlinghaus, Sandra L. and De la Sierra, Ruben. 1998. Revitalizing Maps or Images? *Solstice: An Electronic Journal of Geography and Mathematics*, Institute of Mathematical Geography, Ann Arbor, MI.

Arlinghaus, Sandra L.; Drake, William D.; and, Nystuen, John D. with data and other input from: Audra Laug, Kris S. Oswalt, and Diana Sammataro. 1998. Animaps. *Solstice: An Electronic Journal of Geography and Mathematics*, Institute of Mathematical Geography, Ann Arbor, MI.

Arlinghaus, S., Goodman, F., and Jacobs, D. 1997. Buffers and Duality, *Solstice: An Electronic Journal of Geography and Mathematics*, Institute of Mathematical Geography, Volume VIII, Number 2.

Arlinghaus, Sandra; Haidar, Salma; and, Wilson, Mark. 2002. Animated Map Timeline, Syria. *Solstice: An Electronic Journal of Geography and Mathematics*, Institute of Mathematical Geography, Ann Arbor, MI.

Arlinghaus, Sandra L. and Nystuen, John D. 1990. "Geometry of boundary exchanges: Compression patterns for boundary dwellers." *The Geographical Review*, Vol. 80, No. 1; pp. 21-31.

Arlinghaus, Sandra L.; Nystuen, John D.; Woldenberg, Michael J. 1992. "An application of graphical analysis to semidesert soils." *The Geographical Review*, published by the American Geographical Society, July.

Association of American Geographers, Online Abstract, Blackwell Synergy Ann Assoc Am Geog, Vol 73, Issue 1, pp_ 51-54 Walter Christaller1 (Abstract)_files

Astronomy Online: http://www.algonet.se/~sirius/eaae/aol/market/collabor/erathost/

Atkin, R.H.

- 1974. *Mathematical Structure in Human Affairs*. Crane, Russak, New York. 212p.
- 1981. *Multidimensional Man*. Penguin, New York, 196p.

Austin, Robert F. Personal Communication (concerning merits of hexagonal arrangements in relation to telephone and other communications networks).

Batty, Michael.

- 1985. "Fractals---Geometry between Dimensions." *New Scientist* 4, 31-35.
- The Emergence of Cities: Complexity and Urban Dynamics, Draft paper, May 19, 2003.

Batty, M., and Longley, P.

- 1985. "The Fractal Simulation of Urban Structure." *Papers in Planning Research* #92, University of Wales Institute of Science and Technology, Colum Drive, Cardiff, CF1 3EU
- 1996. *Fractal Cities*. Academic Press, London and San Diego.

Beavon, K. S. O. 1977. *Central Place Theory: A Reinterpretation*. London: Longman.

Beavon, K. S. O. and Mabin, A. S. 1978. "The Lösch system of market areas: derivation and extension." *Geographical Analysis.*

Beckmann, M. J.

- 1958. City hierarchies and the distribution of city sizes. *Economic Development and Cultural Change* 6:243 48.
- 1968. *Location Theory*. New York: Random House.

Beguin, H.

- 1982. City size distribution and central place models: a suggestion. *Journal of Regional Science* 22:225 3.
- 1984. The shape of city size distributions in a central place system. *Environment and Planning A* 16:749 58.
- 1985. A property of the rank size distribution and its use in an urban hierarchy context. *Journal of Regional Science* 25:437 41.

Bell, Sarah B. M., B. M. Diaz, Fred C. Holroyd, M. J. Jackson. 1983. Spatially referenced methods of processing raster and vector data. *Image Vision Comput.* 1(4): 211-220.

Bell,Sarah B. M., Fred C. Holroyd. 1991. Tesseral amalgamators and hierarchical tessellations. *Image Vision Comput.* 9(5): 313-328.

Sarah B. M. Bell, Fred C. Holroyd. 1996. Lattice Rings: Coordinates for Self-Similar Hierarchies and Their Relevance to Geographic Information Systems. *International Journal of Geographical Information Science* 10(2): 147-177.

Bell,Sarah B. M., Fred C. Holroyd, David C. Mason. 1989. A digital geometry for hexagonal pixels. *Image Vision Comput.* 7(3): 194-204.

Benns, F. Lee and Seldon, Mary E. 1971. *Europe: 1939 to the Present*, Revised Edition. Appleton-Century-Crofts.

Berentsen, W. H. 1991. Regional socioeconomic implications of German unification for Eastern Germany: problems of settlement systems and regional development in the former GDR. Paper presented at the conference on "Decentralization and alternative rural-urban configurations" Barcelona.

Berry, B. J. L. 1971. City size and economic development. In Urbanization and National

Development, eds. L. Jakobson and V. Prakash, pp. 111 55. Beverly Hills: Sage Publications.

Berry, B. J. L. and Garrison, W. L. 1958. "Recent developments of central place theory." *Papers*, Regional Science Association.

Berry, B. J. L. and Harris, C. D. 1970. Walter Christaller: an appreciation. *Geographical Review* 60, 116-119.

Berry, Brian J. L. and Marble, Duane F. 1968. *Spatial Analysis: A Reader in Statistical Geography.* Englewood Cliffs: Prentice Hall.

Berry, B. J. L., Parr, J. B., Epstein, B. J., Ghosh, A. and Smith, R. H. T. 1988. *Market Centers and Retail Locations: Theory and Applications*, Englewood Cliffs: Prentice Hall.

Berry, B. J. L. and Pred, A. 1961. *Central Place Studies: A Bibliography of Theory and Applications*. Philadelphia: Regional Science Research Institute.

Binder-Johnson, H. 1978. Walter Christaller: another personal memoir. *Ontario Geography* 12, 93-101.

Birkhoff, G., and Mac Lane, S. 1960. A Survey of Modern Algebra. New York: Macmillan.

Boesler, K. 1982. *Raumordnung*. Erträge der Forschung, 165. Darmstadt: Wissenschaftliche Buchgesellschaft.

Bollobas, B. and Stern, N. "The optimal structure of market areas." *Journal of Economic Theory*, 1972.

Bogue, Donald J. 1950. The structure of the metropolitan community: a study of dominance and subdominance. Ann Arbor, MI.

Boys, Charles Vernon. 1902. *Soap Bubbles and the Forces which Mould Them*. Society for Promoting Christian Knowledge.

Brañas-Garza, P. and F. Alcalá-Olid, F. Different Paths of Urban Agglomeration in Spanish Regions: Evidence from 1960-2000 Globalization and World Cities Study Group and Network, Research Bulletin 24

Brecht, A. 1945. Federalism and Regionalism in Germany: the Division of Prussia. New York: Russell & Russell.

Burgess, Michael. <u>New Perspectives On Teaching Afro-American History</u>

Burkardt, John. www.psc.edu/~burkardt/src/graph_paper/graph_paper.html graph paper showing grid, triangular and hexagonal regions, Pittsburgh Supercomputing Center, Carnegie Mellon University, University of Pittsburgh.

Campbell, C. S. and S. L. Egbert. 1990. Animated cartography: Thirty years of scratching the surface. *Cartographica* 27(2): 24-46.

Carol, H. 1970. Walter Christaller: a personal memoir. *Canadian Geographer* 14, 67-69.

<u>Chicago Metropolis 2020</u>

Christaller, W. (<u>photo</u> of Christaller, from Marvin Mikesell).

- 1933. *Die zentralen Orte in Süddeutschland: Eine ökonomisch-geographische Untersuchung über die Gesetzmässigkeit der Verbreitung und Entwicklung der Siedlungen mit städischen Funktionen*. Jena: Gustav Fischer Verlag. Doktor-Dissertation.
- 1933. Grundsätzliches zu einer Neugliederungdes Deutschens Reiches un seiner Verwaltungsbezirke. *Geographische Wochen*schrift I, 913-919.
- 1933. Gebietseinheiten in der Provinz Starkenburg. *Darmstadter Tagesblatt*, 26 Sept.
- 1934. Allgemeine geographische Voraussetzungen der deutschen Verwaltungsgliederung. *Jahrbuch für Kommunalwissenschaft I,* 2, 48-72..
- 1937. *Die ländliche Siedlungsweise im Deutschen Reich und ihre Beziehungen zur gemeindeorganization.* Kommunalwissenschaftlichen Institutes an der Universität Berlin, VII. Stuttgart und Berlin. W. Kohlhammer Verlag. Habilitationsschrift.
- 1937. Literaturberichte. Kommunalwissenschaft und Siedlungsgeographie. *Jahrbuch für Kommunalwissenschaft* 4, 2; 492-500.
- 1938. Siedlungsgeographie und Kommunalwissenschaft. *Petermanns Geographische Mitteilungen* 84, 49-53.
- 1938. Literaturberichte. Kommunalwissenschaft und Siedlungsgeographie. *Jahrbuch für Kommunalwissenschaft 5, 2; 371-377.*
- 1938. Rapports Fonctionnels entre les Agglomerations Urbaines et les Campagnes. *Comptes Rendus du Congrès International de Géographie, Amsterdam 1938*, Leiden: E. J. Brill, 2, 123-138.
- 1939. Literaturberichte. Kommunalwissenschaft und Siedlungsgeographie. *Jahrbuch für Kommunalwissenschaft 6, 1; 279-289.*
- 1940. Die Kultur und Marktbereiche der zentralen Orte im Deutschen Ostraum und die Gliederung der Verwaltung. *Raumforschung und Raumordnung* 4, 498-503.
- 1940. Grundgedanken zum Siedlungs- und verwaltunsaufbau im Osten. *Neues Bauerntum* 32, 305-312.

- 1941. Raumtheorie und Raumordnung. *Archiv für Wirtschaftsplanung* 1, 116-135.
- 1941. Das Land im der Verwaltungsgliederung des Altreichs. In Meyer, K., ed. *Landvolk im werden*, Berlin: Deutsche Landbuchhandlung, 283-288.
- 1941 Die zentralen Orte in den Ostgebieten und ihre Kultur und Marktbereiche. Teil 1 in *Gemeinschafswerk im Auftrage der Reichsarbeitsgemeinschaft für Raumforschung*. Struktur und Gestaltung der zentralen Orte des Deutschen Ostens. Leipzig: K. F. Koehler Verlag, 1-22.
- 1945. Bildung einer Arbeitsgemeinschaft für funktionale Landes und Verwaltungsgliederung. *Berichte zur deutschen Landeskunde* 5, 35-37.
- 1947. Die Raumidee des Föderalismus und die Neugestaltung Deutschlands. *Neues Abendland* 11, 19-81.
- 1948. Das geographische Problem der Wahlkreiseinteilung. *Deutsche Wählergesellschaft Mittelungen*, Apri, 13-15.
- 1950. Das Grundgerüst der räumlichen Ordnung in Europa: Die Systeme der europäischen zentralen Orte. *Frankfurter Geographische Hefte* 24, 1.
- 1950. Wesen und Arten sozialraumlicher Landschaftseinheiten und Darstellung auf der Karte 1:200 000. *Berichte zur deutschen Landeskunde* 7, 357-367.
- 1962. Die Hierarchie der Städte. In Norborg, K., ed. *Proceedings of the IGU Symposium in Urban Geography, Lund 1960,* Lund: C. W. K. Gleerup Pubs, 3-11.
- 1966. *Central Places in Southern Germany* (translated with omissions by C. W. Baskin). Englewood Cliffs, N.J.: Prentice Hall, Inc.
- 1968. Wie ich zu der Theorie der zentralen Orte gekommen bin. *Geographische Zeitschrift* 56, 88-101.

Churchill, R. V. 1960. *Complex Variables and Applications*, 2nd Edition, New York: McGraw-Hill.

Clark, Alan. 1965. *The Russian-German Conflict, 1941-45*. New York: William Morrow & Company.

Cornwall, B. and A. Robinson 1966. Possibilities for computer animated films in cartography. *Cartographic Journal* 3(2): 79-82.

Crampton, J. 1999. Online Mapping: Theoretical Context and Practical Applications. In W. Cartwright, M. Peterson, and G. Gartner (Eds.) *Multimedia Cartography*, Springer Verlag.

Conway, J. H. and Sloane, N. J. A. 1993. Sphere Packings, Lattices, and Groups, 2nd ed. New York: Springer-Verlag.

Coxeter, H. S. M. 1961. *Introduction to Geometry*. New York: John Wiley & Sons, pp. 53-54; "Close Packing of Equal Spheres." Section 22.4 pp. 405-411.

Dacey, Michael F.

- 1964.   A Note on Some Number Properties of a Hexagonal Hierarchical Plane Lattice. *Journal of Regional Science* 5, 63-67.
- 1965. The geometry of central place theory. *Geografiska Annaler*, B, 47, 111-124.
- 1965. An Interesting Number Property in Central Place Theory." *Professional Geographer* 17, 32-33.

Dacey, Michael F.; Davies, Omar; Flowerdew, Robin; Huff, James; Ko Angela; Pipkin, John. 1974. *One-dimensional Central Plact Theory*. Northwestern University, Studies in Geography, 21, Evanston.

Deutscher Verband für Angewandte Geographie

Dickinson, R. E.

- 1938. The economic regions of Germany. *Geographical Review* 28, 609-626.
- 1945. *The Regions of Germany*. London: Kegan Paul, Trench, Trubner and Company, Ltd.
- 1964. *City and Region: A Geographical Interpretation*. London: Routledge and Kegan Paul Ltd.

Dickson, Leonard E. 1920. *History of the Theory of Numbers, Volume II, Diophantine Analysis*. Carnegie Institute of Washington, 256. (reprinted by Chelsea, N.Y., 1971)

Diggins, J. E. *The Whole Round Earth*, http://www.anselm.edu/homepage/dbanach/erat.htm

Disney, website history, http://disney.go.com/studiooperations/welcome/history.html

Edit Tools 3.1. http://www.ian-ko.com/howto.htm

Ehlschlaeger, C. R., A. M. Shortridge, and M. F. Goodchild 1997. Visualizing spatial data uncertainty using animation. *Computers and Geosciences* 23(4): 387-395.

Eisenstein, Elizabeth L. 1979. *The Printing Press as an Agent of Change*. Cambridge University Press.

Estonian conference. From Native and Landscape Research to Urban and Regional Studies

Euler, Leonhard.

- *Commentarii Arithmeticae* I, p. 570.
- 1773. Novi. *Comentarii Acad. Petrop.*, 18, p. 218.
- *Opera Omnia*, (1), III, p. 310.

Faulkner, William. 1949. Nobel Prize Acceptance Speech. http://www.nobel.se/literature/laureates/1949/faulkner-acceptance.html

Fejes Tóth, L.

- 1940. "Über einen geometrischen Satz." *Math. Z.* 46, 78-83, 1940.
- 1960/61. "On the Stability of a Circle Packing." *Ann. Univ. Sci. Budapestinensis*, Sect. Math. 3-4, 63-66.
- 1964. *Regular Figures*. New York: Macmillan.

Fonseca, James W. 1989. *The Urban Rank-size Hierarchy: A Mathematical Interpretation.* Monograph 8, Institute of Mathematical Geography.

Fuhrmann, S. and A. M. MacEachren 2001. Navigation in Desktop Geovirtual Environments: Usability Assessment. Proceedings of the 20th International Cartographic Conference, Beijing, China, August 6-10, 2001.

Gahegan, M. N. 1996. Visualisation strategies for exploratory spatial analysis. Paper presented at *Third International Conference on GIS and Environmental Modelling*, January 21 to January 25, 1996, Santa Fe, New Mexico.

Gardner, M. 1992. "Tangent Circles." Ch. 10 in *Fractal Music, Hypercards, and More Mathematical Recreations from Scientific American Magazine.* New York: W. H. Freeman, pp. 149-166.

Gauss, C. F. 1876. "Besprechung des Buchs von L. A. Seeber: Intersuchungen über die Eigenschaften der positiven ternären quadratischen Formen usw." Göttingsche Gelehrte Anzeigen (1831, July 9) 2, 188-196, 1876.

Gersmehl, P. J. 1990. Choosing tools: Nine metaphors for four-dimensional cartography. *Cartographic Perspectives*, Spring: 3-17.

Getis, A. Link to home page.

Getis, A. and Boots, B. 1978.   Models of Spatial Processes: An Approach to the Study of Point, Line and Area Patterns, Cambridge: Cambridge University Press. Reprinted in Russian.

Gleick, J. 1987. *Chaos: Making a New Science*. New York: Penguin Books.

Goodchild, M. F. 1979: The aggregation problem in location-allocation. *Geographical Analysis*, 11, pp. 240-255.

Goodchild, Michael F. and Janelle, Donald G. Thinking Spatially in the Social Sciences.

Goodchild, M. F. and Mark, D. M. 1987. The fractal nature of geographic phenomena. *Annals* of the American Association of Geographers 77:265 278.

Haggett, P.; Cliff, A. D.; and, Frey, A. 1977. *Locational Analysis inHumanGeography2*: *Locational Methods*. Second Edition. New York: John Wiley & Sons. (Section 13.5).

Hahn, H.: The crisis in intuition, lecture reprinted in Newman, J. R., 1956: *The World of Mathematics*. Simon and Shuster, New York, pp. 1956-1976.

Haines, C. Grove and Ross, J. S. Hoffman. 1943. *The Origins and Background of the Second World War*. Oxford University Press.

Hanjoul, Pierre; Beguin, Hubert; and Thill, Jean-Claude. 1988. *Theoretical Market Areas Under Euclidean Distance*. Monograph 6, Institute of Mathematical Geography.

Hargrove, William W., Winterfield, Richard F. and Levine, Daniel A. Dynamic segmentation and Thiessen polygons: a solution to the river mile problem.
http://research.esd.ornl.gov/CRERP/DOCS/RIVERMI/P114.HTM

Harris, Chauncy D.

- Letter as follow-up to query by first author about article with Berry.
- Personal communication as telephone conversation following the letter above.

Heath, T. L. 1910. *Diophantos of Alexandria: A Study in the History of Greek Algebra*, second edition, Cambridge University Press.

Higgs, R. 1970. Central place theory and regional urban hierarchies: an empirical note. *Journal of Regional Science* 10:253 55.

Hite, James. The Thünen Model as a Paradigm for Rural Development

Honey, Rex. 1983. Versatility versus continuity -- the dilemma of jurisdictional change. In Kliot, N. and Waterman, S., eds. *Pluralism and Political Geography: People, Territory, adn*

State. London: Croom Helm, 228-244.

Hottes, K., Hottes, R., and Schöller, P. 1984. Walter Christaller, 1893-1969. *Geographers: Bibliographical Studies* 7, 11-16.

Hottes, K. and Schöller, P. 1968. Werk und Wirkung Walter Christallers. Geographische Zeitschrift 56, 81-84.

Hottes, R. 1981/82. Walter Christaller--Ein Überblick über Leben und Werk. *Geographische Taschenbuch* 59-70. Appears in part in Hottes, R. 1983, Walter Christaller, 1893-1969, *Annals*, Association of American Geographers 73, 51-54.

Infrastructure Canada, Research and Analysis. An Overview of the LIterature on Linkages between Communities (March 3, 2005).

Institute of Historical Research, First Industrial Revolution North-West England c_ 1700-60

Institute of Mathematical Geography. 1983-present. URLs (all point to same location): http://www.imagenet.org/ ; http://www.InstituteOfMathematicalGeography.org/ ; http://www.InstituteOfMathematicalGeography.com/ ; http://www.MathematicalGeography.org/ ; http://www.MathematicalGeography.com/

Isard, W. *Location and Space-economy.* Dambridge, Mass. MIT Press.

Iturriaga, C. and Lubiw, A. 2003. Elastic labels around the perimeter of a map. *Journal of Algorithms*, 47 14-39.

Jefferson, Mark. 1928. The Civilizing Rails. *Economic Geography*, 1928, 4, 217-231.

Kim, Sukkoo. 1998. Urban Development in the United States, 1690-1990

Kim, Dooil and Park, Kyung Ho. Spatial Analysis of Military Vehicle Maneuver in Tactical Situation on ArcView

King, Leslie J. 1984. *Central Place Theory*, Beverly Hills: Sage Publications.

Kolars, John F. and Nystuen, John D. drawings by Derwin Bell. 1975.

- *Physical Geography: Environment and Man*, McGraw-Hill
- *Human Geography*, McGraw-Hill.

Kopec, R. J. 1963. An alternative method for the construction of Thiessen polygons. *Professional Geographer*, 15, (5), 24-26.

Krumme, Günter.

- Walter Christaller

- Homepage: http://faculty.washington.edu/krumme/

Kwon, Taejung; Lazzaro, Adrien; Oppenheim, Paul; Rosenblum, Aaron. 2003. Ann Arbor, Michigan: Virtual Height Experiments, Part III, *Solstice: An Electronic Journal of Geography and Mathematics*, Volume XIV, No. 2, Institute of Mathematical Geography.

Ladak, Alnoor and Martinez, Roberto B. Automated Derivation of High Accuracy Road Centrelines Thiessen Polygons Technique. http://www.esri.com/library/userconf/proc96/TO400/PAP370/P370.HTM

Langsam, Walter C. and Mitchell, Otis C. 1971. The World since 1919. Eighth Edition. New York: The Macmillan Company.

Lavenda, Bernard H. 1985. "Brownian Motion." *Scientific American*. v. 252, no. 2. 70-85.

Leibniz-Institut für Länderkunde e.V. Aktuelles, Tagungen, Veranstaltungen,...

Leibniz Institute of Regional Geography.

Loeb, Arthur L.

- 1976. Space Structures: Their Harmony and Counterpoint. Addison-Wesley.
- Personal Communication with S. Arlinghaus.

Lösch, August. *The Economics of Location*. Yale University Press, 1954.

MacEachren, A. M. 1998. Cartography, GIS and the World Wide Web. *Progress in Human Geography*: 575-585.

Mandelbrot, B. F.

- 1977. *Fractals: Form, Chance, and Dimension*. W. H. Freeman, San Francisco, 365 p.

- 1983. *The Fractal Geometry of Nature*. W. H. Freeman, San Francisco. 468p.

von Manstein, Field-Marshal Erich. 1958. *Lost Victories*. London: Methuen and Co. Ltd.

Marshall, John U.

- 1975. The Löschian Numbers as a Problem in Number Theory. *Geographical Analysis* 7, 421-426.
- 1977. The construction of the Löschian landscape. *Geographical Analysis* 9

McCoy, N. H. 1965. *The Theory of Numbers*. New York: Macmillan.

McLuhan, M. 1967. *The Medium is the Message*. New York: Bantam Books.

McPherson, J. C. "The implications of central place theory for urban structure in a declining region: the North American experience." *Papers*, Regional Science Association, v. 47.

MapQuest 2002. About MapQuest. http://www.mapquest.com/about/main.adp (Jan. 19, 2002)

Mellor, R. 1978. *The Two Germanies: A Modern Geography.* New York: Barnes and Noble.

Mennis, J. L. and D. J. Peuquet 2000. A conceptual framework for incorporating cognitive principles into geographic database representation. *International Journal of Geographic Information Science* 14(6): 501-520.

Meusburger, Peter. <u>Organisations and Institutions of German Geography</u> German Association of Geography - Deutsche Gesellschaft für Geographie

Meyer, K. 1970. *Walter Christaller: Handwörterbuch der Raumforschung und Raumordnung,* Band I. Teil A-H. Akademie für Raumforschung und Landesplanung, Hannover: Gebruder Janecke Verlag, 403-410.

Moellering, H.

- 1976. The potential uses of a computer animated film in the analysis of geographical patterns of traffic crashes. *Accident Analysis and Prevention* 8: 215-227.
- 1980. The real-time animation of three-dimensional maps. *The American Cartographer*, 7(1):67-75.
- 1978: Professor of Geography, The Ohio State University, Columbus, OH, Personal communication.

Monmonier, Mark.

- 1991. Ethics and Map design: Six strategies for confronting the traditional one-map solution. *Cartographic Perspectives* 10 (summer): 3-8.
- 1996. *How to Lie with Maps.* The University of Chicago Press.

Mordell, L. J. 1969. *Diophantine Equations.* New York and London: Academic Press.

Morrill, R. L. 1981. *Political Redistricting and Geographic Theory*. Resource Publications in Geography, Washington, DC: Association of American Geographers.

Morrill, R. L. and Dormitzer, J. M. 1979. *The Spatial Order: An Introduction to Modern Geography*, North Scituate, MA: Duxbury Press.

Mulligan, G. F. 1984. "Agglomeration and Central Place Theory. A Review of the Literature," *Int. Reg. Sci. Rev*. v. 9, 1-42.

Müncheimer, W. 1949. Die Neugliederung Deutschlands: Grundlagen, Kritik, Ziele, und die Plane zur Reichareform von 1919-1945. *Frankfurter Geographische Hefte* 23, 1.

Murray, Alan and Gottsegen, Jonathan. The Influence of Data Aggregation on the Stability of Location Model Solutions http://www.ncgia.ucsb.edu/~jgotts/murray/murray.html

Nakamura, Kei. On the Fibonacci Numbers. http://www.math.ucdavis.edu/~nakamura/teaching/resources/s01math55fibo.pdf

Natural Neighbor Interpolation. http://www.ems-i.com/smshelp/Scatter_Module/Scatter_Scattermenu/Natural_Neighbor.htm

Niven, I., and Zuckerman, H. S. 1960. An Introduction to the Theory of Numbers. New York and London: John Wiley and Sons.

Niven, I; H. S. Zuckerman, and Montgomery, H. L. 1991. An Introduction to the Theory of Numbers. John Wiley & Sons, Inc.

Nystuen, John D.

- 1963: Identification of some fundamental spatial concepts. *Papers of the Michigan Academy of Science, Arts, Letters*, 48pp. 373-384.
- 1966. "Effects of boundary shape and the concept of local convexity;" Michigan

Interuniversity Community of Mathematical Geographers (unpublished). Reprinted, Ann Arbor: Institute of Mathematical Geography.

- 1967: Boundary shapes and boundary problems. *Papers, Peace Research Society International*, 7, 107-128.
- 1978, 1984, Personal communication concerning a general interest in fractal geometry (not as associated with central place theory).

Nystuen, J. and Brown, D. 2001. Coordinators, UM GIS Lecture Series. Lecture by Arthur Getis: "Spatial Analytic Approaches to the Study of the Transmission of Disease: Recent Results on Dengue Fever in Iquitos, Peru".

Okabe, A.; Boots, B.; and, Sugihara, K. 1992. *Spatial Tesselations: Concepts and Applications of Voronoi Diagrams*. Wiley Series in Probability and Mathematical Statistics. Chichester: John Wiley & Sons.

Online bibliography of Development - Tourism

Online references from a site on the FAO server.

Openshaw, S., D. Waugh, and A. Cross (1994). Some ideas about the use of map animation as a spatial analysis tool. In Hilary M. Hearnshaw and David J. Unwin (Eds.) *Visualization in Geographic Information Systems*, Wiley: New York. pp. 131-138.

Ord, J. Keith and Getis, Arthur. 2001. "Testing for Local Spatial Autocorrelation in the Presence of Global Autocorrelation." *Journal of Regional Science*, Vol.. 41, No. 3, pp. 411-432.

Parr, J. B.

- 1969. City hierarchies and the distribution of city size: a reconsideration of Beckman's contribution. *Journal of Regional Science* 9:239 54.
- 1978. Models of the central place system: a more general approach. *Urban Studies*, 15, 35-49.
- 1980. Frequency distributions of central places in sourthern Germany: a further analysis. *Econ. Geog.*

Parr, J. B. and Denike, K. G. 1970. Theoretical problems in central place analysis. *Econ. Geog*.

Perkal, Julian, 1966. "An attempt at objective generalization;" Michigan Interuniversity Community of Mathematical Geographers (unpublished). Reprinted, Ann Arbor: Institute of Mathematical Geography.

Peterson, M. P. 1995. *Interactive and Animated Cartography*. Englewood Cliffs, NJ: Prentice Hall.

Place and Space in Sociology and the Social Sciences

Polya, G., 1954.   Patterns of Plausible Inference, Vol. II of *Mathematics and Plausible Reasoning*. Princeton University Press, Princeton, NJ, 190pp.

Preston, Richard E.

- 1971. "The structure of central place systems." *Econ. Geog.*
- 1985. "Christaller's neglected contribution to the study of the evolution of central places." *Progress in Human Geography*, 9, 177-193.
- 1991. "Christaller's contribution to a mixed hierarch interpretation of settlement structure. *Acta Geographica Lovaniensia* 31, 62-73.
- 1992. "Christaller's research on the geography of administrative areas." *Progress in Human Geography* 16, 4, 523-539.

Public Broadcasting Service (1996). Triumph of the Nerds: The Rise of Accidental Empires. National PBS Broadcast, first aired Wednesday, June 12, 1996 at 8:00p.m. ET. http://www.pbs. org/nerds/tvdes.html

Puu, Tonu. *Mathematical Location and Land Use Theory.* Springer-Verlag.

Raisz, E., 1948. *General Cartography*. McGraw-Hill, New York. 354pp.

Rhynsburger, Dirk, 1973. Analytic delineation of Thiessen polygons. *Geographical Analysis*, 5, 133-144.

Rosen, K. H. 1988. *Discrete Mathematics and Its Applications*. New York: Random House.

Rosen, K. T., and Resnick, M. 1980. The size distribution of cities: an examination of the Pareto law and primacy. *Journal of Urban Economics* 8:165 86.

Rosing, K. E. 1966. A rejection of the Zipf model (rank size rule) in relation to city size. *Professional Geographer* 18:75 82.

Rössler, M. 1989. Applied geography and area research in Nazi society: central place theory and planning, 1933 to 1945. *Environment and Planning D: Society and Space* 7, 419-431.

Rushton, G. 1971.   "Postulates of central-place theory and the properties of central place

systems." *Geog. Analysis.*

Society for the Advancement of Socio-Economics 2003 Abstracts

Scott, A. 1983. "Location and linkage systems: a survey and reassessment." *The Annals of Regional Science.*

Seaton, Albert. 1970. The Russo-German War 1941-45. New York: Praeger Publishers.

Smith, H. J. S.

- Collected Mathematical Papers, I, pp. 195-202.
- 1861. Report, British Association, paragratphs 96, 97; 313-319.

Snow, John. 1855. *Communication of Cholera*

Snyder, John P. 1993. *Flattening the Earth: Two Thousand Years of Map Projections.* The University of Chicago Press.

Speer, Albert. 1970. *Memoirs: Inside the Third Reich*. The Macmillan Company.

Steen, L. A. and Seebach J. A. Jr., 1970. *Counterexamples in Topology*. Holt, Rinehart and Winston, Inc., New York, 210pp.

Steinhaus, H. 1999.   Mathematical Snapshots, 3rd ed. New York: Dover, p. 202, 1999.

Stewart, C. T. 1958. The size and spacing of cities. *Geographical Review* 48:223 45.

Stone, Glenn Davis. References. http://www.artsci.wustl.edu/~anthro/demo/bib.html

Stutz, Frederick P. and de Souza, Anthony R. 1998. The World Economy: Resources, Location, Trade, and Development (3rd ed.), Prentice Hall; Chapter 7: Cities as Retail and Service Centers (p.307) (http://faculty.washington.edu/krumme/207/stutz/7.html)

Sullivan., 1982: Geometry, iteration and group theory: colloquium lectures, 88th annual American Mathematical Society Meetings, Jan. 13-16. Personal communication via attendance at lectures.

Tagliaventi, Gabriele The Romantic Tradition in 20th Century Town Planning

Taylor, Telford. 1958. *The March of Conquest: The German Victories in Western Europe 1940*. Simon and Schuster.

Thiessen, A. H., and Alter, J. C.. 1911. Climatological Data for July, 1911: District No. 10, Great Basin. *Monthly Weather Review,* July:1082-1089.

Thiessen Polygons. http://www.geog.ubc.ca/courses/klink/g472/class97/eichel/theis.html

Thomas, I. 1985. City size distribution and the size of urban systems. *Environment and Planning A* 17:905 913.

Thompson, D. W. 1961. *On Growth and Form* (abridged and edited by J. T. Bonner). Cambridge: Cambridge University Press.

Thrower, N. J. W.

- 1959. Animated cartography. *The Professional Geographer* 11(6): 9-12.
- 1961. Animated cartography in the United States. *International Yearbook of Cartography* 1:20-30.

Tobler, W. R.

- 1970. A computer movie simulating urban growth in the Detroit region. *Economic Geography* 46: 234-240.
- 1984. Professor of Geography, University of California, Santa Barbara. Personal communication.
- Three Presentations on Geographical Analysis and Modeling

Tsigaris, Peter and Dumouchel, Lian. Complex Systems in Tourism

Tufte, E. R. 1983. *The Visual Display of Quantitative Information*. Cheshire, CT. Graphics Press.

Tufte, E. R. 1995. *Envisioning Information*. Cheshire, CT. Graphics Press.

University of the Philippines, Geography Curricular Programs Homepage

University of Wales, Aberystwyth. Fieldwork Opportunities

Uspensky, J. V. and Heaslet, M. A. 1939. Elementary Number Theory, McGraw-Hill, New York.

Von Boventer, E. 1968. Walter Christallers zentrale Orte und periphere Gebiete. *Geographische Zeitschrift* 56, 102-111.

Waldrop, M. M. (2001). Origins of personal computing. *Scientific American* 285(6): 84-91.

Weimar, Jörg. Cellular Automata

Wells, D. 1986. *The Penguin Dictionary of Curious and Interesting Numbers.* Middlesex, England: Penguin Books, p.30.

White, Denis. Global Grids Bibliography

White, R. W. 1977. Dynamic central place theory: results of a simulation approach. *Geographical Analysis.*

Woldenberg, Michael J. 1968. Energy flow and spatial order: mixed hexagonal hierarchies of central places. *Geographical Review*, 58, 552-574.

Zacks, Stephen. 2001. Can Nigeria live up to the democratic ideals inherent in its new capital city's design?

Zipf, G. K. 1949. *Human Behavior and the Principle of Least Effort.* Cambridge: Addison Wesley.

Software used in the course of making this book was made by the following firms:

- Environmental Systems Research Institute, ArcView and ArcGIS software
- MacroMedia, Dreamweaver, MX.
- Adobe, Photoshop and ImageReady, 7.0
- Sun Microsystems
- Microsoft
- Alta 4 (Germany), ImageMapper
- Discreet, 3D Studio Max
- Animal Movement (Alaska Biological Station)
- Fractal Music 1.9, http://www.fractal-vibes.com; free download.

Hardware used centered on the equipment in the "Usability Lab" of the Duderstadt Center (with two flat screen monitors working together for a wide view) and on a Hewlett-Packard Pavilion

f1903, with an Intel Pentium 4 Processor, 512 MB PC3200 DDR SDRAM memory, Intel Graphics Media Accelerator, 200GB hard drive and a 19 inch flat screen monitor set to highest resolution.

Bibliography

Appendices

- ## **Eratosthenes's Measurement of the Earth**
- ## **Latitude and Longitude**
- ## **Earth-Sun Relations**
- ## **Trigonometry**
- ## **Thiessen Polygons**

Institute of Mathematical Geography. Copyright, 2005, held by authors.

Spatial Synthesis: Centrality and Hierarchy, Volume I, Book 1.

Sandra Lach Arlinghaus and William Charles Arlinghaus

I-Maps: Interactive Maps

- **I-Map 6.1:** Click here for a link to an interactive map showing building footprints and height (on mouse-over) as well as building address and street names (on mouse-over). Parcel boundaries are shown on the underlying aerial and on the green Downtown Development Authority (DDA) area. The Allen Creek floodway (underground) and flood plain are shown, shaded, respectively in blue and turquoise. Click on a building or a street to see associated entries in the underlying database.

- **I-Map 6.2:** Click here for a link to an interactive aerial showing parcel boundaries, zoning, building height (on mouse-over), and street name. DDA outline, only, is shown in light yellow so the user may zoom in to get a closer view of the aerial within the DDA (up to 800% enlargement--can see cars clearly). The Allen Creek floodway (underground) and flood plain are shown, outlined, respectively in blue and light blue; again, because the shading is removed, the viewer may look at the content of the floodway/floodplain in greater detail than above. Click on a building or a street to see associated entries in the underlying database.

- **I-Map 6.3:** Click here for a link to an interactive aerial showing zoning boundaries in the downtown, zoning type (on mouse-over), building height (in the "zoneht" record of the database), and street name. Click on a building or a street to see associated entries in the underlying database.

Institute of Mathematical Geography. Copyright, 2005, held by authors.

Spatial Synthesis: Centrality and Hierarchy, Volume I, Book 1.

Sandra Lach Arlinghaus and William Charles Arlinghaus

Mapplets

- ## K=3 Central Place Mapplet
- ## K=4 Central Place Mapplet
- ## K=7 Central Place Mapplet
- ## Historical Place Name Mapplet

Institute of Mathematical Geography. Copyright, 2005, held by authors.

Spatial Synthesis: Centrality and Hierarchy, Volume I, Book 1.

Sandra Lach Arlinghaus and William Charles Arlinghaus

Virtual Reality

Requires Cosmo Player of other viewer to be loaded in the Browser.

K=3 Poles   _K_=3 central place dot scatter produces a field of poles of height varying according to the principles of the associated central place hierarchy.

K=4 Poles   _K_=4 central place dot scatter produces a field of poles of height varying according to the principles of the associated central place hierarchy.

K=7 Poles   _K_=7 central place dot scatter produces a field of poles of height varying according to the principles of the associated central place hierarchy.

K=3 Solid   Interactive virtual model showing single tile at three levels of detail.

K=3 Translucent   Interactive virtual model showing single tile at three levels of detail.

K=4 Solid   Interactive virtual model showing single tile at three levels of detaill.

K=4 Translucent   Interactive virtual model showing single tile at three levels of detail.

K=7 Solid   Interactive virtual model showing single tile at three levels of detail.

K=7 Translucent   Interactive virtual model showing single tile at three levels of detail.

Core   Downtown Ann Arbor, existing core scene

1000   Downtown Ann Arbor, one scenario for 1000 new residential units

2500   Downtown Ann Arbor, one scenario for 2500 new residential units

---